

AUTOMATED SATELLITE CLOUD ANALYSIS - TACTICAL NEPHANALYSIS (TACNEPH)

Atmospheric and Environmental Research, Inc.
840 Memorial Drive
Cambridge, MA 02139

Final Report

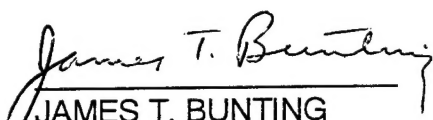
1 April 1990 - 30 November 1994

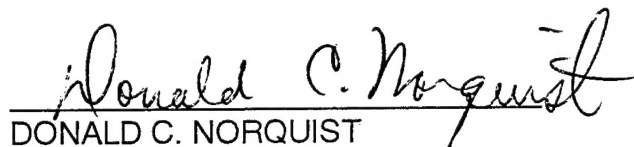
DEB Q. 1. 2. 3. 4. 5. 6. 7. 8. 9. 10. 11. 12. 13. 14. 15. 16. 17. 18. 19. 20. 21. 22. 23. 24. 25. 26. 27. 28. 29. 30. 31. 32. 33. 34. 35. 36. 37. 38. 39. 40. 41. 42. 43. 44. 45. 46. 47. 48. 49. 50. 51. 52. 53. 54. 55. 56. 57. 58. 59. 60. 61. 62. 63. 64. 65. 66. 67. 68. 69. 70. 71. 72. 73. 74. 75. 76. 77. 78. 79. 80. 81. 82. 83. 84. 85. 86. 87. 88. 89. 90. 91. 92. 93. 94. 95. 96. 97. 98. 99. 100. 101. 102. 103. 104. 105. 106. 107. 108. 109. 110. 111. 112. 113. 114. 115. 116. 117. 118. 119. 120. 121. 122. 123. 124. 125. 126. 127. 128. 129. 130. 131. 132. 133. 134. 135. 136. 137. 138. 139. 140. 141. 142. 143. 144. 145. 146. 147. 148. 149. 150. 151. 152. 153. 154. 155. 156. 157. 158. 159. 160. 161. 162. 163. 164. 165. 166. 167. 168. 169. 170. 171. 172. 173. 174. 175. 176. 177. 178. 179. 180. 181. 182. 183. 184. 185. 186. 187. 188. 189. 190. 191. 192. 193. 194. 195. 196. 197. 198. 199. 200. 201. 202. 203. 204. 205. 206. 207. 208. 209. 210. 211. 212. 213. 214. 215. 216. 217. 218. 219. 220. 221. 222. 223. 224. 225. 226. 227. 228. 229. 230. 231. 232. 233. 234. 235. 236. 237. 238. 239. 240. 241. 242. 243. 244. 245. 246. 247. 248. 249. 250. 251. 252. 253. 254. 255. 256. 257. 258. 259. 260. 261. 262. 263. 264. 265. 266. 267. 268. 269. 270. 271. 272. 273. 274. 275. 276. 277. 278. 279. 280. 281. 282. 283. 284. 285. 286. 287. 288. 289. 290. 291. 292. 293. 294. 295. 296. 297. 298. 299. 300. 301. 302. 303. 304. 305. 306. 307. 308. 309. 310. 311. 312. 313. 314. 315. 316. 317. 318. 319. 320. 321. 322. 323. 324. 325. 326. 327. 328. 329. 330. 331. 332. 333. 334. 335. 336. 337. 338. 339. 340. 341. 342. 343. 344. 345. 346. 347. 348. 349. 350. 351. 352. 353. 354. 355. 356. 357. 358. 359. 360. 361. 362. 363. 364. 365. 366. 367. 368. 369. 370. 371. 372. 373. 374. 375. 376. 377. 378. 379. 380. 381. 382. 383. 384. 385. 386. 387. 388. 389. 390. 391. 392. 393. 394. 395. 396. 397. 398. 399. 400. 401. 402. 403. 404. 405. 406. 407. 408. 409. 410. 411. 412. 413. 414. 415. 416. 417. 418. 419. 420. 421. 422. 423. 424. 425. 426. 427. 428. 429. 430. 431. 432. 433. 434. 435. 436. 437. 438. 439. 440. 441. 442. 443. 444. 445. 446. 447. 448. 449. 450. 451. 452. 453. 454. 455. 456. 457. 458. 459. 460. 461. 462. 463. 464. 465. 466. 467. 468. 469. 470. 471. 472. 473. 474. 475. 476. 477. 478. 479. 480. 481. 482. 483. 484. 485. 486. 487. 488. 489. 490. 491. 492. 493. 494. 495. 496. 497. 498. 499. 500. 501. 502. 503. 504. 505. 506. 507. 508. 509. 510. 511. 512. 513. 514. 515. 516. 517. 518. 519. 520. 521. 522. 523. 524. 525. 526. 527. 528. 529. 530. 531. 532. 533. 534. 535. 536. 537. 538. 539. 540. 541. 542. 543. 544. 545. 546. 547. 548. 549. 550. 551. 552. 553. 554. 555. 556. 557. 558. 559. 560. 561. 562. 563. 564. 565. 566. 567. 568. 569. 570. 571. 572. 573. 574. 575. 576. 577. 578. 579. 580. 581. 582. 583. 584. 585. 586. 587. 588. 589. 590. 591. 592. 593. 594. 595. 596. 597. 598. 599. 600. 601. 602. 603. 604. 605. 606. 607. 608. 609. 610. 611. 612. 613. 614. 615. 616. 617. 618. 619. 620. 621. 622. 623. 624. 625. 626. 627. 628. 629. 630. 631. 632. 633. 634. 635. 636. 637. 638. 639. 640. 641. 642. 643. 644. 645. 646. 647. 648. 649. 650. 651. 652. 653. 654. 655. 656. 657. 658. 659. 660. 661. 662. 663. 664. 665. 666. 667. 668. 669. 670. 671. 672. 673. 674. 675. 676. 677. 678. 679. 680. 681. 682. 683. 684. 685. 686. 687. 688. 689. 690. 691. 692. 693. 694. 695. 696. 697. 698. 699. 700. 701. 702. 703. 704. 705. 706. 707. 708. 709. 710. 711. 712. 713. 714. 715. 716. 717. 718. 719. 720. 721. 722. 723. 724. 725. 726. 727. 728. 729. 730. 731. 732. 733. 734. 735. 736. 737. 738. 739. 740. 741. 742. 743. 744. 745. 746. 747. 748. 749. 750. 751. 752. 753. 754. 755. 756. 757. 758. 759. 760. 761. 762. 763. 764. 765. 766. 767. 768. 769. 770. 771. 772. 773. 774. 775. 776. 777. 778. 779. 780. 781. 782. 783. 784. 785. 786. 787. 788. 789. 790. 791. 792. 793. 794. 795. 796. 797. 798. 799. 800. 801. 802. 803. 804. 805. 806. 807. 808. 809. 810. 811. 812. 813. 814. 815. 816. 817. 818. 819. 820. 821. 822. 823. 824. 825. 826. 827. 828. 829. 830. 831. 832. 833. 834. 835. 836. 837. 838. 839. 84


PHILLIPS LABORATORY
Directorate of Geophysics
AIR FORCE MATERIEL COMMAND
HANSCOM AIR FORCE BASE, MA 01731-3010

19970116 063

"This technical report has been reviewed and is approved for publication."


JAMES T. BUNTING
Contract Manager


DONALD C. NORQUIST
Acting Chief, Satellite Analysis and Weather
Prediction Branch
Atmospheric Sciences Division


DONALD A. CHISHOLM, Acting Director
Atmospheric Sciences Division

This report has been reviewed by the ESC Public Affairs Office (PA) and is releasable to the National Technical Information Service (NTIS).

Qualified requestors may obtain additional copies from the Defense Technical Information Center (DTIC). All others should apply to the National Technical Information Service (NTIS).

If your address has changed, or if you wish to be removed from the mailing list, or if the addressee is no longer employed by your organization, please notify PL/IM, 29 Randolph Road, Hanscom AFB, MA 01731-3010. This will assist us in maintaining a current mailing list.

Do not return copies of this report unless contractual obligations or notices on a specific document requires that it be returned.

REPORT DOCUMENTATION PAGE			Form Approved OMB No. 0704-0188	
Public reporting burden for this collection of information is estimated to average 1 hour per response, including the time for reviewing instructions, searching existing data sources, gathering and maintaining the data needed, and completing and reviewing the collection of information. Send comments regarding this burden estimate or any other aspect of this collection of information, including suggestions for reducing the burden, to Washington Headquarters Services, Directorate for Information Operations and Reports, 1215 Jefferson Davis Highway, Suite 1204, Arlington, VA 22202-4302, and to the Office of Management and Budget, Paperwork Reduction Project (0704-0188), Washington, DC 20503.				
1. AGENCY USE ONLY (Leave blank)		2. REPORT DATE 30 November 1994		3. REPORT TYPE AND DATES COVERED Final Report 1 April 1990 - 30 November 1994
4. TITLE AND SUBTITLE Automated Satellite Cloud Analysis - Tactical Nephanalysis (TACNEPH)			5. FUNDING NUMBERS PE 35160F PR 6670 TA 17 WUAT	
6. AUTHOR(S) G.B. Gustafson, R.G. Isaacs, J.M. Sparrow, D.C. Peduzzi, J.S. Belfiore			Contract F19628-90-C-0112	
7. PERFORMING ORGANIZATION NAME(S) AND ADDRESS(ES) Atmospheric and Environmental Research, Inc. 840 Memorial Drive Cambridge, MA 02139			8. PERFORMING ORGANIZATION REPORT NUMBERS (none)	
9. SPONSORING / MONITORING AGENCY NAME(S) AND ADDRESS(ES) Phillips Laboratory 29 Randolph Road Hanscom AFB, MA 01731-3010 Contract Manager: James Bunting/GPAB			10. SPONSORING / MONITORING AGENCY REPORT NUMBER PL-TR-94-2160	
11. SUPPLEMENTARY NOTES				
12a. DISTRIBUTION / AVAILABILITY STATEMENT Approved for public release; distribution unlimited			12b. DISTRIBUTION CODE	
13 ABSTRACT (Maximum 200 words) The TACNEPH program was a four year effort to develop a relocatable regional cloud analysis model for operational use in a transportable satellite ground station facility. Key features of the model are the ability to assimilate and analyze data from both military and civilian polar orbiting satellites in real time and to perform cloud analyses in the absence of any data source other than direct satellite sensor transmissions. In particular, data from the DMSP OLS, SSM/I, and SSM/T are used together with NOAA AVHRR multispectral imagery. In addition to direct broadcast satellite data, the only additional data requirements are for surface temperature climatology and geographic classification databases. Algorithms were developed to perform nephanalysis over the range of conditions expected to be encountered in a tactical environment (e.g., variable mix of sensor and supporting data and the absence of conventional observations). The TACNEPH program has the capability to operate in a "gracefully degrading" mode wherein different algorithms are employed as various sources of data are lost. Cloud algorithms consist of a series of cloud tests, each sensitive to a different satellite sensor spectral signature. Since the model must be able to operate when no conventional data are available, clear scene characteristics are inferred from climatology and sensor data. A technique has been developed to predict clear-scene satellite brightness temperatures through dynamic adjustments to climatological surface temperatures derived from shelter measurements. A multispectral algorithm operates using a decision tree structure to classify individual scene features (e.g., snow, low cloud, cirrus) separately through evaluation of a selected set of spectral signatures at each branch. Spectral signatures are combinations of channel ratios, differences, and absolute magnitudes. Other program tasks addressed database, mission sensor analysis, quality control and tuning issues. An experimental algorithm for retrieval of cloud thickness and base using multispectral imager data was developed to complement the nephanalysis algorithms. Extensive real-data algorithm testing and validation was performed based on comparisons with manual analysis of test data sets.				
14. SUBJECT TERMS loud analysis nephanlaysia satellite meteorology AVHRR OLS tactical terminal			15. NUMBER OF PAGES 108	
			16. PRICE CODE	
17. SECURITY CLASSIFICATION OF REPORT Unclassified	18. SECURITY CLASSIFICATION OF THIS PAGE Unclassified	19. SECURITY CLASSIFICATION OF ABSTRACT Unclassified	20. LIMITATION OF ABSTRACT Unlimited	

TABLE OF CONTENTS

	<u>Page</u>
1 Introduction	1
1.1 TACNEPH Program Task Requirements.....	2
2 External Data Requirements and Sources.....	4
2.1 Visible Sensor Data.....	6
2.1.1 AVHRR Visible Sensor Data Calibration.....	6
2.2 Infrared Sensor Data	6
2.2.1 AVHRR Infrared Sensor Data.....	7
2.3 Mission Sensor Data	8
2.3.1 SSM/I	8
2.3.2 SSM/T-1	8
2.4 Earth Location.....	9
2.5 Sun - Satellite Geometry.....	9
2.6 Climatology Databases.....	10
2.7 Geography Database	10
2.8 1000-mb Height Profile Database	10
3 TACNEPH Database.....	10
3.1 AIMS Database Management.....	11
3.1.1 Database Management System Design.....	12
3.1.2 Database Structure.....	13
3.1.3 TACNEPH Database Implementation.....	16
3.1.4 TACNEPH Database Summary	17
3.2 Image Processing and Display	17
4 Clear-Scene Background Characterization.....	18
4.1 Clear-Scene Visible Databases for OLS and AVHRR.....	19
4.2 Clear-Scene Infrared Databases for OLS and AVHRR.....	20
4.3 SSM/I Surface Temperature	24
4.3.1 SSM/I Antenna Pattern Correction.....	25
4.3.2 Application of SSM/I Derived Surface Temperature.....	27
5 Nephanalysis Algorithms.....	27
5.1 DMSP/OLS Cloud Analysis Algorithm Description	28
5.1.1 Threshold Calculation.....	28
5.1.2 Single Channel Test.....	31
5.1.3 Bispectral Test	32
5.1.4 Use of Visible Data.....	34
5.1.5 OLS Cloud Analysis Results.....	34
5.1.6 OLS Cloud-Clearing Procedure.....	35
5.2 NOAA/AVHRR Cloud Analysis Algorithm Description.....	37
5.2.1 Background Surface Filter Tests.....	37
5.2.1.1 Sun Glint Test.....	38
5.2.1.2 Desert Test	39
5.2.1.3 Snow Background Test.....	40

TABLE OF CONTENTS (continued)

	<u>Page</u>
5 Nephanalysis Algorithms (continued)	
5.2.2 Cloud Tests	40
5.2.2.1 Solar Independent Cloud Tests	41
5.2.2.2 Daytime Cloud Tests	43
5.2.2.3 Night Tests.....	46
5.2.3 Noise Filter.....	47
5.2.4 Intermediate Cloud Analysis Result.....	48
5.2.5 Final Cloud Analysis Result	49
5.2.6 AVHRR Output Product.....	51
5.2.7 AVHRR Cloud-Clearing Procedure.....	52
5.3 Testing and Validation of Cloud Algorithms.....	52
5.3.1 Algorithm Testing.....	53
5.3.2 Validation Procedure.....	57
5.3.3 Validation Results.....	59
6 Quality Control and Tuning.....	62
6.1 Analysis Confidence Flags	62
6.1.1 OLS Confidence Flag Determination	63
6.1.2 AVHRR Confidence Flag Determination.....	64
6.2 Tuning.....	65
6.3 Quality Control Recommendations.....	69
7 Assignment of Cloud Top Altitudes	70
7.1 Quantitative Relationships of Cloud Top Altitude and Temperature Profile.....	70
7.2 Qualitative Tailoring of TACNEPH Guidance	76
7.3 Expected Improvements in VTP/Cloud Height Assignment.....	77
8 Cloud Thickness and Base From Multispectral Cloud Imager Data	79
8.1 Algorithm Description.....	80
8.2 Cloud Type	82
8.3 Cloud Thickness.....	84
8.4 Cloud Top Height	85
8.5 Results	87
8.6 Conclusions.....	94
9 Recommendations for Use of Surface Observations of Cloud.....	94
10 TACNEPH Computer Program	95
10.1 Research Grade Code.....	96
10.2 Implementation on the AIMS System.....	96
11 References.....	98

LIST OF FIGURES

<u>Figure</u>	<u>Page</u>
1 Satellite-earth-solar geometry (after Taylor and Stowe, 1984); γ - satellite zenith angle, Θ - solar zenith angle, and Φ - azimuth angle.....	9
2 Example histogram of comparison between satellite brightness temperature and corresponding climatology temperature value for 89,763 clear pixels obtained from an AVHRR scene from 1947 UTC on 6 June 1992. Vertical lines represent 2 standard deviations about the mean.....	21
3a Comparison of the NRL and AFGWC level 1 corrections to the 37 GHz horizontal polarization channel for approximately 125 consecutive scan lines taken from a single orbit.	26
3b Magnitude of the level 2 corrections for the same set of scan lines contained in Figure 3a	26
4 IR single channel test dual threshold classification approach.....	30
5 Bispectral classification approach.....	33
6 Example histogram of comparison between satellite brightness temperatures and corresponding climatological temperatures for a case in which some cloudy pixels have been incorrectly classified as cloud-free. Solid vertical lines represent 2 standard deviations about the mean of the entire, bimodal distribution. Broken vertical lines represent manually adjusted values for which the cloud contaminated pixels have been eliminated.	36
7 Cloud test result data filter examples. Each group of boxes represents the cloud analysis results for one filter window. A black box signifies cloud has been detected; a white box means clear; stippled boxes have been changed by the noise filter from cloud to clear (a) or clear to cloud (b).	48
8 Initial ROIs for testing of nephanalysis algorithms.	54
9 Regions of interest selected for nephanalysis testing using DMSP and NOAA data from the PL/GPA direct-broadcast satellite ground stations.	54
10 Selected regions of interest for validation study; the land ROI covers the area 35-40 N latitude, 78-83 W longitude; the water ROI covers the area 35-40 N latitude, 73.5 - 58.5 W longitude.	58
11 Schematic of recommended AVHRR cloud algorithm tuning option.....	68
12 Cloud altitude algorithm flow chart.....	71
13 Deficit between cloud top and EBBT as a function of look angle and integrated water vapor for a mid latitude atmosphere.....	74
14 Vertical distribution of SSM/T-1 temperature profile retrieval errors.....	75
15 Cloud thickness and base procedure.....	81
16 Cloud type calculation.....	83
17 Radiative transfer-based LUT generation.	84

LIST OF FIGURES (continued)

<u>Figure</u>		<u>Page</u>
18	Cloud thickness look up tables (LUTs) for five cloud types.....	86
19	Integrated cloud height calculation.	86
20	AVHRR channel 2. Julian day: 183; Year: 1992.	88
21	Cloud mask (cloudy pixels are white).....	89
22	Cloud typing: 1: cumulonimbus (black); 2: cumulus; 3: stratus; 4: stratocumulus; 5: altostratus; 6: altocumulus; 7: cirrostratus; 8: cirrus; 9: clear.	90
23	Cloud height. Low - 300 m (white); high - 9000 m (black).	91
24	Cloud thickness. Low - 200 m (white); high - 6000 m (black).	92
25	Cloud base. Low - 100 m (white); high - 8000 m (black).	93

LIST OF TABLES

<u>Table</u>		<u>Page</u>
1	TACNEPH Task Breakdown Summary.....	3
2	Satellite Sensor Channel Data Attributes.....	5
3	External Supporting Databases	5
4	TACNEPH Database Data Dictionary Descriptions.....	16
5	Clear-Scene Internal Database Characteristics	19
6	Intermediate DMSP Cloud Analysis Bit Assignments.....	35
7	Background Surface Test Summary.....	37
8	AVHRR Cloud Test Summary	41
9	Predicted Clear-Scene Channel 4-5 Brightness Temperature Differences (from Saunders and Kriebel, 1988).....	43
10	Intermediate Output Format Bit Encoding.....	49
11	Background Surface Filters for Cloud Tests.....	50
12	AVHRR Cloud Analysis Algorithm MCF File Bit Assignments.....	51
13	Statistical Comparison of Fractional Cloud Amount Differences (%) for the AVHRR Algorithm (a) and the OLS Algorithm (b)	60
14	Confidence Flag Criteria.....	63
15	DMSP Confidence Flag Assignment.....	64
16	AVHRR Quanta Value Classification Assignments.....	66
17	Default Threshold Increments.....	67
18	Temperature Error Budget (K) for Cloud Top Temperature Assignment (multiply by 0.15 for cloud top altitude error in km)	76
19	Summarized Recommendations for Improved Retrieval of Cloud Top Altitude in a Tactical Environment	79
20	Variance Table for Low Level Clouds.....	83
21	Cloud Type Dependence.....	85

1. INTRODUCTION

The Tactical Nephanalysis (TACNEPH) program was a four-year research effort conducted by Atmospheric and Environmental Research, Inc. (AER) for the Satellite Meteorology Branch of the Phillips Laboratory Geophysics Directorate (PL/GPAS) and sponsored by the Defense Meteorological Satellite Program (DMSP) Systems Program Office (SPO), Space and Missile Systems Center (SMC), Los Angeles, CA. The TACNEPH objective was to develop and validate a set of robust, relocatable regional cloud (neph) detection and analysis algorithms capable of generating gridded fields of analyzed cloud amount and altitude using only the resources available on a tactical terminal such as Mark IV-B or the Small Tactical Terminal (STT). Key requirements are global applicability, the ability to assimilate data from both military and civilian polar orbiting satellites in real-time, and support for a range of available sensor data required to accommodate data-impaired or data-denied situations.

Required attributes of the TACNEPH analysis are autonomy, transportability, reliability, and graceful degradation. Autonomy requires that the cloud analysis be performed without timely updates to supporting data from a central site such as the Air Force Global Weather Central (AFGWC). Transportability means that the TACNEPH cloud algorithms must operate within the constraints of tactical terminal ingest, computing, and display capabilities. Reliability demands that the algorithms operate successfully for any location around the world over a range of data availability conditions. Graceful degradation implies that TACNEPH algorithms adapt to changes in available satellite data resources to produce the most accurate analysis possible under all conditions. The TACNEPH heritage lies in the global RTNEPH model which, along with its predecessor the 3DNEPH, the Air Force has operated continuously for over 20 years (Hamill et al., 1992). However, while the fundamental requirement to operationally analyze satellite sensor data to obtain cloud information is the same for both models, TACNEPH requirements depart from RTNEPH capabilities in a number of areas. Important differences are the regional vs. global nature of the models, the TACNEPH requirements to exploit multiple sensor data sources and to operate in the absence of supporting databases from non-satellite sources, and the processing environments in which the two models operate.

Relevant dynamic data resources assumed to be available to a tactical terminal include digital satellite sensor data from: DMSP Operational Linescan System (OLS), Special Sensor Microwave Imager and Temperature Sounder (SSM/I and SSM/T, respectively), and National Oceanic and Atmospheric Administration (NOAA) Advanced Very High Resolution Radiometer (AVHRR). Static climatological databases of surface shelter temperature and 1000 mb geopotential heights along with a rudimentary geographic type database are also assumed to be carried on the tactical terminal. Conventional surface and upper air observations are assumed to be unavailable on the tactical terminal, but may be available at a nearby or collocated facility (e.g. Combat Weather System, CWS). Other potentially useful satellite data sources are not currently used by TACNEPH; these include the NOAA TIROS Operational Vertical Sounder (TOVS) package and all geostationary environmental satellites (both U.S. and foreign).

Required TACNEPH cloud parameters are cloud amount and altitude. Experimental algorithms to retrieve cloud thickness and base from OLS and AVHRR data were also developed. Cloud attributes are reported on a pixel level and, as such, can be adapted to any gridded field format that may be required by a particular application.

1.1 TACNEPH Program Task Requirements

During the TACNEPH research and development program work was performed on new algorithm development, validation, testing and software maintenance. Nine tasks, some with multiple subtasks, were originally identified as necessary to successfully complete the program requirements. Subsequent to the start of the program one task involving evaluation of a government furnished SSM/I cloud analysis algorithm was dropped when results from other investigations demonstrated that the algorithm was unsuitable for TACNEPH applications. Midway through the development effort it was recognized that insufficient satellite data were available to the program for testing and validation of the nephanalysis algorithms. To solve this problem, the contract was modified to add two new subtasks to provide real-time access to DMSP/OLS and NOAA/AVHRR polar-orbiting satellite data. The remaining eight tasks, with applicable subtasks, are summarized in Table 1.

All algorithms developed in support of the tasks listed in Table 1 were implemented for testing purposes on the Air Force Interactive Meteorological System (AIMS). AIMS is a system of networked general purpose computers, image processing systems, and satellite ground stations maintained at the Phillips Laboratory (Ivaldi et al., 1992). Documentation on computer programs is available separately in the required TACNEPH Software Design Report. All software development for TACNEPH was for the sole purpose of testing algorithm performance under real-world conditions using actual satellite data (see Section 10.1).

Task 1 activities were designed to provide a suitable environment for algorithm testing by simulating the database capabilities expected to be available on a tactical terminal. These were primarily directed toward satellite sensor data ingest and management but also included a significant effort to develop a visualization capability for examining algorithm internal databases and results. As part of this effort, two real-time satellite ground receiving stations to ingest direct-broadcast transmissions from the DMSP F10 and F11 and NOAA-11 and NOAA-12 satellites were installed and integrated as part of AIMS.

An SSM/I all-weather multiple regression algorithm designed to estimate brightness temperatures that would be measured by the OLS under cloud-free conditions has been used at AFGWC in the RTNEPH model. Task 2 was designed to evaluate the usefulness of that technique in the TACNEPH cloud retrieval algorithms. Unfortunately, regression coefficients for the F10 and F11 satellites could not be supplied to the TACNEPH program during the period of performance so formal testing could not be accomplished.

Addressing Task 3 requirements comprised the principal effort under TACNEPH. Each subtask was a major research effort in its own right and resulted in a set of cloud algorithms capable of analyzing any combination of sensor channel data from the OLS or AVHRR. In addition, an important part of the cloud analysis work was accomplished under Task 3.3 where algorithms were developed to predict the brightness temperatures that would be measured by the long-wave infrared (LWIR) channels on the OLS and AVHRR under cloud-free conditions. Accurate clear-scene temperature estimates are critical to OLS cloud algorithm performance and also have a significant impact on AVHRR cloud algorithm accuracy.

The only information on upper air characteristics expected to be available on the tactical terminals are temperature and moisture profiles that can be derived from satellite data. TACNEPH requirements under Task 4 specified evaluation of a government

Table 1. TACNEPH Task Breakdown Summary

Task	Name	Description
1.	Tactical Terminal Database Management	Develop capability to ingest, calibrate, Earth locate, process, and display databases needed for TACNEPH
1.1	AIMS database management	Modify AIMS database manager to support TACNEPH files
1.2	AVHRR data acquisition	Develop software to ingest, calibrate, and Earth locate AVHRR data
1.3	Satellite ground station	Install DMSP and NOAA direct broadcast ground stations
1.4	Real-time data ingest	Develop a real-time satellite data ingest and processing capability for DMSP and NOAA sensor data
1.5	Objective analysis of point data	Write high-level AIMS application to generate regular gridded fields from unevenly spaced point data
1.6	Image processing	Adapt AIMS image processing software to support TACNEPH visualization requirements
2.	SSM/I surface temperature retrieval	Evaluate impact of government furnished SSM/I surface temperature retrieval algorithm on cloud analysis accuracy
3.	OLS and AVHRR cloud analysis	Develop cloud and surface temperature retrieval algorithms
3.1	OLS nephanalysis algorithm	Develop OLS cloud detection algorithm
3.2	AVHRR nephanalysis algorithm	Develop AVHRR cloud detection algorithm
3.3	OLS and AVHRR surface temperature	Develop OLS and AVHRR clear-scene temperature retrieval algorithm
4.	SSM/T cloud height assignment	Evaluate utility of SSM/T derived vertical temperature profiles for assignment of cloud top altitude
5.	Cloud base and thickness	Develop improved algorithm for estimating cloud thickness and base altitude from satellite sensor data only
6.	Quality control and tuning	Investigate QC and tuning techniques to support interactive manipulation and monitoring of cloud analyses
7.	Conventional data processing	Integrate government furnished software to process surface-based cloud observations with nephanalysis results
8.	TACNEPH computer program	Develop software to implement algorithms developed under other tasks for test and validation purposes

furnished SSM/T temperature profile retrieval computer program for use in deriving cloud top altitude. The basis for this evaluation is the accuracy of the retrieved temperature profiles relative to radiosonde measurements.

Task 5, to develop algorithms for retrieval of cloud thickness and base altitude, differed in substance from the other TACNEPH tasks in that it required a research effort not necessarily intended to produce an operational algorithm. Estimation of cloud optical properties from imaging sensor data alone (i.e., OLS and AVHRR) is problematic. AER

derived a hybrid technique to estimate cloud thickness using estimates of cloud type to infer required optical characteristics. Cloud base is then derived using the thickness and cloud top altitude.

Accuracy of TACNEPH derived cloud analyses will vary with the quality and mix of available sensor data and, potentially, with local conditions. Since tactical users are unlikely to be familiar with the underlying principals of the TACNEPH algorithms, additional information is required to provide estimates of the relative accuracy of a given cloud analysis. It was also necessary to develop a capability to adjust algorithm sensitivity to particular cloud types to support different end-user applications and location specific conditions. Task 6 addresses these requirements by providing relative accuracy indicators, or analysis quality flags, as a by-product of the cloud analysis. It also specifies an interactive tuning capability that will allow the user to modify the algorithm characteristics to satisfy a particular application with no knowledge of the algorithmic approach.

While no conventional surface or aircraft observations of cloud are available on tactical terminals, it is likely that some end users will have access to these types of data from other external sources. Task 7 was modified during the program from the initial requirement of simply implementing government furnished software for processing of surface-based observations of cloud parameters to recommendations on how to combine TACNEPH cloud analysis results with surface observations in a post-processing sense.

Possibly the single most important aspect of the entire TACNEPH program was the emphasis throughout on real-data testing. It is worth noting that while there are a large number of satellite cloud retrieval techniques reported in the literature, only a small number have been tested using real satellite data, and of those most are based on results from only a few case studies. Even during initial TACNEPH algorithm development, testing was based on real satellite data. Case study data were collected over four geographically diverse locations for two seasons, winter and summer. Later, following installation of the DMSP and NOAA ground stations, real-data testing steadily grew into what became a daily process that entailed automatic analysis of every satellite pass within view of the ground station antennas and a subsequent evaluation by a trained analyst. Feedback from the analyst to algorithm developers was direct and resulted in numerous improvements and modifications to the algorithms. Ultimately both the OLS and AVHRR cloud algorithms were subjected to this level of daily review for one full year. Task 8 requirements provided the framework for all algorithm testing by providing a full functioned environment for exercising the algorithms over a broad range of conditions through the integration of data ingest, database management, data processing, and display functions.

2. EXTERNAL DATA REQUIREMENTS AND SOURCES

TACNEPH nephanalysis algorithms are designed to operate on satellite data from the DMSP OLS, Special Sensor Microwave Imager (SSM/I) and Temperature Sounder (SSM/T-1), and NOAA-AVHRR sensors. The DMSP and NOAA satellites are in polar, sun-synchronous orbits whose periods are approximately 104 minutes. Data from DMSP-F10 and F11 and NOAA-11 and 12 satellites were used during TACNEPH algorithm development and testing. Sensor data requirements are summarized in Table 2. A full discussion of the sensor data including instrument characteristics, sensor calibration and data format is given in Sections 2.1 (visible), 2.2 (infrared), and 2.3 (mission sensor). In addition to the sensor data, TACNEPH algorithms require five supporting databases: Earth location (Section 2.4), sun-satellite geometry (Section 2.5), surface temperature climatology, (Section 2.6) geography classification (Section 2.7) and 1000-mb height field (Section 2.8). These databases are summarized in Table 3. It should be emphasized that

Table 2. Satellite Sensor Channel Data Attributes

Satellite	Sensor	Channel (μm)	Data Format	Resolution ¹ (km)	Bits per Pixel ²	Pixels per Scan Line ³
NOAA	AVHRR	0.58-0.68	percent albedo	1.1	10	2048
		0.72-1.10	percent albedo	1.1	10	2048
		3.55-3.93	EBBT ⁴	1.1	10	2048
		10.3-11.3	EBBT	1.1	10	2048
		11.5-12.5	EBBT	1.1	10	2048
DMSP	OLS	0.40-1.10	counts	2.7	6	1468
		10.5-12.6	EBBT	2.7	8	1468
	SSM/I	19V & H (GHz)	EBBT	25	12	64
		22V	EBBT	25	12	64
		37V & H	EBBT	25	12	64
		85V & H	EBBT	12.5	12	128
		50.5 (GHz)	EBBT	214		7
	SSM/T-1	53.2	EBBT	214		7
		54.35	EBBT	214		7
		54.9	EBBT	214		7
		58.4	EBBT	214		7
		58.825	EBBT	214		7
		59.4	EBBT	214		7

¹Sensor resolution at satellite subpoint.

²AVHRR radiance data are transmitted at 10-bit resolution. The TACNEPH development system could only accommodate 8-bit brightness temperature data; however, the full 10-bit resolution is used in the radiance to brightness temperature transformation.

³Maximum width of data swath. The number of scan lines is variable, dependent on the satellite-ground station line of sight.

⁴Equivalent Blackbody Brightness Temperature.

Table 3. External Supporting Databases

Type	Resolution	Projection	Description
Earth Location		Scan	latitude/longitude for each pixel
Sun-satellite Geometry		Scan	solar zenith, satellite zenith, azimuth for each pixel
Geography	10-Minute	Lat-Lon	ocean, lake, coast, land, desert
Surface Temperature	8th-Mesh	Polar-Stereo	monthly climatology at 3-hour intervals (T_{clim})
Climatology	(47 km)		
1000 mb Height	Whole-Mesh	Polar-Stereo	monthly climatology at 12-hour intervals (z_{clim})
Profile			

TACNEPH data requirements are consistent with available databases on tactical terminals such as Mark IV-B. It is important to note however, that database resolution and projection information provided in Table 2 are provided only to document how the data were used in the TACNEPH algorithm development work and should not be interpreted as firm requirements. TACNEPH databases were constructed solely to satisfy research needs with no attention to optimizing data access or processing operations. They were not intended to be used as a model for operational implementation. Actual operational data formats will be dictated by the host tactical terminal database capabilities and processing environment. For the research program all data were maintained in the native satellite sensor projection.

2.1 Visible Sensor Data

The majority of TACNEPH cloud analysis algorithms process visible reflectance data in a relative or band-differencing sense. As such, visible sensor data are not required to be absolutely calibrated. The primary reason for this is that visible counts have different physical meanings for DMSP and NOAA satellite sensors. For OLS, visible counts are proportional to upwelling reflected solar energy (Heacock, 1985). For AVHRR, visible counts are linearly proportional to percent albedo (Kidwell, 1988). Thus, to more precisely characterize the physical meaning of each data source the following naming conventions are adopted for this report: references to AVHRR visible data are termed albedo, while all other sources of visible data are referred to as visible counts. All nephanalysis algorithms described in this document expect visible satellite sensor data to conform to these conventions.

2.1.1 AVHRR Visible Sensor Data Calibration

AVHRR visible and near-IR data were calibrated according to the procedures published by Kidwell (1988). Sensor counts are converted to a percent albedo using a linear function:

$$A_i = S_i X + I_i \quad (2-1)$$

where A_i is the percent albedo for channel i , X is the sensor count reported in the telemetry data stream, and S_i and I_i are calibration coefficients established prior to launch. Percent albedo is defined as the ratio of effective scene radiance measured by the sensor to the effective radiance that would be measured from a 100% reflecting diffuse surface at a solar zenith angle of 0° . To convert from percent albedo to radiance the albedo values are convolved with the sensor response function. This is done numerically as follows:

$$I_i = A_i \left(\frac{F_i}{100\pi W_i} \right) \quad (2-2)$$

where I_i is spectral radiance in ($\text{W m}^{-2} \mu\text{m}^{-1} \text{ster}^{-1}$), F_i is the solar radiance integrated over the response function of the sensor (W m^{-2}), W_i is the width of the response function (μm), and i indicates AVHRR channel (1 or 2). Tabular values for the AVHRR visible and near-IR channel calibration and sensor response coefficients are provided by Planet (1988).

OLS visible data are proportional to upwelling reflected solar energy and are not absolutely calibrated following launch (Heacock, 1985).

2.2 Infrared Sensor Data

In contrast to visible sensor data, infrared radiance measurements from all platforms are required to be absolutely calibrated and subsequently converted to equivalent blackbody brightness temperature (EBBT). Throughout this document the term "brightness temperature" is treated as synonymous with EBBT. Calibration is performed differently for the individual sensors but generally requires a linear calibration function to convert IR counts to radiance. Conversion to EBBT is then performed by inverting the Planck function over the bandpass-weighted spectral range of each infrared sensor channel. The exception to this convention is the DMSP OLS sensor which performs calibration and data conversion onboard the satellite and then transmits an 8-bit IR count that is linearly proportional to

brightness temperature. Note that for surfaces where the blackbody assumption is not correct (i.e., emissivity less than 1.0), computed brightness temperatures can be significantly different than the physical temperature of the surface being viewed. This phenomena is recognized and addressed separately by the individual analysis algorithms (see Sections 5.1 and 5.2), and can be useful for discriminating between different types of clouds and background surfaces. Other factors in addition to surface emissivity, such as atmospheric attenuation, can also result in satellite-derived brightness temperatures that are different from the actual temperature of the viewed surface. These conditions are addressed in Section 4.2.

2.2.1 AVHRR Infrared Sensor Data

AVHRR mid wave and long wave IR data were calibrated following the procedures of Planet (1988). For all three IR channels a two-point linear calibration is performed to convert reported sensor counts to radiances and finally to equivalent blackbody brightness temperatures. The response of the channel 3 sensor is taken to be linear with radiance and the two-point calibration is sufficient; however, for the channel 4 and 5 detectors, an additional second-order, nonlinear calibration step is required. The two-point calibration is performed based on sensor measurements of an onboard hot source and cold space once every five AVHRR HRPT scans. The hot source is monitored by four redundant platinum resistance thermistors (PRT). Initially it is necessary to convert PRT counts to temperature for each thermistor:

$$T_i = \sum_{j=0}^4 a_{i,j} \bar{X}_i^j \quad (2-3)$$

where T_i is the temperature measured by thermistor i , $a_{i,j}$ are conversion coefficients determined from a pre-launch calibration, and X_i is the reported count. A weighted average of the four thermistors is used as the hot source reference temperature:

$$\bar{T} = \sum_{i=1}^4 b_i T_i \quad (2-4)$$

where b_i is the weighting coefficient for PRT i , also determined prior to launch. To perform the calibration, the measured hot source temperature is converted to radiance by convoluting the Planck function with the sensor response function. This is done numerically through:

$$I(\bar{T}) = \frac{\sum_i B(v_i, \bar{T}) \phi(v_i) \Delta v}{\sum_i \phi(v_i) \Delta v} \quad (2-5)$$

where I is the equivalent spectral radiance that would be measured from a blackbody having a temperature of \bar{T} , $B(v_i, \bar{T})$ is the calculated Planck radiance at wave number v for a temperature of \bar{T} , $\phi(v_i)$ is the measured response function of the sensor at wave number v_i , and Δv is a wave number interval suitable for the numeric integration. In practice v_i and $\phi(v_i)$ are provided by NESDIS in published tables (Planet, 1988). Once the hot source equivalent radiance has been computed, the linear calibration coefficients (g and h) for each IR channel can be calculated directly:

$$g = \frac{I(\bar{T}) - I_{sp}}{\bar{X}_T - \bar{X}_{sp}} \quad (2-6)$$

and

$$h = I_{sp} - g \bar{X}_{sp} \quad (2-7)$$

where I_{sp} is radiance from deep space (3 K), and \bar{X}_T and \bar{X}_{sp} are average sensor-measured counts for the hot source and cold space respectively. \bar{X}_T and \bar{X}_{sp} are averaged over some number of scan lines (generally 10) to minimize the effect of any noise in $I(T)$ or the sensor measurements. The coefficients are applied to the measured count for each pixel to compute a scene radiance:

$$I(X) = gX + h. \quad (2-8)$$

For channel 3 data the scene radiance is immediately converted to a brightness temperature by inverting the Planck function.

As stated above, an additional second-order nonlinear correction is necessary to correctly compute the channel 4 and 5 radiances. NOAA provides tables for the correction values based on laboratory calibration measurements made prior to launch (Planet, 1988). Tabulated values are provided as brightness temperature corrections that are to be applied to the temperatures obtained from the first-order calibration above. Correction factors are derived from a quadratic fit to the instrument calibration response at 10 K intervals over the range 205-325 K for a range of internal hot source temperatures between 10 and 20 C. For TACNEPH, the non-linear corrections are applied by first converting the tabulated temperature values back to radiance using Eq. 2-5 and then fitting a quadratic to the resultant values. The non-linear corrections are applied to the channel 4 and 5 radiances obtained from Eq. 2-8, and the corrected radiances are then converted to brightness temperatures.

2.3 Mission Sensor Data

In addition to imagery channel data described above in Section 2.2, TACNEPH requires use of microwave data from DMSP SSM/I and SSM/T mission sensors.

2.3.1 SSM/I

The SSM/I is a passive microwave imager used to estimate various geophysical properties of the Earth and atmosphere including surface skin temperature, ice and snow cover, soil moisture, precipitation, and precipitable water. It has seven channels: 19V, 19H, 22V, 37V, 37H, 85V and 85H GHz. The SSM/I uses a conical scan which results in footprints that have the same spatial dimensions across the scan for a given frequency.

2.3.2 SSM/T-1

The SSM/T-1 is a passive microwave temperature sounder used primarily to provide temperature and pressure height profiles of the atmosphere. T-1 also has seven channels: 50.5, 53.2, 54.35, 54.9, 58.4, 58.825, and 59.4 GHz. The 50.5 GHz channel is an atmospheric window channel. Each subsequent channel has greater sensitivity to higher altitudes in the atmosphere, up to 30 km for the 59.4 GHz channel.

2.4 Earth Location

The TACNEPH database was set up such that orbital parameters are not maintained for each satellite scene (in some cases, depending on the source of the satellite data, they were not even available). Therefore, to provide the required Earth location information it is necessary to maintain separate latitude-longitude (LL) files for each scene. These files are produced automatically during sensor data ingest and are maintained in the same spatial projection as the sensor data but at degraded spatial resolution. A linear run-time interpolation technique is used to access the LL files and calculate the location of each pixel. For the operational implementation of the program the only requirement is to provide Earth location information on demand for each analysis location. This requirement holds regardless of whether the data are pre-registered to a standard grid or left in scan projection. In either case it is not necessary to duplicate the LL file scheme used in the development program.

2.5 Sun - Satellite Geometry

Similar to the Earth location information described above, satellite and solar zenith angle and sun-satellite azimuth angle data must also be provided for each analysis point. Figure 1 provides a schematic representation of the angle definitions. These angles are used to classify solar illumination conditions and to characterize sun glint in visible reflectance data. Like the LL files, the angle data are maintained in separate files generated during the sensor data ingest operation. They are also carried at reduced spatial resolution and are retrieved using a linear run-time interpolation routine. Again, the only requirement that affects the operational implementation is a capability to retrieve the angle data for each pixel on demand.

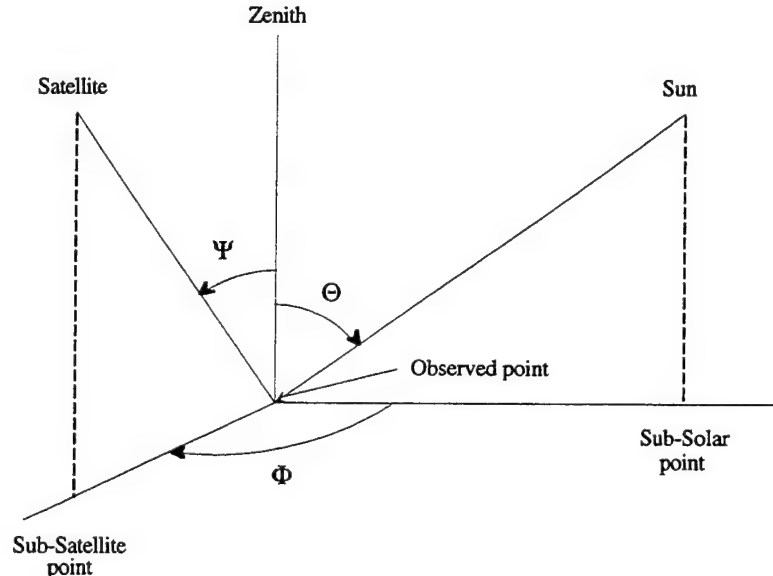


Figure 1. Satellite-earth-solar geometry (after Taylor and Stowe, 1984);

Ψ - satellite zenith angle, Θ - solar zenith angle, and Φ - azimuth angle.

2.6 Climatology Databases

Information on the radiating temperature of the terrestrial background is needed for cloud detection schemes and background characterization. The only database available on the Mark IV-B that provides any information on surface temperature is a global "surface temperature" climatology. For the TACNEPH program, a surface temperature database was obtained from the Air Force Environmental Technical Applications Center (ETAC) that is believed to be the same as that available in the Mark IV-B database. The information we have received about this database is that it was compiled from RTNEPH surface temperature data over a multi-year period and is representative of shelter, rather than skin, temperatures (personal communication, James T. Bunting). These data are maintained at a resolution of 0.1 K and are comprised of monthly average temperatures at three-hour intervals (i.e., 0, 3, 6, 9, 12, 15, 18, and 21 UTC) stored on an 8th-mesh grid. Temperature data are retrieved from the database by identifying the 8th-mesh grid box that contains the target pixel and then time interpolating to match the observed sensor data. Additional information on the use of surface temperature data is provided in Section 4.2.

2.7 Geography Database

Geography data are needed to characterize the background conditions for several of the cloud detection tests. Of particular importance is the boundary between land and water backgrounds. Highly reflective surfaces such as snow, ice, desert, and sun glint also have significant impact on any tests that rely on measurements of reflected solar energy for a signature. The geography database developed for TACNEPH provides a characterization of the background type at 10 arc-minute resolution. Background types include ocean, lake, land, coast and desert. While it is recognized that this database does not currently exist on the Mark IV-B, it could easily be made available and should be considered for transition along with the TACNEPH algorithms. If available a higher resolution database approaching satellite sensor resolution, with specific emphasis on accurate placement of coastlines, would significantly improve the overall cloud analysis.

2.8 1000-mb Height Profile Database

A 1000-mb height database is required for the retrieval of atmospheric temperature height profiles using SSM/T-1 microwave sounder data. This profile is in turn used to specify cloud height. The 1000-mb database was available for development purposes as part of the Sea Space DMSP ground station system on site at the Phillips Laboratory.

3. TACNEPH DATABASE

Database related work (Task 1, Table 1) was a major effort during TACNEPH. The basic requirement was to emulate the relevant database capabilities that would be available in a tactical terminal, particularly as they relate to satellite sensor data. This was necessary to handle the large amount of data required to support algorithm testing and validation (see Section 5.3). All work was performed on the AIMS computer system which had only rudimentary satellite database capabilities at the start of the program. Database management as it applied to TACNEPH involved three separate functions:

- 1) data ingest (data unpacking, calibration, Earth location);
- 2) database organization (query, retrieve, add, modify, delete); and
- 3) data visualization (image processing, interactive evaluation and testing, and synthetic image rendering).

Data ingest was handled on an ad hoc basis for each separate source of data and as such is not generally applicable and will not be detailed here. However, there has been considerable interest in the database management and visualization functions expressed at numerous TACNEPH program reviews, so descriptions of these functions are provided.

3.1 AIMS Database Management

AIMS database management work was performed under Task 1.1 (Table 1). The goal of this task was to modify existing, and to develop new, AIMS database management software to support and maintain the TACNEPH data file suite. For this task it was first necessary to specify the database requirements in terms of the types and volume of data that needed to be handled, how the data were to be used at the user-application level, how and where to store it, and how to optimize data access while minimizing the impact on user applications.

Three major types of satellite data are of concern to the TACNEPH project. The foremost is satellite imagery, encompassing raw sensor data measured by visible, infrared, or microwave detectors onboard an orbiting satellite. The second is imagery-supporting data, including Earth location, sensor calibration, and viewing geometry information. These data compliment the imagery data by providing ancillary information that is known at data collection time but not directly stored or encoded with the imagery data. The third data type is analysis data. Generally, when sensor data are processed through a cloud analysis algorithm, pixel resolution product data are generated. As an example, a given analysis data file might contain information describing which pixels of a given multi-channel scene are classified as cloudy. Another analysis might form a more generalized result, or only represent subsets of imagery data. The results for these and other user-specified analysis products compliment the imagery data in the same manner that the supporting ancillary data do and, as such, are logically tied to the input imagery database files by the database manager.

For TACNEPH a database management strategy was developed that addresses multiple requirements. The amount of data handled in the TACNEPH effort is large. Data from one pass of a multi-channel polar-orbiting satellite can easily occupy 30 to 40 megabytes of storage space, even before any ancillary or analysis data have been generated. A unique unit of data had to be defined such that accessing of data by user applications would not cause conflicts or aliasing with other data in the database. The storage strategy had to support migration of data from one physical media to another. Migration of data implies that the user could move the actual location of the raw data sets (for, say, space allocation concerns) without any impact on the functionality of applications that use the data. A method for storage and retrieval of data from the entire database was engineered such that both permanent and removable media could be used in a manner transparent to any user applications. The removable media encompasses the same file structure as the permanent storage hardware currently residing with the AIMS systems.

Once a strategy for storing data was established, a method for accessing the data was devised. Providing the applications user with a list of all data-directories and disks containing information about what sensor data is available places a heavy burden on that user. A linearly organized list of all raw data sets is a minimal asset when the data list is large. In order to manage the data as a resource shared by many users at all levels of investigation and research, it became essential that information about the data be clearly specified and defined, easily accessible, and well-controlled.

There is much ancillary and inferred data that describes imagery data such as the observing satellite, location, time, and other information that can assist a user to identify and access required data. Metadata are a specialized type of information used to describe large data sets that can be encoded in a compact computer-readable form for optimized storage processing and end user availability. A series of metadata databases were developed to describe the large volumes of raw data for the TACNEPH.

Two software products were designed, developed, and implemented in accordance with the above requirements. They consist of a low-level user library of metadata management routines, and a high-level metadata scanning utility. A software library consisting of numerous database management routines was developed, and fully implemented on the AIMS cluster. These routines operate on metadata that describe the contents of the entire TACNEPH data set. The routines are low-level, that is, a user may call any of these modules from a variety of applications. Each low-level routine has a single, well defined function. Status codes are used to report the success or failure of specific operations and are the only control information passed back to the calling application. As such these low-level routines do not exert control over the operation of a calling application.

The high-level utility was developed to perform search and retrieve operations on the combined metadata databases from the command line. This utility serves as a front-end product to the applications user, in many cases eliminating the need for application specific software development. It is used to search and sort through metadata records from some or all metadata databases for information about specific records, or groups or records to retrieve information on database entries that match specified criteria.

3.1.1 Database Management System Design

The TACNEPH database management system (TDB) was designed to satisfy both data-storage and relational data-management requirements. In addition to the project-imposed requirements discussed in Section 3.1, the AIMS computer systems imposed their own set of requirements on the database design. Left unchecked, the volume of data represented by the TACNEPH data set would overwhelm AIMS resources and make it unusable to the other research efforts concurrently dependent on this system. Further, the TACNEPH data set is dynamic and open-ended forcing the database management strategy to incorporate expansion and adaptability to increasing volumes of data, especially as those volumes increase rapidly. To address these issues a requirement that the database implementation allow for removable storage media was imposed. This requirement was satisfied via the use of optical disks.

The data to be used for the TACNEPH project is scan-formatted multi-channel satellite imagery with supporting Earth location ancillary data. To facilitate processing and exploit the natural organization of the sensor data, all data are maintained in scan line format. One file is created for each imager channel, another for earth-location data, and another for additional scan geometry information. For an average case which covers roughly 15 minutes of high-resolution coverage, one set of files occupies approximately 35 megabytes of disk space. Supporting data are stored in formats specifically developed for TACNEPH applications.

In considering the problem of how to physically store all types of TACNEPH data, a single data entity that conceptualized the smallest common denominator for all data types had to be defined. That unit was determined to be the case-study day. With this definition of a data unit, a method for the actual storage of data evolved. The method is as follows:

under a generic disk name a directory structure is created that contains a series of subdirectories. These subdirectories are named in accordance with the Julian date corresponding to the valid time of the satellite data. The files contained within these subdirectories are uniquely named to reflect both the origin of the data (i.e., which satellite and sensor collected the data) and the site over which the data was taken. An example of a directory listing for a TACNEPH data subdirectory is provided below:

Directory of TDB\$DISK:[TACNEPH.DATA.<YYYDDD>]:

```
N12_001_JAM_121_13.DAT
N12_002_JAM_121_13.DAT
N12_003_JAM_121_13.DAT
N12_004_JAM_121_13.DAT
N12_005_JAM_121_13.DAT
N12_LAT_JAM_121_13.DAT
N12_ANG_JAM_121_13.DAT
N12_001_ALB_121_13.DAT
N12_002_ALB_121_13.DAT
N12_003_ALB_121_13.DAT
N12_004_ALB_121_13.DAT
N12_005_ALB_121_13.DAT
N12_LAT_ALB_121_13.DAT
N12_ANG_ALB_121_13.DAT
```

Note that in the example "TDB\$DISK" is a logical definition pointing to the specific disk on which the data directory structure resides. TACNEPH.DATA is the generic data directory structure and <YYYDDD> is the date of the observation. The file names are unique mnemonics that not only identify the file, but the satellite, data type, location, date and time of observation. This allows for multiple cases observed during a single day to be stored in the same directory, uniquely. In this sample directory listing, there are files from two separate data runs, taken on the same day, but over different locations.

The disk name and data directory structure are important to execution of the second part of the storage strategy. Under VMS, a disk name is a logical representation of an actual device. If this device is formatted in the Digital Equipment Corporation (DEC) Files-11 standard, then the device can be accessed in a consistent way independent of the type of medium used. At the beginning of this project, several erasable optical disk drives were installed on the AIMS cluster to exploit this format convention. The optical drives use removable disks that store 600 megabytes of data, and can perform access operations at speeds comparable to those of the permanent hard drives installed on the cluster. Using logical names instead of physical disk names, and adhering to the Files-11 standard, provides a method for implementing a generic storage strategy over multiple media types, independent of their type (e.g., removable vs. non-removable), that is invisible to the applications user. Supporting software was developed to inform the user whether loading an optical disk is necessary to run an application. Everything else about the storage structure (e.g., data sub-directory) is independent on the actual location of the data and thus transparent to the user.

3.1.2 Database Structure

The next stage of the design addressed data access. This was solved through use of a relational metadata database model. The management of all the data sets of the types described in Section 3.1 is handled by a collection of metadata files. All data management

software acts only on the metadata files which are maintained separately from the sensor and supporting data files.

Recall that metadata describes a specific class of data that are used to describe other data. Typically, metadata records are much smaller than the units of data they describe. For example, a satellite image requires tens of megabytes, however, the information that describes the data (e.g., location, time, satellite...) typically only requires a few tens, or at most hundreds, of bytes. For TDB, metadata files are organized based on the information content inherent in each data set. For example, separate metadata files were created to describe imagery and supporting data. The metadata are permanently associated with the data file they describe by the database management software. Supporting data are linked to the appropriate imagery data by relations inherent in the metadata entries.

When gathering metadata entities to be used in a data management strategy, the organization of these entities becomes important. Randomly organized metadata are of no more use than randomly organized raw data sets. For the TACNEPH application, the organization of metadata entities into conceptual units was necessary. These units are referred to as (meta) data dictionaries. For TACNEPH, satellite imagery and supporting data are described by metadata entries in a data dictionary. Each set of entries describes one database entry (i.e., one data file), and each dictionary describes one type of data (e.g., imagery, supporting). In the TACNEPH implementation of this design, the data dictionaries are themselves organized in a relational manner, thus providing the logical links between different types of data. Each of the data-dictionaries are described in brief below:

The CORE data-dictionary contains the minimal set of metadata elements which can describe every physical data object (i.e. image file, analysis file) registered in the TACNEPH database. Its primary function is to provide a link to every piece of data in the TACNEPH database.

The SATIMG data-dictionary contains metadata elements which describe imagery files in the TACNEPH database. Parameters such as number of rows, number of columns, and number of bit-planes are stored in these meta-records with reference links to associated non-imagery data objects in the TACNEPH database.

The ANGLES and LATLON data-dictionaries contain metadata elements which describe scene/satellite-geometry and geopositional files in the TACNEPH database. Parameters such as satellite orientation, sensor footprint, and subsampling resolution are stored in these meta-records with reference links to associated non-angles/non-latlon data objects in the TACNEPH database.

The PRODUCTS data-dictionary contains metadata elements which describe analysis files in the TACNEPH database. The parameters in these dictionaries vary depending on the type of analysis being tracked by the database. Reference links to all the associated raw data (imagery, angles, latlon, etc.) used in generating the analysis are also tracked.

The COMMENTS data-dictionary contains subjective user-comments associated with a single entry in the TACNEPH database. There is no limit to the number of individual comments that can be tracked by the TACNEPH database software.

The CORE data-dictionary contains entries for every data object in the TACNEPH database. The other data-dictionaries contain entries for unique sub-sections of the database, but are linked with associated database entries such that a query made on any of these data-dictionaries will guide the retrieval application to the appropriate data. The power of this design becomes apparent when one considers the problem of accessing a

specific data file. Assume one data file occupies 30 MB and the database contains 100 images of this size to track. A metadata database-record that contains information about one of these images would require no more than a few hundred bytes. A metadata database containing records for 100 images would require only a few kilobytes of storage space. It is likely that even a purely random search of the metafiles would be fast enough to satisfy most applications while any type of search of the raw data files would probably be prohibitively long. This becomes even more apparent given the distributed nature of the TACNEPH data set. The TACNEPH database structure is a collection of organized metadata data-dictionary files. All data dictionaries are maintained on-line in a centralized location while the data files themselves are distributed and can be located anywhere including off-line media. Optimization of the search and access process is attained through organizing the data dictionaries based on the most common query parameters.

The TACNEPH database functions on a one-to-one (or linear) relational model. The linear model offers uniqueness such that every member of the data set is represented by a separate, rudimentary data dictionary entry. In the TACNEPH application, there are various classes of raw data sets to be organized. Each of these can be described by metadata, but results in a collection of metadata groups that themselves require an organization strategy to optimize their usefulness. A database management design that enhances the robustness of a (single) relational metadata model was sought to impose a structure on the evolving groups of metadata. This was accomplished through the introduction of a high level core data dictionary that provides the relationships between the lower level dictionaries.

The "atomic-unit" of the TACNEPH data set is the individual data file. The atomic-unit of the TACNEPH database is an individual core data-dictionary meta record. The core dictionary file contains entries for all data files in the database. Each entry has a unique entry number and contains metadata describing the I/O characteristics of a single data file independent of type. Lower level dictionaries (i.e., SATIMG, LATLON, ANGLES, PRODUCT, COMMENT) describe data-specific characteristics of only one type of data file (imagery, earth location, satellite geometry, analysis data). For example, sensor data obtained from a single OLS pass generates a number of entries in different data dictionaries. Five entries in the core dictionary are made since there are five data files from this pass to track (visible and IR sensor channel data plus LATLON, ANGLES, and PRODUCT data). The visible and infrared data are described by two entries in the SATIMG dictionary. The metadata which describe this pass in the SATIMG dictionary include: the satellite and sensor type, the number of rows and columns in the image, the image resolution (km/pixel), offset information for mapping software, and time stamps for both the time of ingest and time of orbital pass. Earth location and scan geometry data associated with the pass are described in the LATLON and ANGLES dictionaries respectively. It should be noted that unlike imagery data which are stored at pixel-level resolution, earth-location and satellite geometry data are not required at such high resolution and thus are stored at a sub-sampled resolution to minimize mass storage requirements. The sampling frequency varies with the satellite type. Sub-sampled data are interpolated at run time when pixel-level data retrievals are processed. The impact on processing performance and positional/geometric accuracy has been minimal. Metadata in these dictionaries include information on the sampling frequency of the data, and any positional shift in the data imposed on interpolation routines.

Derived analyses files are described in the product dictionary. The metadata in this dictionary describe characteristics that are similar to the SATIMG and core dictionaries, but also take into account the multiple occurrence of analyses per single data entry in the other data dictionaries. User comments can also be registered about this pass in a comment dictionary. All of these data files are also registered in the core data dictionary. One dictionary is distinguished from another by the information they contain.

The core dictionary provides pointers between the various data dictionary entries that are all related to the same pass. For the TACNEPH application, this is a very powerful design for several reasons. When searching through multiple related data dictionary entries only limited information on one specific data type can be obtained from a single data dictionary. Complete descriptions of the entire related data set can only be obtained by accessing all related metadata dictionaries. To facilitate this process all data dictionary files are organized using a file structure known as Indexed Sequential Access Method (ISAM). ISAM provides a format for rapidly accessing individual entries based on a specified descriptor known as a key. In TDB, each database entry is assigned a unique entry number. In all cases the dictionary files use the entry number as the primary key. For a given set of related data files, the core dictionary maintains the entry numbers for all related entries in the various lower level dictionaries. Thus, from any data dictionary, access to any other related dictionary entry is straight-forward and direct through a query of the core dictionary for the related entry number. Keyed access of data is a property of the VMS operating system that is handled well. The combination of robust design and the existence of VMS tools that allow its easy implementation made this solution an attractive one for TACNEPH.

3.1.3 TACNEPH Database Implementation

The TACNEPH database was successfully implemented on AIMS and used extensively for several years to handle both real-time and retrospective data. All software was developed using the required VMS FORTRAN-77 programming language and making extensive use of VMS specific utilities and programming libraries. A hierarchy of data dictionaries was used to organize the descriptor data by category. Table 4 provides a description of the data dictionaries. Metadata dictionary files are organized into primary and secondary databases. A primary metadata database is one that contains unique indexed entries related to other data dictionaries along structured hierarchical lines which converge at the master (core) database. A primary descriptor entry would describe attributes for only one entry in the core database, and thus is distinguishable along the primary index of the core data dictionary. A metadata database of secondary design is one that contains non-unique (related) indexed entries that may be associated to multiple other databases (primary or secondary). An example of a secondary database is a user comment database. Multiple comments might describe a common core database entry, and thus are not distinguishable along the core database's primary index.

Table 4. TACNEPH Database Data Dictionary Descriptions

Name	Description
CORE	Contains list of related data dictionary entries and file access information
SATIMG	Describes imagery files generated from satellite sensor data
LATLON	Describes files containing Earth location information
ANGLES	Describes files containing satellite scan and solar geometry information
COMMENT	Contains anecdotal information provided by research scientists and users
PRODUCT	Describes files containing analysis algorithm results

In the TACNEPH database application, the structure of the primary and secondary databases serves to order and control the organization of metadata. The structural hierarchy of the primary databases defines the data flow control for search and retrieval algorithms. This structure orders the complete metadata about a given data object by most important and relevant qualities. The non-hierarchical structures between secondary and primary

databases act as operators on the primary metadata. Secondary data are incomplete by themselves but can operate on any primary database anywhere within the hierarchy tree and augment the information content of the primary metadata. For example, when a user comment about a particular image is accessed, it signifies relatively little objective information. However, when combined with a related primary metadata field, the comment augments that objective information by providing a subjective depth. As such, secondary databases may operate on any level of primary metadata, but provide little or no objective information by themselves.

3.1.4 TACNEPH Database Summary

Requirements for the TACNEPH database management task were satisfied through the development of a dynamic, relational database management and storage capability; a low-level database-management software library; and a high-level utility program. The relational database and its associated management strategy optimally represent and control large sets of meteorological data, and support database growth as a part of its design. The low-level software library is a collection of independent modules that manage the TACNEPH metadata data dictionary files. The high-level application program is a user-interface to the metadata files that assist the user in making informed and rapid queries into the contents of the TACNEPH data sets. The application is open-ended to allow for expansion of the data types to accommodate future needs of the TACNEPH database.

3.2 Image Processing and Display

In support of the image processing and cloud analysis tasks, software interfaces have been developed to tie products developed for these tasks into the database management structure. Image processing and display functions include programs to selectively query the database and load satellite imagery and analysis products onto a display device, functions to manipulate the imagery data, and a program to assist with manual analysis of satellite imagery data.

An image display utility called TLOAD loads user-specified areas of an AVHRR or OLS image into Adage memory. The utility takes advantage of the TDB interface modules which were designed to return platform-specific information to an application which calls them. In this case, the number of channels which are associated with a particular satellite are loaded as 8-bit gray shade images into specific areas of Adage refresh memory, in an order which will also support display of multispectral color composites. Intermediate results from a cloud analysis algorithm are also loaded as an 8-bit synthetic image in the overlay planes of Adage memory. Each of the cloud and background tests is represented as a different color in overlay memory and can be viewed separately using an image manipulation and data retrieval program called BIT_TOGGLE. TLOAD and BIT_TOGGLE make extensive use of high level TDB utilities for fast, easy access to data and analyses.

BIT_TOGGLE provides an interactive utility to manipulate and display satellite imagery and analysis algorithm results quickly and easily. It was used extensively during the cloud algorithm test and evaluation phases of the project described in Section 5.3. The main program feature is a user interface that combines keyboard and mouse-driven features to obtain information about the imagery on a pixel level, such as earth location, satellite brightness temperature or visible count, or corresponding surface temperature climatology values. BIT_TOGGLE display capabilities include rapid toggling through different channels of display memory to view imagery from different sensor channels, full-color multispectral display techniques to distinguish different types of cloud and background surfaces (see d'Entremont et al., 1987), and display of individual color-mapped cloud test results over

single channel and multispectral composites. By altering the selection of individual planes, an analyst can evaluate the algorithm intermediate results for a particular region of interest.

Validation of algorithm results required the manual analysis of a large set of satellite images (see Section 5.3.2). An interactive program called TBLANK was developed to assist the analyst in this process. Visualization of sensor data is controlled through a set of fast interactive person/machine functions that support both single channel gray shade and full color multispectral display, image enhancement, segmentation and thresholding. Actual delineation of cloud boundaries is accomplished through a technique known as threshold blanking. Here the analyst selects a region of interest, displays the sensor data in whatever format allows for optimal interpretation, and interactively raises or lowers a pixel intensity threshold to separate cloud-filled from clear pixels. The threshold can be either coarsely or finely adjusted until it accurately delineates the cloud boundary as determined by the analyst. The magnitude of the threshold level is viewed as a user selectable color shading of the image. For example, if the analyst chooses, say, a green shade then pixels with intensity levels below the threshold are displayed as shades of green while pixels above retain their original color shading. Thus, the analyst can easily see where the threshold level is set without obscuring any features with intensity levels above or below that level. The size and sensor channel selection for each Region of Interest (ROI) are completely at the control of the analyst and can be changed at any time during the process. Normally the analyst segments an image many times using different thresholds and channel combinations depending on the diversity of the cloud and background conditions, thus, the process tends to be iterative. Threshold blanking has been found to be a fast and highly accurate method for transferring an analyst's interpretation into a digital form.

4. CLEAR-SCENE BACKGROUND CHARACTERIZATION

The TACNEPH algorithm generates two internal databases that provide statistical information on the visible and infrared characteristics of the cloud-free background. They comprise clear-scene statistics that are required for discrimination of cloud-free from cloud-contaminated radiative signatures in single channel cloud tests used in both the OLS and AVHRR cloud algorithms. Table 5 summarizes the required internal databases used to characterize the cloud-free background. The data must be stratified by satellite and time of day (i.e., separate clear-scene statistics for ascending and descending orbits of each satellite). The infrared statistics are used indirectly to adjust the surface temperature climatology values in order to predict the AVHRR channel 4 and OLS/T brightness temperatures that would be measured under cloud-free conditions. The visible statistics are used directly for comparison with the measured visible counts (OLS) or albedo (AVHRR). During the TACNEPH development program, algorithm testing and validation was performed over numerous ROI that were boxes that ranged from a few hundred to approximately 1000 km on a side (see Section 5.3 for a description of the ROI regions). Clear-scene statistics were maintained separately for each ROI to individually characterize the natural variability of the measured satellite data under cloud-free conditions. In the tactical terminal implementation, it is likely that a single set of statistics will be sufficient for the entire tactical area unless there is a well-defined boundary between substantially different background types, such as a coastline. In that case it would be necessary to generate two separate statistical databases, one characterizing the land surfaces and the other characterizing water surfaces. This type of situation can be readily automated through use of the TACNEPH geography database to discriminate the two classes. This was in fact done in the research algorithm whenever a given ROI contained a significant fraction of both land and water surfaces. Further discussion of background stratification can be found in Section 5.3.1. The visible and infrared statistics databases are described in Sections 4.1 and 4.2, respectively.

Table 5. Clear-scene Internal Database Characteristics

Type	Resolution	Projection	Description
clear-scene IR statistics	ROI		history of LWIR-T _{clim} differences
clear-scene visible statistics	0.1°	lat/lon	clear-scene albedo normalized by BRDF

4.1 Clear-Scene Visible Databases for OLS and AVHRR

Reference clear-scene background visible channel data are required for the single channel visible or near-IR reflectance tests in the OLS and AVHRR algorithms. Visible/near-IR clear-scene data are processed in a manner similar to the RTNEPH background brightness database. For each ROI a separate database of clear-scene albedo is maintained for each daytime satellite overpass time. The data are maintained over a regular latitude - longitude grid with an interval of 0.1 degrees and are updated continuously as new data are received. Clear-scene information is produced from by-products of the cloud analysis algorithms. As satellite data are received and analyzed through the appropriate nephanalysis algorithm, two passes through the algorithm are performed: 1) cloud detection, and 2) cloud clearing (see Section 5). In cloud detection mode, algorithm thresholds are set to provide an optimal analysis with no preference toward over or under-analysis of cloud. In cloud clearing mode, cloud thresholds are set with a bias toward over-analysis to insure identification and removal of all cloud-contaminated pixels. In the current implementation of the algorithms, the clear scene information obtained from cloud clearing is used to update the databases for the next satellite pass rather than the current analysis. Some small benefit may be gained by updating the databases prior to performing the cloud detection part of the current analysis.

For each 0.1 degree grid box, all clear-scene pixel values are accumulated separately for the OLS-L and AVHRR channel 2 and the mean count (OLS) or albedo (AVHRR) value is calculated. For the AVHRR, the mean albedo is then normalized by an anisotropic reflectance factor (ARF) to adjust for the effect of different relative solar and satellite angles across the scene:

$$A'_i = A_i / \text{ARF}(\psi, \theta, \phi, M) \quad (4-1)$$

where A_i and A'_i are the measured and normalized albedo for channel $i=1, 2$, respectively, M is the Geographic Type of the background surface (i.e., land or water), and ψ , θ , and ϕ are the satellite zenith, solar zenith, and sun-satellite azimuth angles, respectively. Evaluation of the ARF function is performed through look up tables published by Taylor and Stowe (1984). The ARF function is not applied to the OLS data because on-board satellite gain controls are designed to perform this same function. Clear-scene data are filtered through a 60° solar zenith angle threshold to insure only daytime data for which ARF values are available are processed. To ensure that cloud contaminated data does not corrupt the database, new information is added only if the value does not exceed the magnitude of the stored value by more than 0.1 (new data can be darker by any amount). The database is updated using a weighted average of the previous value and the new normalized albedo:

$$V = 0.25 V' + 0.75 V \quad (4-2)$$

where V is the stored clear-scene visible count or normalized albedo and V' the newly measured value. The gross fidelity of this database can be established easily by displaying the data as an image.

4.2 Clear-Scene Infrared Databases for OLS and AVHRR

The AVHRR and OLS cloud algorithms both include a single channel infrared threshold test and as such require estimates of clear-column satellite brightness temperatures to discriminate cloud-free from cloud contaminated radiative signatures. In the TACNEPH program, the only database providing any information related to clear-column brightness temperatures is the Surface Temperature Climatology database described in Section 3. The required predicted clear-scene satellite brightness temperatures are computed using a dynamic correction to the climatology database. The correction accounts for the combined effect of the multiple error sources that can occur when using a fixed climatology of shelter temperatures to predict a satellite derived clear-scene brightness temperature. Of particular concern are shelter temperatures that are not representative of bandpass-weighted satellite infrared brightness temperatures, differing spatial resolutions between the climatology and satellite derived data, satellite sensor calibration errors, and the effect of IR atmospheric attenuation. Accurate modeling of individual errors, let alone their combined effect, is problematic so the approach selected for TACNEPH uses a single correction factor to account for all error sources collectively.

The calculation of the predicted brightness temperature that would be observed by a satellite from the cloud-free terrestrial background at a given location and time is performed as part of the cloud analysis algorithm; however an internal database of clear-scene infrared statistics must first be generated. The initial step is to compile a ten-day record of the deviation of the climatology temperature (T_{clim}) from the satellite derived temperature (T_{sat}) for locations previously classified as cloud-free. This record is used to characterize the natural variability of the difference between the two temperature values when no cloud is present so that future measurements can be tested to see if they fall within the expected range for clear conditions.

Temperature difference information is maintained as an internal statistical database summarizing the distribution of the temperature differences stratified by location, satellite, time of day, and surface type: land, water, or desert. Statistics are accumulated over the tactical region of interest. Thus, a separate database entry is required for each of the ten days, for each polar satellite, its ascending and descending orbits, and the three possible surface types identified in the geographic supporting database.

As with the visible data described above, cloudy pixels are removed by analyzing the data through the appropriate cloud algorithm run in cloud-clearing mode. Once clouds have been identified and removed from further processing and the difference between the sensor channel brightness temperature and the corresponding surface climatology temperature is calculated for all remaining pixels and used to generate a frequency distribution. Figure 2 illustrates a sample temperature difference distribution developed from 89,763 cloud-free pixels observed during a NOAA 11 afternoon ascending pass over land surfaces in the east central United States.

If $n = 1, 2, \dots, N_i$ is the number of clear pixels from the cloud clearing analysis for some day $i = 1, 2, \dots, 10$ then for each pixel n , the temperature difference (ΔT_n) is defined as:

$$\Delta T_n = T_{sat_n} - T_{clim_n} , \quad (4-3)$$

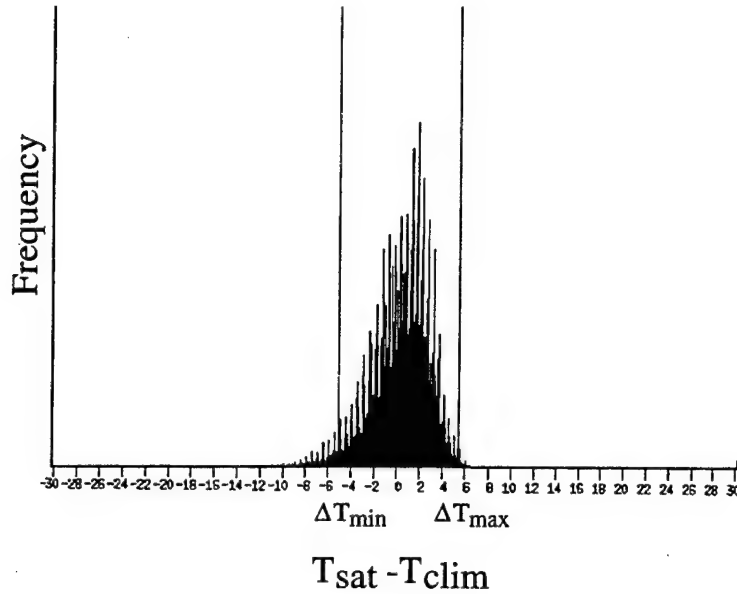


Figure 2. Example histogram of comparison between satellite brightness temperature and corresponding climatology temperature value for 89,763 clear pixels obtained from an AVHRR scene from 1947 UTC on 6 June 1992. Vertical lines represent 2 standard deviations about the mean.

where T_{sat_n} is the OLS or AVHRR brightness temperature of a pixel n and T_{clim_n} is a time interpolated climatology temperature value, derived from the Surface Temperature Climatology database, that corresponds to the time and location of pixel n . T_{clim_n} is defined by first locating the $1/8^{th}$ mesh grid box closest to the latitude and longitude of pixel n (note the AFGWC polar grid convention uses the upper left corner to define the location of a grid box, see Hoke et al., 1981). The two-step time interpolation is used. First, to match the date of the satellite data, and second to match the time of day. The date interpolation is performed to avoid discontinuities in the clear-scene statistics over month boundaries (recall that the three-hourly climatology data are updated monthly). The first step to interpolate the climatology data to the valid satellite date is performed by assuming the climatologies are valid on the 15th of each month. To interpolate to time of day, the two climatology temperature database entries with valid times that bracket the time of the satellite observation are located and the respective shelter temperature values at the specified $1/8^{th}$ mesh grid point are linearly interpolated to the time of the satellite observation:

$$T_{clim_n} = \frac{T_{clim_{t_2}} - T_{clim_{t_1}}}{t_2 - t_1} (t_{sat} - t_1) + T_{clim_{t_1}} \quad (4-4)$$

where t_{sat} is the satellite observation time, t_1 and t_2 are the valid times of the bracketing climatology temperature database entries (i.e., $t_1 \leq t_{sat} \leq t_2$), and $T_{clim_{t_1}}$ and $T_{clim_{t_2}}$ are the respective climatology temperature values for the specified grid box valid at times t_1 and t_2 . The interpolation process is not critical to the clear-scene temperature estimation except that it tends to eliminate artificial boundaries in the analysis when the sensor data passes from one climatological time regime to another (e.g., from one synoptic time to another or over the end of one month into the next).

The general Gaussian shape of the distribution in Figure 2 is typical, therefore it was decided that the range of ΔT_i values found for each day i could be represented using the limits defined by two standard deviations taken about the mean of the temperature difference distribution (labeled ΔT_{\min} and ΔT_{\max} in Figure 2). Thus, the IR Temperature Statistics database contains an historical record of the ΔT values corresponding to the 2σ limits for each location, satellite, orbit, and background combination. For day i the mean difference:

$$\overline{\Delta T}_i = \frac{1}{N_i} \sum_{n=1}^{N_i} \Delta T_n \quad (4-5)$$

and the standard deviation:

$$\sigma_i = \left(\sum_{n=1}^{N_i} \frac{(\Delta T_n - \overline{\Delta T}_i)^2}{N_i - 1} \right)^{\frac{1}{2}} \quad (4-6)$$

are computed and used to define the 2σ limits (ΔT_{\min_i} and ΔT_{\max_i}) that represent the extremes of the ΔT distribution:

$$\Delta T_{\min_i} = \overline{\Delta T}_i - 2\sigma_i \quad (4-7)$$

and

$$\Delta T_{\max_i} = \overline{\Delta T}_i + 2\sigma_i. \quad (4-8)$$

Once the IR-Climatology Temperature Statistics have been accumulated for the previous 10 days they are used by the OLS and AVHRR cloud detection algorithms to help predict the brightness temperature (T_{pred}) that would be measured from the satellite in the absence of cloud for the current time, location and background type. The procedure is applied to the thermal infrared channel data from each sensor (AVHRR channel 4 and OLS-T). First, the satellite data being analyzed are segmented into a series of small analysis regions. During TACNEPH it was set empirically at 16×16 pixels. However, these numbers should be considered a minimum size since testing has indicated that, in practice, it can be increased if necessary to improve computational efficiency. The critical factor in determining the size of the analysis region is whether the spatial variability of the background temperature resolved by the satellite data is captured in the climatology temperature database (i.e., is the magnitude of the temperature variation over the analysis region approximately the same in the climatology temperature database as in the satellite IR channel data).

After the data are segmented the next step is to compute a separate correction factor for each analysis region. Recall that the correction will be added to the $1/8^{\text{th}}$ mesh climatology temperatures to predict the local (i.e., 16×16) clear-scene brightness temperatures. One pixel from the analysis region that is considered most likely to be cloud-free is selected and used to establish a reference satellite-climatology temperature difference value (ΔT_{ref}) for the entire local region. To minimize the likelihood of cloud contamination the reference pixel is taken as the warmest pixel in the analysis region. To avoid using a warm anomaly to establish the reference value, the warmest 1% of all pixels in the analysis region are first

removed before the reference pixel is selected (e.g., for a 16 x 16 region, pixels with the two highest brightness temperatures are excluded). Thus, ΔT_{ref} is defined as:

$$\Delta T_{\text{ref}} = T_{\text{ref}} - T_{\text{clim}} \quad (4-9)$$

where T_{ref} is the brightness temperature of the reference pixel and T_{clim} is the time interpolated climatology temperature corresponding to the time and location of the reference pixel (calculated in the same way as T_{clim_n} in Eq. 4-4).

If the reference pixel can be established to be cloud-free then ΔT_{ref} is used as the climatology temperature correction for its respective analysis region. However, the critical step affecting cloud analysis accuracy is testing of the reference pixel for possible cloud contamination. If the reference pixel does contain cloud then the predicted clear-scene brightness temperature, T_{pred} , will be representative of the cloud brightness temperature and not that of the terrestrial background. Testing of the reference pixel is accomplished by comparing the magnitude of ΔT_{ref} against the range of expected clear-scene temperature differences established from the ten-day IR-Climatology Temperature Statistics. If ΔT_{ref} falls within the expected range, then the reference pixel is assumed to be cloud-free, otherwise it is assumed to be cloud contaminated and a default value is used for ΔT_{ref} . To establish the expected range of clear-scene values a time and frequency-weighted average of the historical clear-scene ΔT limits is used:

$$\Delta T_{\text{min}} = a \frac{\sum_{i=1}^{10} t_i \Delta T_{\text{min}_i}}{\sum_{i=1}^{10} t_i} + b \frac{\sum_{i=1}^{10} N_i \Delta T_{\text{min}_i}}{\sum_{i=1}^{10} N_i} \quad (4-10)$$

and

$$\Delta T_{\text{max}} = a \frac{\sum_{i=1}^{10} t_i \Delta T_{\text{max}_i}}{\sum_{i=1}^{10} t_i} + b \frac{\sum_{i=1}^{10} N_i \Delta T_{\text{max}_i}}{\sum_{i=1}^{10} N_i} \quad (4-11)$$

where a and b are empirically defined coefficients for the temporal and frequency average terms, respectively: the sum of $a + b$ must equal 1.0, currently $a = 0.9$ and $b = 0.1$. The time weighting factor t_i is defined to give greatest weight to the most recent day and decreases as the clear-scene data age. To avoid the use of anomalous data in the time-frequency averaging process, a minimum sample size is required. For data from a given day to be included in the ten-day average, the number of clear-scene data points in the distribution, N_i , must exceed 5000. Any days for which N_i is less than 5000 are excluded from the averaging process and data from the next oldest day are added to the series to maintain the ten-day total. The value of t_i is assigned to 1 for the oldest day in the series and increases in value by the difference in Julian date from the date of the oldest day. For example, if the Julian date for the first day in the series (i.e., $i=1$, $t_1=1$) were, say, 140, and two subsequent days had sample sizes, N_i , of less than 5000 then the Julian date of the tenth day in the series would be 152 and the time weight, t_{10} , would be 12 (152-140).

Thus to calculate a predicted brightness temperature corresponding to any pixel n within the analysis region ΔT_{ref} is first tested for cloud contamination. If:

$$\Delta T_{\min} \leq \Delta T_{\text{ref}} \leq \Delta T_{\max} , \quad (4-12)$$

then ΔT_{ref} is assumed to be cloud-free and is added to the time interpolated climatology temperature corresponding to that pixel as the correction factor:

$$T_{\text{pred}_n} = T_{\text{clim}_n} + \Delta T_{\text{ref}} , \quad (4-13)$$

otherwise ΔT_{ref} is assumed to be cloud contaminated and a default correction based on the mean of the time-frequency weighted average ΔT limits is used to calculate the predicted clear-scene brightness temperature:

$$T_{\text{pred}_n} = T_{\text{clim}_n} + \frac{1}{2} (\Delta T_{\min} + \Delta T_{\max}) . \quad (4-14)$$

As stated above, the predicted clear-scene brightness temperature (T_{pred}) is calculated in exactly the same way by both the OLS and AVHRR cloud analysis algorithms. However, once established it is used differently by each algorithm in the cloud detection process (see Sections 5.1 and 5.2 for descriptions of how the predicted temperature is used in the OLS and AVHRR algorithms, respectively).

4.3 SSM/I Surface Temperature

Microwave data from the SSM/I represent another potential source, in addition to the Surface Temperature Climatology database, for information on clear-scene brightness temperature. An all weather multiple regression algorithm was developed at AFGWC to use SSM/I seven channel radiometer data to estimate OLS IR brightness temperature measurements that would be observed from the terrestrial surface. Since many clouds are transparent at the SSM/I frequencies, this technique has the potential to provide useful information on the clear-scene OLS brightness temperature under both clear and cloudy conditions. This would be potentially very useful to the TACNEPH application since, as described above, accurate information on the cloud-free environment has a first-order impact on cloud analysis accuracy.

The SSM/I algorithm provided by AFGWC is a two-step linear regression algorithm. Both steps use a series of linear coefficients applied to the seven SSM/I channels to retrieve the desired parameters. Since the measured radiance at each channel is strongly affected by the background surface (largely due to variations in surface moisture), the first step characterizes the background surface type into one of 30 categories. Ideally, for each category a separate set of regression coefficients would be available for the second step which is to retrieve the clear-scene IR brightness temperature.

Unfortunately, the source code and regression coefficients provided for the TACNEPH program had been developed for the SSM/I instrument on the DMSP F8 satellite and were incomplete. Of the 30 possible background surface categories, coefficients were available to classify and process data over only five. Also, the only DMSP data available to TACNEPH were obtained from the F10 and F11 satellites via the PL ground stations. No F8 data could be received because the appropriate decryption codes were not available. However, the F8 coefficients were applied to data from F11 on an experimental basis to determine if they were useful for estimating OLS clear-scene temperatures. Results for both the surface type classification and temperature retrieval portions of the algorithm were poor. The surface classification could not even accurately discriminate land from water backgrounds and temperature values frequently differed from

coincident OLS clear-scene brightness temperatures by greater than 30 K. Conversations with personnel at AFGWC confirmed that the disappointing performance of the algorithm was probably due to the use of F8 coefficients with F11 data.

During the TACNEPH program period of performance, work continued at AFGWC to implement a capability to develop regression coefficients for new satellites and to monitor performance of the temperature retrieval algorithm over time. While this effort was apparently successful, no additional coefficients were received in time to be included in the TACNEPH effort. Because of this, the technique could not be directly evaluated for use in the TACNEPH algorithms. However, based on work that was accomplished, some observations and recommendations related to the TACNEPH program can be provided.

4.3.1 SSM/I Antenna Pattern Correction

SSM/I sensor measurements are calibrated to produce antenna temperatures. These must be corrected for interactions between antenna characteristics and the upwelling radiation (i.e., antenna pattern corrections, APC) to produce physical brightness temperatures required by the EDR algorithms. In the course of early investigations on this task it was discovered that at least two different approaches are available to perform antenna pattern corrections to the SSM/I (Wentz, 1988 and Hollinger et al., 1987). The principal difference between the two is that the NRL technique, in addition to correcting for feed horn characteristics and cross-polarization coupling, applies a second order side lobe correction that is absent in the Wentz approach. Additional information was requested and received from AFGWC on the APC technique in use there. The AFGWC technique was a variation on the Wentz technique through a somewhat different implementation of the cross-polarization coupling correction. However, APC adjusted brightness temperatures obtained from the two algorithms showed good agreement over a range of temperatures.

Independent experiments using the NRL two level technique also showed good agreement with both the Wentz and AFGWC correction algorithms for cases where a uniform array of antenna temperatures were used to exercise the algorithms. This confirms that the three techniques are comparable for feed horn and cross-polarization coupling corrections since the NRL second order corrections account for contributions from side lobes and should not cause any change in temperature if the side lobe energies are the same as the main beam. Figure 3a compares the NRL and AFGWC level 1 corrections to the 37 GHz horizontal polarization channel for approximately 125 consecutive scan lines taken from a single orbit. For the level 2 corrections to be non-zero some gradient has to exist in the array of antenna temperatures. Anecdotally, it was learned that there is generally little variation over in-band antenna temperatures across a single scan, but along scan there can be a wide range of differences. Figure 3b illustrates the magnitude of the level 2 corrections for the same set of scan lines contained in Figure 3a.

It was not possible to evaluate the impact of the NRL level 2 corrections on retrieved IR brightness temperatures due to our inability to successfully run the SSM/I algorithm using the outdated coefficients. However, the information in Figure 3 is suggestive of some general observations. NRL level 2 corrections do not appear to significantly affect the magnitude of the derived brightness temperature under most conditions. Although for some situations, presumably when there is a strong along track gradient, the level 2 corrections become significant and can exceed the magnitude of the level 1 corrections.

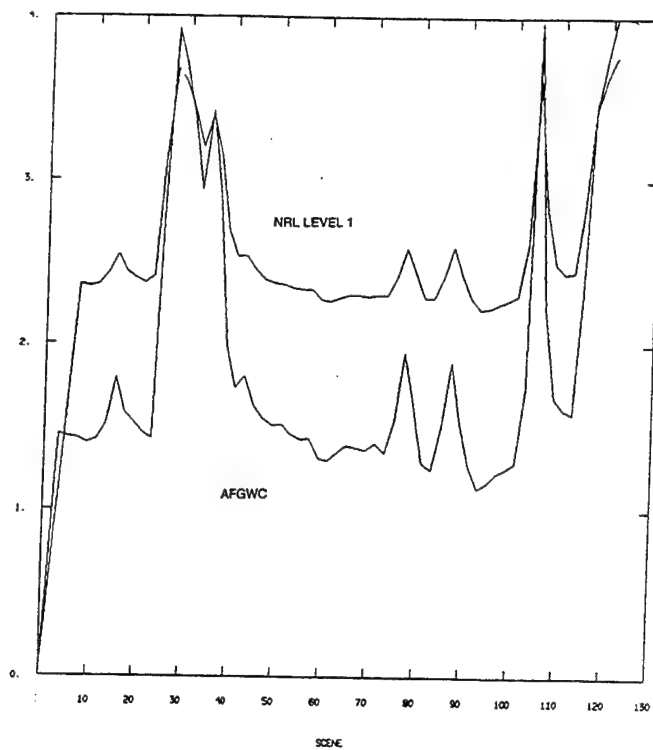


Figure 3a. Comparison of the NRL and AFGWC level 1 corrections to the 37 GHz horizontal polarization channel for approximately 125 consecutive scan lines taken from a single orbit.

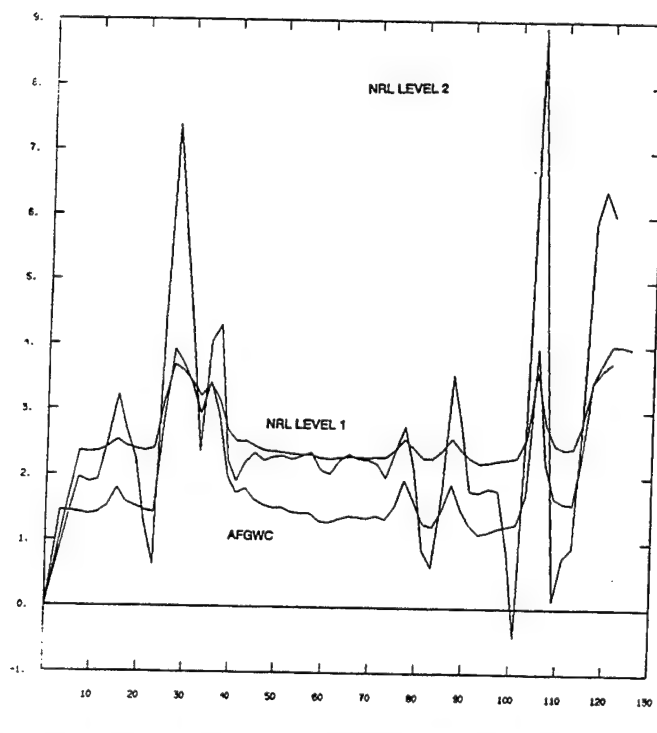


Figure 3b. Magnitude of the level 2 corrections for the same set of scan lines contained in Figure 3a.

4.3.2 Application of SSM/I Derived Surface Temperature

Estimates of OLS clear-scene IR brightness temperatures retrieved from the SSM/I are potentially useful in TACNEPH in some situations. As expected, the existing Surface Temperature Climatology data have been found to vary significantly from the satellite observed IR temperatures over clear-scene conditions. While the dynamic correction described in Section 4.2 that is used to predict the clear-scene IR temperature works well over most situations, there are certain conditions where improved first-guess estimates would be particularly beneficial. One class of conditions where this is true is when there has been a rapid change in the thermal characteristics of the terrestrial background, particularly since the last satellite overpass. Examples include a snow fall or snow melt or even, under extreme conditions, a frontal passage. In these cases the ten day historical record used to characterize the expected range of variation between satellite and climatological temperatures may not be applicable. Generally the algorithm requires a few days to react to these types of rapid change, during which time algorithm performance degrades. This is particularly important for OLS processing since that algorithm is most dependent on the single channel IR test.

Where they overlap the OLS, SSM/I data have the obvious advantage over climatology of temporal consistency. As such they would be expected to resolve the types of situations discussed above that currently impact OLS algorithm performance. The recommended approach to using SSM/I derived temperatures is identical to that described in Section 4.2 for using climatological temperatures. A record of the comparative differences between OLS and SSM/I temperatures would be generated for locations classified as cloud-free. From this an expected range of allowable differences would be generated for each pass and compared to the actual measured differences. This would be necessary to account for variations in the SSM/I retrievals caused by different terrestrial backgrounds and certain cloud types (e.g., precipitating cloud). If, as expected, it turns out that the SSM/I derived temperatures are a better first-guess to the OLS brightness temperatures than climatology, the result would be a smaller range of 2σ values in equations 4-7 and 4-8, which in turn should translate to an improved cloud analysis.

5. NEPHANALYSIS ALGORITHMS

This section provides a description of the TACNEPH cloud detection algorithms which are designed to analyze DMSP/OLS and NOAA/AVHRR sensor data. It is intended as the primary resource for further implementations of the algorithm in operational environments. Other secondary resources that may also be exploited are the separate software design report and source code listings that describe the research grade code produced to support the algorithm development effort. However, it should be kept in mind that the research grade code was designed specifically to meet the requirements of the Research and Development program and not those of an operational tactical terminal program. As such, any use of the research grade code in a Technology Transfer (T²) effort should be for guidance on sizing and as an example of one way to implement the algorithms. Primary reliance should be on the algorithm descriptions contained in this section of the report. It is designed to provide a step by step description of the algorithm process and is not tied to any hardware platform or software environment; however, occasional references to data file formats are included to illustrate how data specific aspects of the program could be implemented. The research grade code was necessarily developed to operate in a VAX/VMS environment and contains many features specifically designed to assist the research scientist in evaluating the algorithm performance and scientific validity of the approach. Any features of this type that have potential use in the operational implementation will be identified in the text.

TACNEPH cloud analysis algorithms were designed to address the graceful degradation requirement imposed on this program. The DMSP and NOAA algorithms are completely separate approaches, each designed to exploit the unique information content of the respective sensors. The algorithms consist of a series of tests that individually analyze multiple cloud signatures in data streams. To produce a final cloud analysis, the combined results of all tests are analyzed. Graceful degradation is achieved through selective evaluation of individual cloud tests based on available data. For example, the OLS algorithm in its optimal configuration uses both visible and infrared channel data. However, at night, in sun-glint conditions, or when visible channel data are noisy the algorithm will operate on single channel data. The fundamental goal during the TACNEPH development effort was to design algorithms that will produce an optimal cloud analysis from whatever data sources are available.

Reliance on external data sources by both algorithms is strictly limited to the data sets identified in Section 2. These particular data sets were identified because they are assumed to be available in a tactical terminal. The only dynamic data requirements are for satellite sensor and ephemeris data, all supporting data are static statistical or fixed parameters. All other required data are generated internally by the algorithms (see Section 4).

For the purposes of algorithm development, cloud analysis results are provided on a pixel-by-pixel basis. Since no final output format was specified it was felt that a pixel analysis would be the most flexible in terms of supporting whatever application specific output format is required operationally. From this format, it is straightforward to compute the required cloud amount and altitude parameters over any regular grid or pixel spacing.

5.1 DMSP/OLS Cloud Analysis Algorithm Description

The TACNEPH OLS cloud detection algorithm relies on three distinct cloud tests which are applied separately depending upon availability of the required image data. The tests are all statistical threshold types of algorithms and consist of single channel visible and infrared tests plus a two channel bispectral test. Results of each test are stored internally as an intermediate database. For the research grade implementation, diagnostic results were also stored for each analysis region (defined as 16 x 16 pixels) where the size of the analysis region was determined at run-time. This information was extremely useful as a diagnostic for algorithm performance and the fine-tuning of parameters which affect cloud detection. If this information should be determined to be useful in the operational implementation, it could be easily produced in a format conducive to a tactical terminal file system.

The multiple cloud tests used in the TACNEPH OLS algorithms are designed to satisfy the graceful degradation requirement of the TACNEPH program. Each test exploits cloud information based upon the presence of infrared and visible data; however, in the event of lost or unusable data, the algorithm will continue to produce a cloud analysis that optimally utilizes whatever data are available.

5.1.1 Threshold Calculation

The TACNEPH OLS algorithms require two dynamic databases to predict the infrared and visible characteristics of the clear-scene background (see Section 4). Clear-scene statistics are required for discrimination of cloud-free from cloud-contaminated radiative signatures in single and dual channel cloud tests. The infrared statistics are used indirectly, to adjust surface temperature climatology values to accurately predict infrared

brightness temperatures for cloud-free conditions. The visible statistics are used directly, for comparison with the measured visible brightness.

The threshold approach utilized by all OLS cloud tests was selected because it allows for multiple uncertainties in the sensor measurements, including sensor calibration, clear-scene characteristics, and atmospheric transmission, to be accounted for with a single value. Recall from Section 4 that an empirically derived dynamic correction factor is used to account for all sources of error collectively without the need to understand and quantify the individual contributions. The magnitude of the cloud thresholds is then dictated by the remaining uncertainty in the corrected temperatures. The performance of the algorithm is directly impacted by the ability to accurately characterize cloud-free backgrounds. This is achieved through the identification or characterization of the following:

- land/water/desert boundaries,
- clear-scene brightness temperature, and
- clear-scene reflectance.

Both single channel and bispectral OLS cloud analysis algorithms use dual threshold cutoff values to classify clear, cloud-filled, and partially cloud-filled pixels within an analysis box. The method employed to select these threshold values is dependent on the sensor data channel being analyzed, infrared or visible.

Infrared thresholds are based on an estimate of the clear-scene brightness temperature derived from a dynamic correction to surface skin temperature estimates obtained from a surface climatology database described in Section 4.2. Once a predicted clear-scene brightness temperature is established, threshold values are computed from statistical estimates of the expected natural variability of the data.

Clear-scene infrared statistics information is used both to establish whether a given reference pixel is cloud-contaminated and to calculate the magnitude of the clear and cloud threshold values. Thresholds are used to account for the uncertainty in the predicted clear-scene brightness temperature calculation. The cloud threshold is defined by the equation:

$$\Delta T_{\text{cld}} = |\Delta T_{\text{max}} - \Delta T_{\text{min}}| * \alpha_{\text{cld}}, \quad (5-1)$$

and the clear threshold is defined by:

$$\Delta T_{\text{clr}} = |\Delta T_{\text{max}} - \Delta T_{\text{min}}| * \alpha_{\text{clr}}, \quad (5-2)$$

where ΔT_{max} and ΔT_{min} are computed using Eq. 4-10 and 4-11 from the IR-Climatology Statistics internal database. They are used to represent the natural variability of the difference between the satellite observed and predicted temperatures for the cloud-free background. The values of α_{cld} and α_{clr} are empirically derived coefficients currently defined as 1.5 and 0.75, respectively.

Once the thresholds are calculated then cloud and clear cutoff values used in the analysis algorithms (see following sections) are calculated by subtracting the threshold values from the predicted clear-scene brightness temperature. Thus, the cloud cutoff is defined as:

$$T_{\text{cld}} = T_{\text{pred}} - \Delta T_{\text{cld}}, \quad (5-3)$$

and the clear cutoff value as:

$$T_{clr} = T_{pred} - \Delta T_{clr} \quad (5-4)$$

where T_{pred} is calculated as in Equations 4-13 and 4-14. Calculation and application of the cutoff values is illustrated graphically in Figure 4.

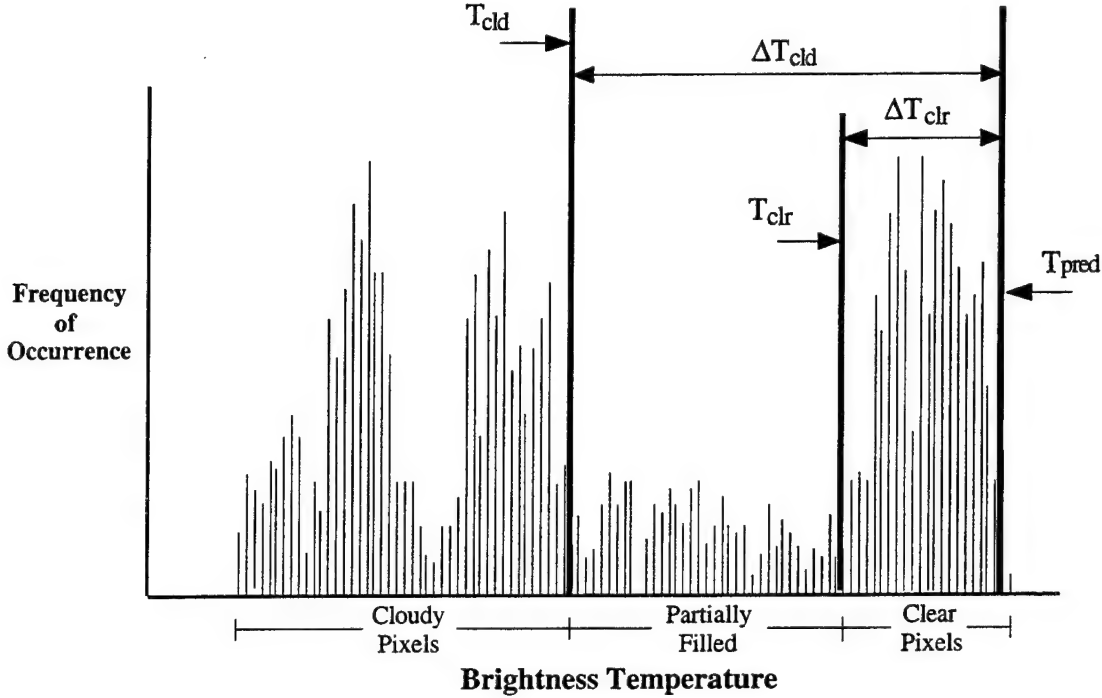


Figure 4. IR single channel test dual threshold classification approach.

The procedure for establishing cutoff values for the visible channel follow an approach similar to that for the infrared channel. Fundamental differences are that cloud and clear threshold cutoff values are calculated individually for each pixel rather than using one pair of values over a whole analysis box, and the technique used to establish cutoff values varies depending on the geographic type of the scene. Over land areas, where surface reflectance is expected to change with time and geographic region, cutoff values are set with the use of the dynamically maintained Visible Background Count internal database described in Section 4.1. Data from the Visible Background database are used in a way analogous to the way clear-scene brightness temperature data are used in the infrared technique. However, since the background data are generated directly from satellite observed radiances no correction factors need to be applied.

If the pixel being analyzed is located over land, then the method for determining the cloud cutoff threshold value (R_{cld}) is defined by the equation:

$$R_{cld} = R_{sfc} * \rho_{cld} \quad (5-5)$$

where R_{sfc} is the brightness count from the Visible Background database (Section 4.1) that corresponds to the satellite pixel and ρ_{cld} is an empirically derived coefficient used to account for uncertainty in the background database. Note that the uncertainty coefficient is multiplied by the background value rather than added as in the IR cutoff calculation (Eq. 5-3). This is to account for increasing uncertainty as the value (i.e., brightness) of the

background increases. Similarly, the method for determining the clear cutoff value (R_{clr}) is defined by the equation:

$$R_{clr} = R_{sfc} * \rho_{clr} , \quad (5-6)$$

where ρ_{clr} is a second empirically derived coefficient. The values of ρ_{clr} and ρ_{cld} are 0.4 and 0.1, respectively. Once the visible and infrared cutoff values are established they are used in the bispectral algorithm to classify cloud-filled, cloud-free or partially cloud-filled pixels. Since there is not a one-to-one correspondence between the latitude/longitude mapping of the background database (i.e., 0.1°) and the satellite data, new clear and cloud cutoff values are calculated for each pixel.

Over water, variations in surface reflectance are considered negligible compared to land. These cutoff values are fixed at R_{cld} and R_{clr} are fixed. These cutoff values are $R_{cld}=40$ and $R_{clr}=37$.

5.1.2 Single Channel Test

The DMSP visible and infrared single channel cloud analysis algorithm is applied when data from only one OLS channel are available. Obviously, the most common occurrence is missing visible data; however, the algorithm can be applied equally to either the visible or infrared channel as the situation demands. If both visible and infrared data are available, then the bispectral test described below is applied. The single channel algorithms utilize the dual threshold approach as illustrated in Figure 4. Separate cutoff thresholds are defined to segregate pixels classified as partially cloud-filled from those that are completely cloud-filled or completely cloud-free. Cloud analysis accuracy is dependent on the accurate prediction of the clear-scene brightness temperature used to define the clear and cloudy cutoff values as described above in Section 5.1.1.

The single channel algorithm consists of two tests. First, a test is performed to determine if the brightness temperature of the IR channel is less than the cloud cutoff or the visible count is greater than the cloud cutoff:

- $T_{IR} < T_{cld}$ or
- $R_{vis} > R_{cld}$

where T_{IR} is the OLS infrared brightness temperature, T_{cld} is the IR cloud cutoff value defined by Eq. 5-3, R_{vis} is the OLS visible count, and R_{cld} is the visible cloud cutoff value defined by Eq. 5-5. For the IR algorithm, a pixel is classified as cloudy if the OLS brightness temperature is less than the cutoff value. Similarly, the visible algorithm classifies a pixel as cloudy if the visible count is greater than the cutoff value.

If the sensor data do not meet the cloudy criteria then a second test is performed to determine if the pixel is completely cloud-free. This is done by testing the sensor against the clear cutoff values:

- $T_{IR} > T_{clr}$ or
- $R_{vis} < R_{clr}$

where T_{clr} is the infrared cloud-free cutoff defined by Eq. 5-4 and R_{clr} is the visible cloud-free cutoff defined by Eq. 5-6. If these tests evaluate as true then the pixel is classified as cloud-free. If both of the cloud and clear tests evaluate as false:

- $T_{\text{cld}} \leq T_{\text{IR}} \leq T_{\text{clr}}$ or
- $R_{\text{cld}} \geq R_{\text{vis}} \geq R_{\text{clr}}$

then the pixel is classified as partially cloud-filled (i.e., the FOV of the sensor contains both cloud and clear).

Once pixels have been classified using the single channel algorithm, fractional cloud amount can be calculated over some spatial region. As discussed above, the size and characteristics of this region are assumed to be application dependent since no specific requirements were imposed on TACNEPH. To compute fractional cloud amount over some arbitrarily defined region wherein pixels have been classified as either clear, partially cloud-filled, or cloudy, the contributions from each class need to be quantified as follows:

$$A_c = \frac{1}{N_{\text{tot}}} \left(N_{\text{cld}} + \sum \frac{(I_{\text{IR}_i} - I_{\text{clr}})}{(I_{\text{cld}} - I_{\text{clr}})} \right) \quad (5-7)$$

where A_c is the effective cloud cover ($0 \leq A_c \leq 1$), N_{tot} is the total number of pixels in the analysis region, N_{cld} is the number of pixels that meet the completely cloudy criteria (i.e., exceed the cloud cutoff value), I_{IR_i} is the measured scene radiance of pixels classified as partially cloudy, I_{cld} is a representative cloud radiance, and I_{clr} a representative clear-scene radiance. The N_{cld} term accounts for the completely filled pixels and the summation term for the partially cloudy contribution; the summation is performed over all pixels classified as partially cloud-filled. The partial term is an adaptation of the spatial coherence energy balance approach developed by Coakley and Bretherton (1982). The representative radiance values, I_{clr} and I_{cld} are computed from the respective cloudy and clear brightness temperature cutoff thresholds.

5.1.3 Bispectral Test

The OLS bispectral algorithm, developed for use during daytime conditions, is similar to the single channel algorithm but is applied in two spectral dimensions simultaneously. Data from both visible and infrared sensor channels are analyzed using two pairs of cutoff values, one pair for each channel. It should be noted that accurate specification of the infrared threshold is not as critical in the bispectral test as in the one channel IR algorithm since low (warm) liquid water clouds reflect well and will generally be detected from the visible data when not over highly reflective backgrounds.

Figure 5 provides an illustration of how the two dimensional visible-infrared space is divided into nine classification regions by the four cutoff values. In this figure T_{cld} and T_{clr} represent the infrared brightness temperature cloud and clear cutoff values defined by Eqs. 5-3 and 5-4, respectively, while R_{cld} and R_{clr} represent the visible count cloud and clear cutoffs defined by Eqs. 5-5 and 5-6, respectively. Infrared temperatures that are less than the infrared cloud threshold value:

- $T_{\text{IR}} < T_{\text{cld}}$

are unambiguously classified as cloud-filled. Data that are both warm in the infrared and dark in the visible channel (R_{vis}):

- $T_{\text{IR}} > T_{\text{cld}}$

and $\bullet R_{vis} < R_{cld}$

and $\bullet T_{IR} > T_{clr} \text{ or } R_{vis} < R_{clr}$

are unambiguously classified as clear. Warm bright regions:

$\bullet T_{IR} > T_{cld}$

and $\bullet R_{vis} > R_{cld}$

require an a priori clear-scene classification to remove the ambiguity caused by the similarity in radiative signatures of backgrounds such as deserts and low cloud. Data that fall between all four threshold values:

$\bullet T_{cld} < T_{IR} < T_{clr}$

and $\bullet R_{cld} > R_{vis} > R_{clr}$

are classified as partially cloud-filled. These rules are used to define the classification bins labeled in Figure 5.

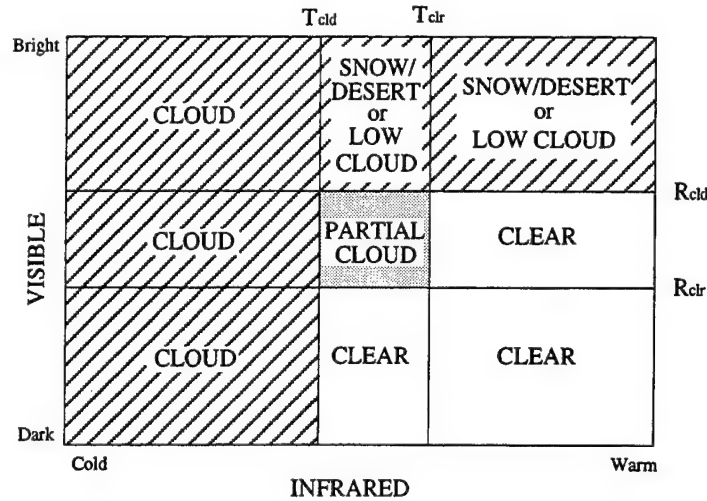


Figure 5. Bispectral classification approach.

Like the single channel algorithm, fractional cloud amount is calculated based on the individual pixel classifications within an analysis region. Again, contributions to cloud amount are calculated separately for completely filled and partially filled FOVs:

$$A_c = \frac{1}{N_{tot}} \left[N_{cld} + \frac{1}{2} \sum \left(\frac{I_{IR} - I_{clr}}{I_{cld} - I_{clr}} + \frac{R_{vis} - R_{clr}}{R_{cld} - R_{clr}} \right) \right] \quad (5-8)$$

where A_c is effective cloud amount, N_{tot} is the total number of pixels in the analysis region, N_{cld} is the number classified as completely cloud-filled, R_{vis} and I_{IR} are the measured reflectance and calculated radiance, respectively, of the partially cloud-filled pixels and I_{clr} and I_{cld} are calculated from the brightness temperature cutoff values, T_{clr} and

T_{cld} respectively. The N_{cld} term accounts for the contribution of cloudy pixels and the summation is performed over all pixels classified as partially filled.

5.1.4 Use of Visible Data

Any algorithm that uses visible data requires filters for highly reflective terrestrial backgrounds. Three background types or conditions have been identified as problematic for visible processing: desert, snow and ice, and sun glint over water. Desert regions are identified in the geographic type supporting database (Section 2.7). No dynamic information on snow cover is assumed to be available on tactical terminals. Possible options for providing snow and ice cover information to the TACNEPH algorithms should be considered since this will directly impact the accuracy of the cloud analysis. For example, if the tactical user suspects there is snow in the analysis region, based on personal observation or other information sources (e.g., pilot reports), a snow flag user input could be introduced. Additionally, SSM/I and AVHRR data could be used to generate a separate snow and ice cover supporting database that could be input to the TACNEPH model. A sun glint test, based on local satellite observing and solar geometry, was developed for use over water background surfaces (as defined by the geographic support database described in Section 2.7). Potential sun glint areas are defined by the following test:

- Background surface type must be water,
- and
- $|\psi - \theta| < 40$,
- and
- $120 < \phi < 240$,

where the cutoff values are empirically set to define the geographic extent over which sun glint may be expected to occur (see Section 2.5 for angle definitions).

No visible data processing is performed over an analysis region that contains desert or snow backgrounds or where the sun glint test evaluates as true. Also visible processing is restricted to locations where the sun is above the horizon and not near the terminator. These conditions are defined by a solar zenith angle test:

- $\theta > 75$.

The minimum zenith angle defining usable visible data is set at this value because dynamic onboard gain adjustments to the visible sensor in the vicinity of the terminator make objective processing of the visible data problematic. In situations where there is a known reflective background or the solar zenith angle is too large, the OLS cloud algorithm reverts to the single channel IR test.

5.1.5 OLS Cloud Analysis Results

To support algorithm testing during the algorithm development process, the research grade software used to implement the OLS algorithm was configured to produce pixel level output products that contained results of all the cloud tests available to the algorithm (i.e., single-channel visible, single-channel IR, and bispectral). Results are encoded into an array of 8-bit values suitable for display as synthetic imagery. Table 6 provides definitions of the bit assignments for the DMSP Cloud Analysis Algorithm output. One 8-bit quantity is produced for each pixel in the input image, and one file is created for each OLS input scene processed through the OLS cloud analysis algorithm.

Table 6. Intermediate DMSP Cloud Analysis Bit Assignments

Bit	Assignment	Description
0	Desert	ON = desert background type
1	Coastline geography	ON = coastline background type
2	VIS partial	Single-channel visible partial cloud test
3	VIS total	Single-channel visible total cloud test
4	IR partial	Single-channel infrared partial cloud test
5	IR total	Single-channel infrared total cloud test
6	Bispectral partial	Bispectral partial cloud test
7	Bispectral total	Bispectral total cloud test

In any future operational implementation it is assumed that the desired output will be a fractional cloud amount based on the single most applicable cloud test. Applicability will be determined by data availability. In situations where both visible and infrared data are available, cloud amount will be determined by the bispectral test. Otherwise, when data from only one sensor channel are available (e.g., nighttime, failure of other sensor channel), cloud amount will be determined by the appropriate single-channel test.

5.1.6 OLS Cloud-Clearing Procedure

In order to generate the clear-scene information required to produce the supporting infrared corrections and visible background databases described in Section 4, it is necessary to operate the OLS algorithm in a cloud-clearing mode. The cloud-clearing procedure is similar to the cloud detection operation described above except that only the clear cutoff value is used to discriminate clear from cloud-contaminated pixels and a smaller threshold (i.e., identifies warmer pixels) is used to define the cutoff value. The intent is to find and remove all cloud in a scene with less concern for overanalysis. However, at the same time it is critically important that at least some clear areas are identified in order to update the clear-scene supporting databases.

Cloud-clearing thresholds are defined as a percentage of the IR cloud-detection thresholds and/or the visible clear cutoff values. Real-data tests showed that different thresholds were needed for different locations and conditions. Over the Canadian ROI, the IR threshold is 30% smaller than the clear visible brightness count threshold:

$$\Delta T_{\text{cld_clr}} = (.70)\Delta T_{\text{clr}} \quad (5-9)$$

and over the Albany, Water and Georgia ROI's the reduction is 15%:

$$\Delta T_{\text{cld_clr}} = (.85)\Delta T_{\text{clr}} \quad (5-10)$$

where ΔT_{clr} is the IR clear threshold defined in Eq. 5-2. Infrared cloud-clearing cutoff values are then defined by replacing ΔT_{clr} in Eq. 5-4 with $\Delta T_{\text{cld_clr}}$ from Eq. 5-9 or 5-10:

$$T_{\text{cld_clr}} = T_{\text{pred}} - \Delta T_{\text{cld_clr}} \quad (5-11)$$

Visible cutoff values are defined by reducing the clear cutoff values directly, for the Canadian ROI by 30%:

$$R_{\text{cld_clr}} = (.70)R_{\text{clr}} \quad (5-12)$$

and for the Albany, Water and Georgia ROI's the percentage is 15%:

$$R_{\text{cld_clr}} = (.85)R_{\text{clr}} \quad (5-13)$$

where R_{clr} is visible clear cutoff value defined in Eq. 5-6.

During the development process, it became apparent that the magnitudes of the cloud-clearing cutoff values are crucial to maintaining an accurate cloud analysis. If no clear areas are identified the clear-scene databases quickly become obsolete. If some cloud is misinterpreted as clear, the background databases become cloud-contaminated resulting in a degradation of the cloud algorithm accuracy. To insure that the cutoff values were properly set, histograms of the clear-scene differences between satellite-observed and climatological temperatures were routinely generated and monitored. Figure 2 illustrates a typical clear-scene temperature difference histogram when there is no cloud contamination. However, if some cloudy pixels remain in the distribution after cloud clearing, the resulting histogram assumes a bimodal shape such as that illustrated in Figure 6. When this occurs it may become necessary, if the accuracy of the cloud analysis begins to degrade, to manually adjust the 2σ limits (ΔT_{min_i} and ΔT_{max_i}) defined by Eqs. 4-7 and 4-8 to remove the contaminated pixels from the clear-scene statistics. Failure to correct for cloud-contaminated pixels can result in a negative feed-back process wherein the time and frequency-weighted minimum ΔT limit from Eq 4-10 becomes too small, allowing some cloud-contaminated pixels to satisfy the inequality in Eq. 4-12 resulting in a predicted clear-scene temperature (T_{pred_n} from Eq. 4-13) that may be unrealistically low. If this T_{pred} value is used in-turn in Eq. 5-11 to detect and eliminate cloud-contaminated pixels, more cloudy pixels can be incorrectly classified as cloud-free and the process builds on itself.

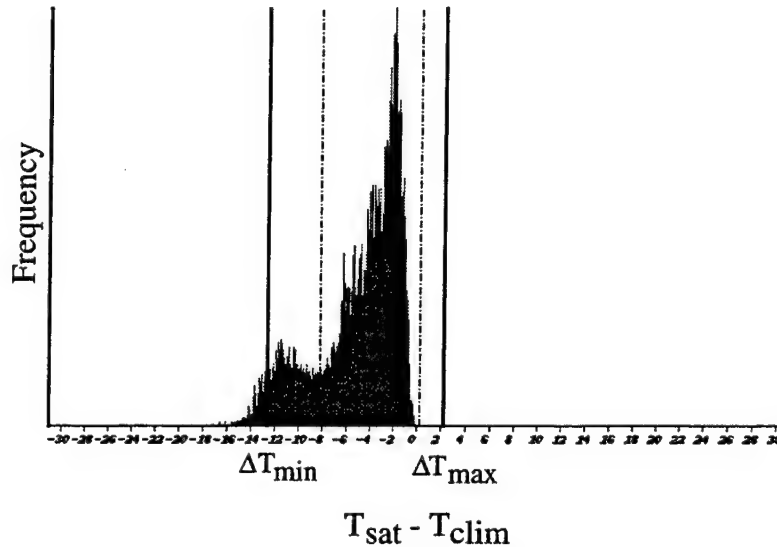


Figure 6. *Example histogram of comparison between satellite brightness temperatures and corresponding climatological temperatures for a case in which some cloudy pixels have been incorrectly classified as cloud-free. Solid vertical lines represent 2 standard deviations about the mean of the entire, bimodal distribution. Broken vertical lines represent manually adjusted values for which the cloud contaminated pixels have been eliminated.*

5.2 NOAA/AVHRR Cloud Analysis Algorithm Description

The TACNEPH AVHRR cloud detection algorithm consists of a series of tests, comprised of cloud and background surface classification tests, each one of which relies on one or a combination of separate cloud spectral signatures. The approach is based on work done by Saunders and Kriebel (1988). The background tests are used to identify problematic background surface conditions that can cause the cloud tests to misclassify the clear-scene as cloudy (e.g. snow/ice, sun glint and desert) (Section 5.2.1). Results of these tests are used to modify affected cloud tests and/or eliminate channels from the analysis process. The algorithm is structured to run each of the tests and store the individual results in a temporary internal buffer termed the intermediate cloud analysis (Section 5.2.4). It is important to note that some of the tests require the results of other tests so the order in which the tests are run is important. Noise effects resulting from problems in the AVHRR channel 3 sensor are removed from specific cloud test results using a noise filter (Section 5.2.3). After all tests have been completed, data stored in this internal buffer are analyzed concurrently to produce the final cloud analysis product (Section 5.2.5). For the purposes of the algorithm development effort, cloud analysis results are output on a pixel by pixel level. Depending on the specific implementation and database requirements on the tactical terminal, these results can be easily reformatted to either a Polar Stereographic or Mercator map projection at the desired grid resolution. It may be useful to note that for the research grade implementation, intermediate results for each of the separate tests were output and visually examined. This information was extremely useful as a diagnostic for algorithm performance and to provide additional insight into specific types of cloud (e.g., certain tests are particularly sensitive to low cloud or cirrus) (Section 5.3.1). If this type of information should be determined to be useful in the operational implementation, it could be easily produced through proper formatting of the internal buffer referred to above.

5.2.1 Background Surface Filter Tests

Background surface tests are used to identify problematic surface backgrounds that have spectral signatures similar to cloud. Results of these tests are used to either modify affected cloud tests or eliminate channels from the final analysis process. Table 7 summarizes the background tests, the sensor channels, and the solar zenith angle requirements.

Table 7. Background Surface Test Summary

Name	Description	AVHRR Channel	Solar Zenith Angle
SNOW	snow and ice detection	1,2,3,4	$\theta < 80^\circ$
GLINT	detection of sun glint over large bodies of water	1,2,3,4,5	$\theta < 80^\circ$
DESERT	highly-reflective non-vegetated land surfaces	2,3,4	$\theta < 80^\circ$

5.2.1.1 Sun Glint Test

The sun glint test (GLINT) is used to detect specular reflection off of water surfaces which could be mistakenly identified as cloud by tests that rely on reflected solar radiation. Sun glint is a potential problem over any water surfaces that can be resolved by the satellite, however, in practice the GLINT test is only applied over permanent water surfaces large enough to be captured in the geography database (Section 2.7). In contrast to the OLS algorithm described above, the AVHRR sun glint test uses spectral information along with geometry considerations to classify glint conditions. There is no sun glint signature that is distinct from all cloud signatures; therefore the GLINT algorithm relies on a series of signatures, any one of which could be representative of either cloud or glint, but when taken together greatly enhance the probability that the cause is glint rather than cloud. This has the additional benefit of discriminating cloud within a sun glint region, eliminating the need to remove glint areas from visible channel cloud processing. A series of conditions involving the background, solar/satellite geometry, and spectral signatures must be met to detect glint. All tests must evaluate positively for glint; the failure of any single test prevents a glint classification.

The first set of tests determine if the background surface type and solar/satellite geometry will support sun glint. These tests are:

- Background surface type must be water ,
- and • $|\psi - \theta| < 40^\circ$,
- and • $120^\circ < \phi < 240^\circ$,

where ψ is the satellite zenith angle and θ is the solar zenith angle, and ϕ is the azimuth angle between the sun and the satellite. The threshold values are empirically derived.

The second set of tests examines the spectral signature of any pixels that passed the background surface type and solar/satellite geometry tests. These tests are:

The albedo must be high in the visible channels:

- BRIGHT Test detects cloud (Section 5.2.2.2) ,
- or • RATIO Test detects cloud (Section 5.2.2.2).

Channel 3 must be nearly saturated:

- $T_3 > 309 \text{ K}$,
- and • $T_3 > T_4 + 14 \text{ K}$.

The IR brightness temperature must be relatively high in the infrared channels (i.e., not indicative of a low liquid water cloud):

- COLD Test does not detect cloud (Section 5.2.2.1) ,
- and • CIRRUS Test does not detect cloud (Section 5.2.2.1).

If all of these conditions are satisfied, the pixel is classified as sun glint and bit 0 of the intermediate output word is set.

5.2.1.2 Desert Test

The Desert Test (DESERT) is used to augment the geographic database (Section 2.7) through identification of clear-scene desert backgrounds by analysis of multispectral daytime AVHRR data. In this application, the term desert is used to indicate any highly reflective, non-vegetated land surface; it does not necessarily follow the geographer's definition based on annual precipitation. The desert geography was developed by thresholding clear-scene visible imagery. This works well for identifying stable surface features but it is restricted to the reflectance information in the scenes used to develop the background classification. It cannot account for daily and long term changes in reflectance resulting from the angle of solar illumination or seasonal effects, for example. A dynamic test, which classifies the background based on the information in the current scene proved necessary. Also, in addition to their run-time use in specifying cloud-free desert pixels in the AVHRR algorithm, desert flags are potentially useful to the DMSP/OLS cloud analysis algorithms as a high resolution source for identifying bright sandy backgrounds. The DESERT test combines a series of spectral signatures as follows:

In addition to the pixel being a land point, a series of five AVHRR spectral conditions must be met in order to classify a pixel as cloud-free desert. The first condition is a modified version of the RATIO cloud test (Section 5.2.2.2):

$$\bullet 0.85 < A_2/A_1 < 1.05,$$

where the empirically determined thresholds bound the range of the near-IR to visible channel ratio for clear-scene desert backgrounds. Note these thresholds are more limiting than the cloud detection RATIO thresholds since highly reflective land surfaces generally do not exhibit as much variability as clouds in near-IR and visible sensor channel measurements.

The second test is an absolute check on the channel 2 albedo testing for a (potentially) clear background. The test is defined as:

$$\bullet A_2 < 0.2,$$

and is employed to ensure the measured albedo is not large enough to be a cloud signature since desert surfaces are not as bright as cloud in channel 2.

The third test determines if the channel 3 brightness temperature is near saturation. Clear non-vegetated surfaces exhibit a strong solar component in channel 3 resulting in a large T_3 brightness temperature. The test is defined as:

$$\bullet T_3 > 300 \text{ K},$$

The fourth test checks for a T_4 temperature that is warmer than all but low cloud:

$$\bullet T_4 > 290 \text{ K} ,$$

The final desert criterion ensure that low clouds do not get classified falsely as desert by restricting the brightness temperature difference between channels 3 and 4 to a specified range. The test is defined as:

$$\bullet 7.0 \text{ K} \leq T_3 - T_4 \leq 17.0 \text{ K}.$$

If all of these conditions are satisfied, the pixel is classified and bit 0 of the intermediate output word is set. Note that the bit assignment of this test does not conflict with the GLINT test as DESERT is applied only over land surfaces.

5.2.1.3 Snow Background Test

The SNOW test is used to discriminate snow and ice backgrounds from cloud. It is a two tiered algorithm; first it uses multispectral data to identify scenes with characteristics consistent with snow (but not necessarily separate from cloud). The second step provides the principal discrimination signature for separating snow from cloud based on the MWIR reflectivity. At the $3.7 \mu\text{m}$ wavelength, water droplet clouds tend to be reflective while snow backgrounds are not. Thus, if the scene is characteristic of either snow or cloud, but is not reflective in channel 3, then it is classified as snow. To establish the basic scene characteristics a series of tests are applied:

The first two tests ensure that the temperature is close to freezing and close enough to the surface temperature not to be cloud,

$$\bullet T_4 < 278 \text{ K};$$

and

$$\bullet |T_4 - T_{\text{pred}}| < 15$$

where T_{pred} is defined in Eqs. 4-13 and 4-14..

The next tests look for reflection in the visible(over land) or near-IR (over water) channels

$$\bullet A_2 > 0.24 \text{ over water or } A_1 > 0.1 \text{ over land.}$$

Then, if the data fall within all of these limits, the final test is applied:

$$\bullet |T_3 - T_4| < 5.$$

If snow is detected, then bit 7 of the intermediate output word is set. Note that if this spectral snow test evaluates as true, the pixel is unambiguously classified as cloud-free and results from other tests are not used. Testing on real data has shown that cloud in cloud shadows exhibit spectral signatures that are very similar to snow and may be misclassified as clear. Stricter thresholds can reduce this misclassification; however, correct snow classifications are also reduced. The cloud shadow effect is minimal compared with the problems resulting from snow so this error is accepted.

5.2.2 Cloud Tests

Recall from Section 5 that each AVHRR cloud detection test is based on a spectral signature that exploits one or more of the AVHRR sensor channels. Each cloud test is designed to be more sensitive to a specific type of cloud; there is no one test that can identify all types of cloud under all conditions. In total, there are seven tests which are divided into three groups: 1) those that are equally applicable without regard to the amount of solar illumination on the scene; 2) daytime tests that rely on reflected solar radiation; and 3) nighttime tests that are applicable only in the absence of sunlight. A solar zenith angle threshold is used to determine which tests are applicable to a particular situation. Daytime is defined as a solar zenith angle less than or equal to 90 degrees; Nighttime is defined as a solar zenith angles greater than 90 degrees. Some of the daytime tests require even stricter

solar zenith angle thresholds. These restrictions will be noted in the appropriate test descriptions.

Each pixel in a scene is subjected to all applicable cloud tests. Data from all five AVHRR channels, the background surface tests (Section 5.2.1), and the supporting clear-scene information (Section 4) are required to analyze the scene. Table 8 summarizes the cloud tests and the solar zenith angle requirements that dictate when they are applied.

Table 8. AVHRR Cloud Test Summary

Name	Description	Channel	Solar Zenith Angle
COLD	single LWIR channel threshold	4	NA
CIRRUS	split LWIR	4,5	NA
BRIGHT	single vis or near-IR channel threshold	1,2	$\theta \leq 60^\circ$
RATIO	comparison of near-IR to visible albedo	1,2	$\theta \leq 80^\circ$
CLF	difference between MWIR and LWIR	3,4	$\theta \leq 90^\circ$
FLS	difference between LWIR and MWIR	3,4	$\theta > 90^\circ$
HIGH	difference between MWIR and LWIR	3,4,5	$\theta > 90^\circ$

5.2.2.1 Solar Independent Cloud Tests

There are two tests used to detect cloud that are independent of the scene solar illumination. The first is a single channel LWIR threshold (COLD) test designed to detect mid-level water droplet clouds, optically thick cirrus, and any other cloud that is thermally distinct from the terrestrial background. The second (CIRRUS) uses the split LWIR channels to detect thin cirrus and small ice or water particles at the edge of mid-level cloud.

The COLD test is similar to the RTNEPH satellite processor and OLS single channel algorithm in that it is a single channel IR threshold test that attempts to separate out the thermal signature of clouds from an estimated terrestrial background signature. The TACNEPH algorithm uses the surface temperature climatology database (Section 2.6) along with the internally generated infrared clear-scene statistics database (Section 4.2) to predict the clear-scene channel 4 radiative temperature. For the research implementation, data were processed over a 32 x 32 pixel analysis array and segregated by background type into two classes: 1) land backgrounds and 2) water backgrounds (in the tactical terminal implementation the 32 x 32 array would be replaced by the desired analysis region). For each background type, channel 4 data are organized in a histogram from coldest to warmest and a reference temperature value is identified for which 5% of the data in the distribution are warmer. A warm temperature is selected to maximize the probability that a cloud-free location will be selected for the reference temperature. The 5% limit is added to eliminate anomalously warm pixels from consideration. A pixel with a brightness temperature equal to the reference temperature is located in the 32 x 32 analysis array and the corresponding climatological surface temperature is calculated from the climatology database. As is the case when generating the clear-scene statistics database, the climatological temperature is obtained by first collocating the sensor and climatology data and then time interpolating the climatological temperatures to match the satellite valid times. The time interpolation is not critical to the clear-scene temperature estimation process except that it tends to eliminate artificial boundaries in the analysis when the sensor data passes from one climatological time regime to another (e.g., from one synoptic time to another or over the end of one

month into the next). Once the reference pixel is identified and a climatological surface temperature is calculated, a predicted clear-scene brightness temperature is calculated for the analysis region using the process described in Section 4.2.

A cloud decision is performed by comparing each T₄ pixel value to its corresponding predicted clear-scene temperature:

- $T_{\text{pred}} - T_4 > \text{THRESH}_{\text{cold}}$.

If the T₄ value is less than the T_{pred} value by an amount greater than a preset threshold, then the pixel is declared cloudy and bit 3 in the intermediate output word is set. The magnitude of the threshold was established empirically as a measure of the uncertainty in the clear-scene temperature prediction. Separate threshold values are maintained as a function of the background type including land, water, desert, snow, and coast. Current THRESH_{cold} values are: 9 K for water backgrounds, 10 K for land, 10 K for desert, 15 K for snow, and 25 K for coastline. Cloud clearing thresholds are 0 K for water backgrounds, 0 K for land, 10 K for desert, 5 K for snow, and 25 K for coastline.

Accurate detection of clouds over coastlines has proven particularly difficult for the COLD test. Over coastlines, there can be a large temperature gradient between the land and water surfaces. Since the reference temperature is representative of the warmer surface, the colder surface may be misclassified as cloud. This problem can be avoided by stratifying the background points into land and water, selecting two reference temperatures, and applying separate corrections to land and water points. However, the coarse resolution of the geography database has made it difficult to correctly stratify the background points. In addition to coastlines, this problem occurs over land areas containing lakes which are too small to be reflected in the geography database. If, for example, the lake is warmer than the surrounding land, the reference temperature will be representative of the lake and the surrounding land will be misclassified as cloudy. A higher resolution geography database with specific emphasis on accurate placement of coastline would eliminate many of these surface classification problems allowing the 5% limit imposed to eliminate anomalously warm pixels from selection as the reference temperature to be reduced. A higher resolution, 64th mesh geography database was developed and used successfully to address this problem as part of the parallel SERCAA research program (Gustafson et al., 1994).

The CIRRUS test exploits the sensitivity of the channel 5 radiance to the presence of small ice crystals present in thin cirrus and small water droplets generally found around the edge of water clouds. The cloud signature derives from the channel 4-5 difference since the emissivity at channel 4 wavelengths is relatively insensitive to the presence of these particles. However, care must be taken when implementing this test since channel 5 radiance is also affected by the presence of water vapor in the atmosphere. Thus the split window difference test uses a theoretically derived table of expected differences between T₄ and T₅ that is maintained as a function of expected water vapor loading and path length through the atmosphere. Saunders and Kriebel (1988) derived such a table for the North Atlantic Ocean region that was found to be generally applicable during TACNEPH testing. Since no direct humidity measurement is assumed to be available in a tactical terminal, the predicted clear-scene temperature (T_{pred}) is used as a surrogate for water vapor (i.e., the higher the surface temperature the greater amount of water vapor that can be maintained). Table 9 contains the expected T₄-T₅ values used in the CIRRUS test. A cloud detection threshold is established by interpolating to the actual T₄ and satellite zenith angle (ψ) values. The CIRRUS test is defined as:

- $T_4 - T_5 > \text{THRESH}(T_4, \psi)$

where $\text{THRESH}(T_4, \psi)$ is the cloud detection threshold obtained through interpolation from the table. If the $T_4 - T_5$ difference exceeds the threshold level, the point is declared cloudy and bit 2 in the intermediate output word is set. There are no separate cloud clearing thresholds used in this test.

Table 9. Predicted Clear-Scene Channel 4-5 Brightness Temperature Differences (from Saunders and Kriebel, 1988)

$T_{\text{pred}} \backslash \psi$	0	36	48	55	60
260	0.55	0.60	0.65	0.90	1.10
270	0.58	0.63	0.81	1.03	1.13
280	1.30	1.61	1.88	2.14	2.30
290	3.06	3.72	3.95	4.27	4.73
300	5.77	6.92	7.00	7.42	8.43
310	9.41	10.74	11.03	11.60	13.39

Real-data tests have shown that the CIRRUS test performs accurately and robustly for the majority of climatological situations. However, the test sometimes has difficulty accurately discriminating cirrus cloud from snow and ice backgrounds. An improved CIRRUS test, which attempts to correct this problem, ideally requires snow and ice field information. However, snow information is currently unavailable to the TACNEPH program other than through the spectral SNOW test. Recall that if the spectral SNOW test identifies snow, the pixel is unambiguously classified as clear. In TACNEPH, a surface temperature dependency is used to identify potentially snow covered surfaces:

- $T_{\text{pred}} < 280 \text{ K}$.

If this criterion is met, an additional requirement is placed on the cloud test. Based on the assumption that channel 4 brightness temperatures measured from cirrus clouds are colder than the terrestrial background, the T_4 brightness temperature is required to be lower than the predicted clear-scene brightness temperature by an amount greater than a cloud detection threshold. This test is defined as:

- $T_{\text{pred}} - T_4 > 5 \text{ K}$.

If the background is potentially snow or ice and both cloud criteria are met, then the pixel is classified as cloud-filled and bit 2 in the intermediate output word is set. If the background is not classified as snow or ice, then only the $T_4 - T_5$ test is required.

Should a snow database become available to TACNEPH in the future, snow and ice covered surfaces should be identified using the database rather than the surface temperature dependency.

5.2.2.2 Daytime Cloud Tests

Three cloud tests are used during daytime passes that rely, at least partially, on reflected solar radiation for a cloud signature. The first is used to detect water droplet clouds that exhibit a high albedo relative to the terrestrial background (BRIGHT); the second uses the ratio of near-IR to the visible albedo to identify signatures that depart from expected cloud-free land and water background signatures (RATIO); and the third contrasts

the brightness temperature derived from both the emitted and reflected components of the MWIR channel for large water droplet clouds to the emitted only component at longer wavelengths (CLF). However, these signatures are not unique to cloud and the tests can be confused by terrestrial backgrounds that exhibit similar reflectance characteristics including snow, desert, and sun glint. To discriminate cloud from these backgrounds, the background surface filter tests described in Section 5.2.1 are used to modify the actual cloud test thresholds or filter ambiguous information from the cloud test results.

The BRIGHT test is a single channel threshold algorithm that attempts to discriminate relatively bright cloud reflectance from a known background. The test requires both channel 1 and 2 data along with the internal clear-scene albedo database. The sensor data are normalized to remove the effects of anisotropic reflection in exactly the same way that the clear-scene albedo database was generated (Section 4.1). These data are only processed out to a solar zenith angle of 60 degrees since ARF data are not available beyond that range and, in any event, it is questionable whether there is sufficient solar illumination to obtain a good cloud signature. The normalized sensor albedo data are compared to the stored clear-scene albedo data for the collocated grid box and, if the sensor data exceeds the stored value by an amount exceeding a preset threshold, the pixel is classified as cloudy and bit 6 of the intermediate output word is set. The threshold was empirically defined as 0.16 over water surfaces and 0.07 over land. Channel 2 data are used over water backgrounds to exploit the relative transparency of the atmosphere relative to the visible data. However, over land surfaces channel 1 data are used because vegetated surfaces exhibit a relatively higher reflectivity in the near-IR that normally outweighs atmospheric transmission effects. In both cases the goal is to use the sensor data that minimize contributions from sources other than cloud.

The RATIO test is unique in that it attempts to detect a visible and near-IR signature that is not representative of a clear terrestrial background rather than explicitly searching for a cloud signature. As discussed above, visible channel data are relatively more susceptible to brightening from atmospheric scattering, particularly from suspended aerosols compared to the near-IR channel data. However, vegetated land surfaces exhibit a reverse trend due to a higher reflectivity in the near-IR compared to visible channel wavelengths. The RATIO test exploits these characteristics by comparing the relative brightness of the channel 1 and 2 data through a channel ratio. No normalization for anisotropic effects is needed since they cancel in the ratio operation. The test is applied by simply dividing the measured channel 2 albedo by the channel 1 value. Vegetated land surfaces tend to have a ratio considerably greater than 1; water surfaces will be less than 1 depending on the transmissivity of the atmosphere. Clouds exhibit a ratio approximately equal to 1. Thus the cloud test is applied by testing whether the channel ratio is approximately 1. Two sets of cutoff values are used depending on the perceived near-surface humidity level. The predicted clear-scene temperature (T_{pred}) is used to identify potentially high humidity regions that could enhance aerosol growth.

If the predicted temperature is less than or equal to 295 K the cloud detection test is defined as:

$$\bullet \quad 0.75 \leq A_2/A_1 \leq 1.1 \quad (\text{cloud clearing } 0.7, 1.2);$$

if warmer than 295 K then the limits are changed:

$$\bullet \quad 0.70 \leq A_2/A_1 \leq 1.0 .$$

If the channel ratio falls within the appropriate limits the pixel is classified cloudy and bit 5 of the intermediate output word is set. Real-data tests have shown that this test can falsely

detect cloud over coastlines. It is believed that the signatures from the mixed land-water field of view result in a spectral signature ratio which is close to 1. To eliminate false detection of cloud, this test is not used for any data for which the background is identified as coast by the geography database (Section 2.7). Coastline which is not identified in this coarse resolution geography, e.g. small lakes and rivers, remains a problem.

Because the BRIGHT and the RATIO tests rely on the reflectance characteristics of cloud to identify cloud, reflective terrestrial backgrounds (i.e. snow or ice, desert and sun glint backgrounds) that exhibit a visible or near-IR signature similar to cloud can be incorrectly identified as cloud. To minimize over-analysis of cloud, these test results are not used when the background has been identified as snow, ice, desert or sun glint by the background surface tests (Section 5.2.1) or the geography database (Section 2.7).

The CLF test also relies on reflected solar to detect low water clouds and fog. The cloud signature is based on the different radiative characteristics of small water droplet clouds at channel 3 and 4 wavelengths. During daylight conditions, the cloud signature in channel 3 is a combination of both emitted and reflected solar energy. At the longer channel 4 wavelength there is only an emitted component. For most other surfaces, the radiative signatures for both channels are approximately equal (e.g. vegetated land is not reflective in channel 3). The result of these characteristics is that brightness temperatures calculated from channel 3 radiance measurements that contain cloud are much larger than for channel 4. The CLF test is applied as a channel brightness temperature difference: if $T_3 - T_4$ is greater than a threshold then cloud is detected. The magnitude of the threshold is defined empirically as:

$$\bullet T_3 - T_4 > 12 \text{ K} \quad (\text{cloud clearing } 4 \text{ K})$$

under normal conditions. However, since this test relies on the reflected component in channel 3, any surface features other than cloud that reflect well at $3.7 \mu\text{m}$ may result in incorrect cloud classification. Sun glint and non-vegetated land surfaces such as desert fall in this category; the CLF test must be modified to handle these surface conditions. Snow is generally not a problem as it does not reflect well at $3.7 \mu\text{m}$. The GLINT test described above (Section 5.2.1) is not sufficient to filter these test results because the CLF test is more sensitive to low levels of sun glint than either the BRIGHT or RATIO tests. Since the level of sun glint that will affect this test cannot be detected directly, additional surface type and geometric conditions are applied to eliminate all conditions that can potentially support glint. These conditions are identical to the geometric requirements for the GLINT test:

- Background surface type must be water ,
- and • $|\psi - \theta| < 40^\circ$,
- and • $120^\circ < \phi < 240^\circ$.

If these conditions are met, then the CLF threshold is increased:

$$\bullet T_3 - T_4 > 54 \text{ K} \quad (\text{cloud clearing } 4 \text{ K})$$

requiring clouds to be extremely bright in channel 3. The CLF threshold is also raised for non-vegetated land backgrounds which are identified either through the spectral DESERT test (Section 5.2.1) or the geography database (Section 2.7):

- if • DESERT

then • $T_3 - T_4 > 20 \text{ K}$ (cloud clearing 20 K).

The desert threshold does not need to be as high as the sun glint threshold because desert reflectance is not as high as sun glint in channel 3. If the $T_3 - T_4$ difference exceeds the appropriate threshold, the pixel is classified cloudy and bit 4 of the intermediate output word is set.

5.2.2.3 Night Tests

The two remaining cloud tests can only be used in the absence of solar illumination. Both tests use channel 3 data and would be adversely affected by the presence of reflected solar radiation in the channel 3 measurements. The first, FLS, is the nighttime equivalent of the CLF test, and again exploits the difference in radiative characteristics of small water droplet clouds between the mid wave and long wave IR bands. The second test, HIGH, exploits the non linearity of the Planck function between the channel 3 and channel 4 bandwidth to detect optically thin cirrus.

The FLS test requires channel 3 and 4 brightness temperature data and is used to detect low cloud and fog at night. Low, nighttime clouds tend to have a lower emissivity at channel 3 wavelengths relative to the longer wavelength channel 4. This results in a slightly lower channel 3 brightness temperature, often less than 1 K difference. The FLS test compares the $T_4 - T_3$ difference against a preset threshold:

• $T_4 - T_3 > 1.0$ (cloud clearing 0.6 K),

if the difference exceeds the threshold, bit 4 of the intermediate output word is set. Real-data tests over desert surfaces commonly exhibited an over-analysis of cloud; this was corrected by raising the threshold for all data identified as desert. For this test, desert is identified in the geography database (Section 2.1.3) as the DESERT test is only applicable under daytime conditions:

if • desert

then • $T_4 - T_3 > 2.0$ (cloud clearing 0.6 K) .

Because the cloud signature used in this test is small, the FLS test can be severely affected by sensor noise in the channel 3 sensor data which often exceeds the cloud threshold. The result of the noise is misclassification of clear data as cloudy. The results of the FLS test are submitted to a noise filter in the TACNEPH algorithm which effectively reduces analysis error due to the noise. The filter is explained in detail in Section 5.2.3.

The HIGH test also uses channel 3 data along with the two long wave channels and is particularly sensitive to optically thin cirrus. In this case the cloud signal is caused by mixed surfaces of different temperatures in the sensor field of view. Due to the non linearity of the Planck function over the channel 3 bandpass, warm radiating surfaces have a proportionally greater influence on the derived channel brightness temperature than do cooler surfaces. This effect is also present at the longer wavelength channels but less pronounced. As a result thin cirrus generally appears warmer at night in channel 3 than at either channel 4 or 5. For detection of cirrus, channel 5 is preferred for comparison with channel 3 since, as discussed earlier in the CIRRUS test, channel 5 temperatures are somewhat lower than channel 4 for ice clouds, thereby enhancing the cloud signature. However, as was also described in the CIRRUS test section, atmospheric water vapor in the field of view will also reduce the channel 5 temperature, potentially causing a false

cloud signature. To test for this, the same technique used in the RATIO test to check for potentially increased low level water vapor is used here; if the adjusted surface temperature climatology exceeds a cutoff level then the channel 4 data are used in preference to channel 5. Thus, the HIGH test checks for:

$$\bullet T_3 - T_5 > 4.0 \text{ K} \quad (\text{cloud clearing } 2.7 \text{ K})$$

if the predicted clear-scene temperature is less than or equal to 295 K, otherwise the test is:

$$\bullet T_3 - T_4 > 4.0 \quad (\text{cloud clearing } 2.7 \text{ K}).$$

If the HIGH test detects cloud, bit 6 in the intermediate output word is set. Since the cloud signature is stronger for the HIGH test than for the FLS test, no noise filtering of the output file is required; however, if in the future the sensor noise increases, filtering may become necessary.

5.2.3 Noise Filter

A well known problem with all extant AVHRR sensors is instrument noise in channel 3. Noise affects the T_3 data differently for each satellite and also changes with time. As such, filtering the sensor data to remove noise effects is problematic. Unfortunately the sensor noise can impact the accuracy of cloud tests that use channel 3 data, particularly at night when T_3 cloud signatures are weakest. Channel 3 noise has not been a significant problem during day conditions since cloud signatures tend to be strong relative to the magnitude of the noise ($< 3^\circ \text{ K}$).

Attempts to filter the $3.7 \mu\text{m}$ sensor data before it was passed to the cloud analysis algorithm were somewhat successful in removing the noise signature but had the undesirable side affect of smearing edges in the imagery (e.g., coastlines, clouds, etc.). Smearing had the same affect as channel registration errors which in turn introduced new errors in the cloud analysis (i.e., false cloud signatures along smeared boundaries). To overcome this problem and still minimize noise effects on algorithm accuracy, a data filter is applied to synthetic images generated from the results of each individual cloud analysis test adversely affected by the sensor noise. In these images, sensor noise is generally manifested as a misclassification of clear pixels as cloud-filled. In clear areas, the noise patterns are interpreted by the cloud algorithms as very small clouds (averaging 1-5 pixels in size), with a characteristic speckled pattern when displayed in image form. The noise filter operates on the spatial characteristics of the synthetic images, relying on the fact that clouds generally form in clusters. The noise filter identifies and removes isolated cloudy pixels that are not part of a cluster (i.e., form a speckled pattern). Less frequently, cloudy areas can be similarly misclassified as clear due to the sensor noise. In these situations the noise filter fills in small clear spots in a generally cloudy area. Currently, sensor noise levels are low enough that only the results of the nighttime FLS test ($T_4 - T_3$) require noise filtering (the cloud signature for this test is relatively small), however, if noise levels increase to a point where other channel 3 tests are affected the same procedure may be applied.

The noise filter is applied to each of the individual cloud analyses as follows. Results from an affected cloud test are placed in an array that has the same spatial coordinates (i.e., rows and columns) as the original satellite image. Each element in the array is assigned a binary number representing the cloud test result for one pixel: 1 = cloud, 0 = clear. An $n \times n$ window is passed over the analysis array, moving one element at a time, and the $n \times n$ elements in the window are summed. If the window sum is less than a minimum threshold value, the center element is set to 0, indicating no cloud detected.

If the sum is greater than the maximum threshold, the center element is set to 1, indicating cloud. If the box sum falls between the thresholds, the value of the center box is left unchanged. The filter operation is always applied to the original rather than modified data so that summation operation is not affected by data points within the current window location that were previously changed by the filter. Figure 7 illustrates examples of the possible window combinations. A sum less than the minimum threshold implies that if the algorithm classified the center element as cloud it is probably anomalous since it is not part of a reasonably sized cluster (see Figure 7a). A window sum greater than the maximum threshold indicates that the majority of elements are cloudy and the center pixel is probably cloudy also (see Figure 7b).

Cloud edges are generally well preserved using this filter method, as illustrated in Figures 7c and 7d. In Figure 7c the window lies at the far edge of the cloud while the window covers more of the cloud in Figure 7d. In both cases the center element would remain unchanged, thereby preserving the actual cloud edge. Currently, window size is defined as 5 x 5 pixels for land areas with a minimum threshold of 8 and a maximum threshold of 17. Over water areas the window size is defined as 3 x 3 pixels with a minimum threshold of 3 and a maximum threshold of 6. The smaller window is used over water backgrounds due to the higher occurrence of small cloud features.

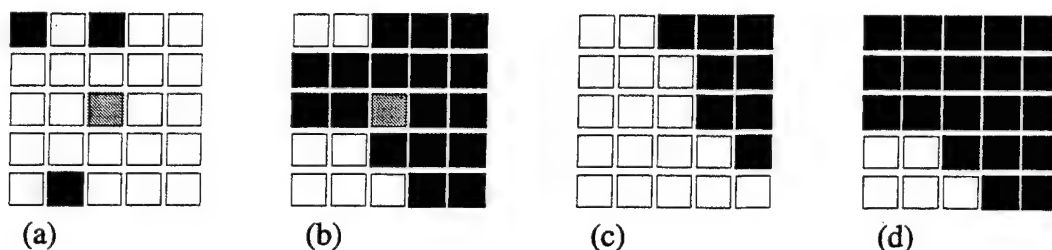


Figure 7. *Cloud test result data filter examples. Each group of boxes represents the cloud analysis results for one filter window. A black box signifies cloud has been detected; a white box means clear; stippled boxes have been changed by the noise filter from cloud to clear (a) or clear to cloud (b).*

5.2.4 Intermediate Cloud Analysis Result

The intermediate cloud analysis provides a synopsis of the cloud and background test results for each pixel in the input image. An 8-bit value is used to characterize the results of the cloud algorithm according to the breakdown in Table 10. Descriptions of the individual background surface and cloud tests are provided in Section 5.2.1 and Section 5.2.2 respectively. Each 8-bit output word represents results for the pixel at the corresponding file location (i.e., row and column) in the input image. This serves two purposes: 1) it simplifies the database management problem in that the resultant array is the same size as the input image and 2) it supports direct visual comparison between the results and input data when both are displayed as raster images on a suitable display device. Note that the intermediate analysis contains the actual results of each cloud test; individual cloud test results are not checked against or modified by the results of the background surface tests until the final analysis step described below in Section 5.2.5. So if a visible channel cloud test misclassifies a clear pixel as cloudy due to problematic surface conditions such as snow or sun glint, the cloud result is maintained in this intermediate analysis. Evaluation of intermediate results proved extremely useful during algorithm development in that the researcher could evaluate the accuracy of the individual cloud detection tests and judge how much of the scene was actually misclassified due to surface conditions.

Table 10. Intermediate Output Format Bit Encoding

Bit	Description
0	GLINT (water), DESERT (land)
1	COAST (1) Or (0) other
2	CIRRUS test (solar independent)
3	COLD test (solar independent)
4	CLF (day) FLS (night)
5	RATIO (day)
6	BRIGHT (day) HIGH (night)
7	SNOW (day)

5.2.5 Final Cloud Analysis Result

As noted in Section 5, results from all tests, cloud tests and background tests, must be interpreted jointly to provide a final cloud analysis. The rules according to which a pixel is declared cloudy or clear are based on results of all the cloud and background tests. For nighttime situations, defined by solar zenith angles greater than 90°, the process is straightforward. If any nighttime test detects cloud, the pixel is classified as cloud-filled. These nighttime tests are the test for fog and low stratus, FLS and the test for thin cirrus cloud, HIGH.

During daytime conditions, the process for evaluating individual cloud test results is more complex. Several of the cloud tests rely on reflected solar radiation and thus can be confused by highly reflective terrestrial backgrounds such as sun glint, snow/ice cover, and desert. These problematic backgrounds may degrade the accuracy of the AVHRR cloud analysis algorithm if they are mistakenly identified as cloud. To avoid this problem individual test results that classify pixels as cloud-filled are not used to generate the final cloud product when it is likely they are erroneous due to problematic surface backgrounds. The background filter tests described in Section 5.2.1, and the Geography database described in Section 2.7, are employed to filter these backgrounds from the final cloud results. Filtering is achieved by negating the results for a particular cloud test if an appropriate background filter flag has also been triggered for the pixel being evaluated. Table 11 provides a look up matrix of the filters employed by each of the seven individual AVHRR cloud detection tests.

In addition to background surface filters, several tests use cloud detection thresholds designed to be more restrictive over problematic background surfaces. All restrictions that must be considered when analyzing results of the individual cloud tests to produce a final cloud classification are summarized below. Included in these descriptions are solar zenith angle requirements and conditions under which the results of the individual cloud tests are not used (filtered) due to problematic background surfaces.

CLF

- Solar zenith angle must be less than or equal to 90°
- Desert and sun glint backgrounds require stricter cloud detection thresholds
- Test result is not used under the following conditions:
 - Spectral snow test is positive (Section 5.2.1)

Table 11. Background Surface Filters for Cloud Tests

	Spectral Test Filters			Supporting Data Filters		
	Sun Glint	Snow/Ice	Desert	Snow/Ice AFGWC	Geographic Desert	Geographic Coast
CLF		✓				
RATIO	✓	✓	✓	✓	✓	✓
BRIGHT	✓	✓	✓	✓	✓	
COLD		✓ ¹				
CIRRUS		✓ ¹				
FLS						
HIGH						

¹ During daytime conditions

RATIO

- Solar zenith angle must be less than or equal to 80°
- Cloud detection threshold maintained as a function of humidity
- Test result is not used under the following conditions:
 - Sun glint test is positive (Section 5.2.1)
 - Spectral snow test is positive (Section 5.2.1)
 - Spectral desert test is positive (Section 5.2.1)
 - Geography database indicates desert background (Section 2.1.3)
 - Geography database indicates background is coast (Section 2.1.3)

BRIGHT

- Solar zenith angle must be less than or equal to 60°
- Water and land backgrounds, identified by the geography database (Section 2.1.3), use separate cloud detection thresholds
- Test result is not used under the following conditions:
 - Sun glint test is positive (Section 5.2.1)
 - Spectral desert test is positive (Section 5.2.1)
 - Spectral snow test is positive (Section 5.2.1)
 - Geography database indicates desert background (Section 2.1.3)

COLD

- Water, land, coast, and desert, identified by the geography database (Section 2.1.3), use separate cloud detection thresholds
- Test result is not used under the following conditions:
 - Spectral snow test is positive (Section 5.2.1)

CIRRUS

- Test result is not used under the following conditions:
 - Spectral snow test is positive (Section 5.2.1)

FLS

- Solar zenith angle must be greater than 90°
- Desert backgrounds identified by geography database (Section 2.1.3) require a stricter cloud detection threshold

HIGH

- Solar zenith angle must be greater than 90°
- Cloud detection test channel combination selected as a function of humidity

5.2.6 AVHRR Output Product

The output product of the AVHRR Cloud Analysis Algorithm is an 8-bit quantity termed the Mask and Confidence Flag (MCF). The MCF is a bit-mapped quantity that stores cloud/no cloud information plus flags for missing data and the confidence flag. Bit assignments for the AVHRR MCF cloud analysis algorithm output are provided in Table 12. One MCF is produced for each pixel in the input AVHRR image. MCF bit assignments are made as follows:

Table 12. AVHRR Cloud Analysis Algorithm MCF File Bit Assignments

Bit	Assignment	Description
0	Cloud Mask	ON = Cloud-Filled OFF = Cloud-Free
1		Not Used By AVHRR Algorithm
2		Not Used By AVHRR Algorithm
3		Not Used By AVHRR Algorithm
4		Not Used By AVHRR Algorithm
5	Data Dropout	ON = Missing or Unreliable Data
6	Confidence	0 = Missing Data; 1 = Low;
7	Flag	2 = Middle; 3 = High

Cloud Mask - Bit 0

The cloud mask bit is set to ON, indicating a cloud-filled pixel, if the pixel is determined to be cloud-filled by the final cloud classification.

Bit 1

Not used in this algorithm

Bit 2

Not used in this algorithm

Bit 3

Not used in this algorithm

Bit 4

Not used in this algorithm

Data Dropout - Bit 5

The data dropout bit is set if the data for the pixel are either missing or unreliable.

Confidence Flag - Bits 6 & 7

The confidence flag bits are set to indicate LOW (1), MIDDLE (2), or HIGH (3) confidence.

5.2.7 AVHRR Cloud-Clearing Procedure

The cloud-clearing procedure of the AVHRR algorithm simply requires running the AVHRR algorithm with less restrictive cloud thresholds. The intent is to find all cloud in the scene with a bias toward overanalysis. Note that the thresholds must be set to insure that some clear areas are identified correctly in order that the clear scene statistics database be regularly updated with new information. Because of the difficulty in discriminating cloud from certain backgrounds, if a pixel is determined cloudy by any cloud test, irrespective of the background type tests, it is not included in the clear scene statistics. AVHRR cloud-clearing thresholds are noted in parentheses () next to the test equations.

5.3 Testing and Validation of Cloud Algorithms

Algorithm testing and validation using real-satellite data was a major component of the TACNEPH program. A major issue related to test and validation of nephanalysis algorithms is the lack of universally recognized ground truth data. For TACNEPH, manual analysis of sensor data was chosen for ground truth over other potential sources, such as surface observations, for two reasons: 1) our belief that comparisons between surface based and satellite based observations are problematic and 2) the high degree of accuracy that can be obtained from careful analysis of sensor data. Satellite and surface based observing systems do not view cloud in the same way, this is manifested in such things as: differences in viewing geometry including, say, a surface observer's tendency to see sides of clouds, the surface observer's sky dome is unlikely to be representative of the larger satellite observed scene, differences in cloud characteristics and obscuration when viewing from above and below, misregistration of sensor data relative to the observers location, and the lack of reliable surface observations over most parts of the world. Problems associated with comparisons of satellite and surface cloud estimates were studied extensively by Hughes and Henderson-Sellers (1983). They point out that while cloud distributions based on surface based observations show good agreement with distributions derived from satellite data, direct comparisons between a given satellite analysis and specific surface observations are problematic. Even the use of data from large mesoscale networks provide formidable obstacles: such networks are scarce and generally do not even report cloud amount. The recent FIRE intensive field observing programs offer a potential source for detailed, high resolution cloud data, however, the coverage area was still relatively small compared to satellite coverage, the data are not easily obtained, and the program concentrated primarily on cirrus cloud.

Manual analysis of sensor data for comparison with automated analyses, while incestuous, has the major advantage of concurrency (i.e., same viewing geometry, solar illumination, time of day, and coverage). Also, trained human analysts, with the aid modern image processing systems, can exploit spectral information in multispectral data in addition to spatial feature recognition that has traditionally been the strength of manual photo interpretation. The interactive image enhancement and display functions described in Section 3.2 were used extensively by the manual analysts to assist in correctly classifying satellite imagery. Surface observations (when available) were not ignored, however, they were used only for guidance by the analyst interpreting a scene and not to replace the satellite based analysis. Surface observations were particularly useful to detect or confirm the presence of low clouds, fog, and multiple layer systems.

5.3.1 Algorithm Testing

Testing of the TACNEPH cloud detection algorithms on real satellite data was an essential part of the development process. Many advances and refinements to the cloud detection capabilities resulted from direct manual analysis of numerous satellite images. Trained satellite data analysts examined the algorithm results by manually comparing the intermediate cloud analysis to the original satellite data by displaying the satellite data as a raster image with a color coded cloud mask overlay. In total, over 1500 images were analyzed in this way. These provided an excellent record of recurring problems such as over or under-analysis of cloud, seasonal effects and sensor noise problems.

Early in the program, initial case studies were performed on a limited AVHRR dataset from four regions representing extensive climatic variation (Figure 8): Saudi Arabia data included desert and warm ocean conditions; Brazil data contained moist tropical regions; the Alaska data had snow, sea ice and intricate coastlines; and the northeast US data provided temperate climatic conditions. However, the data set spanned a maximum of 10 days and only daytime data were available. At that the time, there was no access to DMSP data. Although the AVHRR data provided valuable insight into the effectiveness of the cloud detection scheme over different climatic and surface regimes, it quickly became apparent that an extended time series of data from all satellites was crucial to the development of accurate robust algorithms. Application of the algorithms over both diurnal and seasonal changes was important as was the required historical record of satellite derived corrections to the stored climatology (Section 4.2).

A modification to the TACNEPH contract resulted in the purchase of two satellite ground stations which were installed at the Phillips Laboratory (PL/GPA); a NOAA ground station collected data from NOAA-11 and NOAA-12 starting in the spring of 1992 and a DMSP ground station collected either F10 or F11 data beginning in the fall of 1992. Over the course of a year, real-time transmission data from every pass in the ground station line of sight were collected, ingested into TDB and analyzed for cloud. Four ROIs were selected for testing purposes as shown in Figure 9. These regions were chosen to stress the algorithm over the most variable set of climatic and background conditions for which data were available. The region centered over Hudson's Bay encompassed some of the more difficult conditions over which to detect cloud, including large snow and ice fields over land and water, permanent and new sea ice formations and large, rapid changes in land and water surface temperatures, especially during the fall and spring. The northeast US region provided data representative of a mid-latitude region with moderate climatic conditions. Variations in terrain, small lakes and coastlines provided some difficult challenges. The southeast US region over Georgia and Florida included tropical data with very high humidity. In the ocean region, sun glint and low clouds were the biggest challenges.

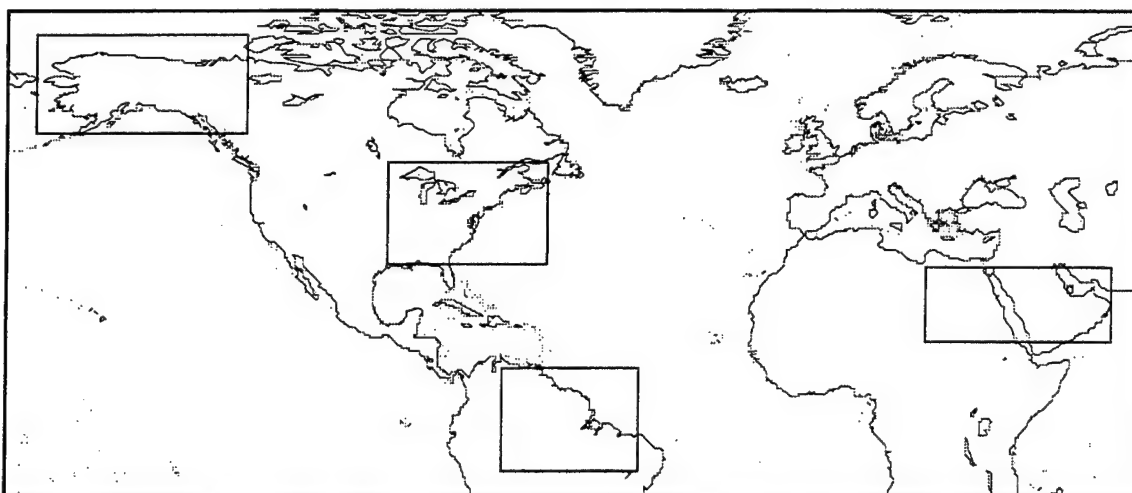


Figure 8. Initial ROIs for testing of nephanalysis algorithms.

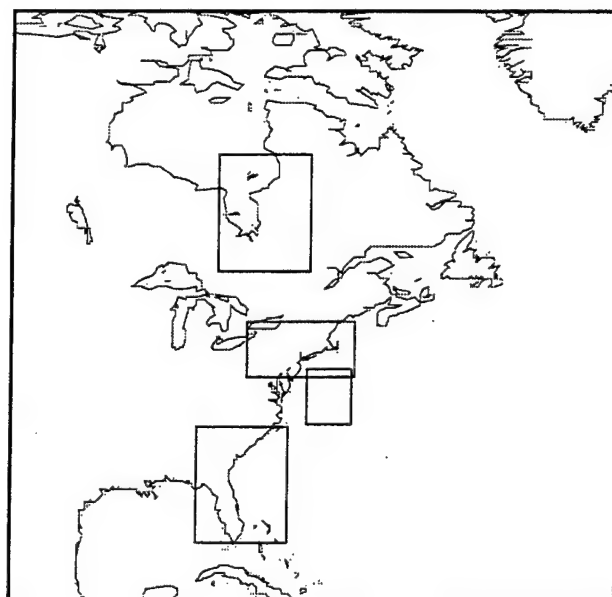


Figure 9. Regions of interest selected for nephanalysis testing using DMSP and NOAA data from the PL/GPA direct-broadcast satellite ground stations.

The large quantity of data to be analyzed, from upwards of 12 passes per day, resulted in the need for image processing and manipulation software to facilitate data access and display. A set of interactive utilities was designed and developed with which the analyst can display sensor data images from any satellite and overlay intermediate cloud results as a color-coded cloud mask on a 32-bit image and retrieve a variety of information about the sensor data and cloud analysis (see Section 3.2). This capability has proven to be an extremely powerful tool for analyzing algorithm performance over different scenes from the case study data. Image information capabilities include pixel-by-pixel retrieval of brightness temperature and albedo equivalents of image gray shades for all sensor channels, latitude and longitude, solar geometry including solar zenith, satellite zenith and solar/satellite azimuth angles, climatology correction information including reference

temperature, 2σ limits, and correction factors, and specific cloud test information including channel differences and ratios. Display software also provides for application of various normalization functions to the displayed imagery. The routine contains a list of mathematical functions, such as solar and bi-directional reflectance distribution function (BRDF) correction factors, which are specified by a coded input parameter. The selected mathematical operation is then automatically applied to the source data loaded in display memory and results are loaded and displayed in a separate area of memory.

Daily algorithm testing was instrumental in highlighting both the strengths and weaknesses of the cloud algorithms. The findings led to major changes in the algorithms, including development of new tests as well as modifications to existing tests. Examples of algorithm characteristics, strengths, and weakness that were identified and addressed during the testing process are provided here to give the reader a sense of how the algorithms perform over different conditions.

Probably the biggest challenge for the algorithms is accurate discrimination of low cloud over highly reflective clear backgrounds, specifically snow and ice, sun glint and desert, using the daytime AVHRR tests, BRIGHT, RATIO, and CLF and the OLS visible and bispectral tests. Low cloud is a difficult problem because it is thermally indistinct from the surface and therefore not readily detected by the infrared cloud tests. As detailed in Section 5.2.1, background surface tests in the AVHRR algorithm were used to identify potentially problematic backgrounds. The discrimination of snow and ice from cloud using SNOW, is good when there is sufficient solar illumination (i.e., solar zenith angle of less than 60°). Between 60 and 80 degrees of solar zenith, the detection of snow is uncertain. Although the SNOW test does not detect all the snow in a scene due to weak spectral signatures, the only condition where the algorithm over analyzes snow is within cloud-on-cloud shadows. The main disadvantage of SNOW is that it is not applicable when the solar zenith angle is greater than 80° , so at night there is no way to classify snow backgrounds. Anytime existing snow backgrounds are not detected, the potential for problems arise. All cloud tests have, at one time or another, misclassified cloud-free snow surfaces as cloud during testing. The problem is most serious for the AVHRR COLD and CIRRUS tests and the OLS bispectral algorithm, which can classify large snow fields as cloud. This problem was seen repeatedly over the Hudson's Bay ROI from early fall through late spring. Modifications to the SNOW test and the cloud tests improved detection accuracy considerably but did not eliminate the problems. In the OLS algorithm, there is no means of detecting snow spectrally; the AVHRR algorithm relies on $3.7 \mu\text{m}$ channel for snow/cloud discrimination, however, there is no comparable band on the OLS instrument.

Sun glint over water surfaces is also a problem for the AVHRR and OLS tests that rely on visible data. In the AVHRR algorithm, the GLINT background filter test detects enough sun glint to remove false cloud classifications from the BRIGHT and RATIO tests. However, the CLF test ($T_3 - T_4$) for low cloud is sensitive to levels of glint too low to be detected by the GLINT test. To compensate, the CLF test is modified for water points whenever the solar/satellite geometry has the potential to support sun glint. Reliance on pure geometric considerations is less restrictive than spectral tests because, depending on sea state (an unknown within TACNEPH), the area of specular reflection can be large and oriented in whatever direction the wind is from. Since there is no way to predict these effects, all locations that could support glint are assumed to be contaminated. For the CLF test, detection of cloud in potential glint regions is restricted by raising the cloud signature threshold. Fortunately this does not significantly impact the accuracy of the AVHRR analysis, since other tests, in conjunction with the GLINT test, do provide good results. The main danger is avoiding over classification in these conditions. In the OLS algorithm, there is no spectral sun glint test so that all cloud tests rely on geometric glint filters. For this algorithm, sun glint is a more serious problem since restrictions on the use of visible

data directly impacts the ability to detect low cloud. For both algorithms, water points incorrectly classified as land in the geography database remain a problem.

Cloud detection over reflective land surfaces such as desert posed an additional problem. While the snow and sun glint filters were part of the original AVHRR algorithm, the DESERT test was developed when real-data tests showed that the geography database desert classification did not sufficiently identify problem locations. This DESERT test has proven to be extremely effective in identifying reflective land surfaces that can cause false cloud signatures in some cloud tests. Using DESERT in conjunction with the geography database correctly classifies almost all problem backgrounds of this type. Again due to the absence of a 3.7 μm sensor channel, the OLS algorithm must rely solely on the geography desert classification resulting in situations where over-analysis of cloud over misclassified desert regions can occur. A proposed solution to the lack of snow and desert tests in the OLS algorithm is to use the AVHRR DESERT and SNOW test results to build dynamic desert and snow databases for the local region.

One source of error in low cloud detection results from a combination of the coarse resolution and the minimal information content of the geography database. Geography problems are seen repeatedly to affect many tests. For example, both the OLS and AVHRR single channel infrared threshold tests rely on a comparison of predicted clear-column surface brightness temperature with the satellite observed brightness temperature to detect cloud. Within an analysis region, the satellite temperature of the warmest pixel is used to estimate the clear column temperature (Section 4.2). When the clear region contains a large temperature gradient, such as often occurs between land and water, the warmer surface is declared clear while the colder surface can be misclassified as cloudy. This problem can be rectified by segregating the land and water points and calculating separate predicted clear-scene temperatures for each group. However, in TACNEPH, the resolution of the available geography database (10') is much coarser than the satellite data (1 km). Coastlines are poorly defined and rivers and small lakes are generally not identified. Accurate division of points by background type is impossible thus perpetuating the problem of over-analysis near coastlines. The problem is made worse by the fact that the geography database contains only a small number of surface classification types making stratification by background type difficult. An example, in addition to coastlines, where rapid changes in background type can cause undetected thermal gradients are high mountain terrain, such as the Himalayas, that are next to low, flat lands. Without some indication in the geography database of their existence, the changes in visible and infrared characteristics between these surfaces that can affect cloud algorithm performance will go undetected.

It is also recognized that both the geography and surface temperature climatology databases are biased towards land classifications. The convention in these databases for mixed land/water locations is to use land characteristics. Anytime this type of misclassification occurs where there is a contrast between either the visible or infrared characteristics of the backgrounds, the possibility for degradation of cloud algorithm performance exists. Examples include sun glint over locations misclassified as land, cold water adjacent to warm land, and mixed fields of view averaging out to a false cloud signature in the AVHRR RATIO test. In the original cloud algorithms, the RATIO test routinely identified mixed land/water fields of view, such as occur along coastlines and rivers, as cloud. The solution was to negate positive results from the RATIO test for points identified as coastline by the geography database. Rivers and other small bodies of water too small to be included in the geography remain a problem.

Areas of high humidity are another problem that affects the AVHRR RATIO and HIGH tests. During testing this was seen most often in the southeast US ROI (Figure 9). In the daytime, high concentrations of suspended aerosols near the surface cause increased

scattering in the visible AVHRR channel 1 relative to channel 2. Over vegetated land this can produce a channel 2/channel 1 ratio that is typical of cloud rather than clear background. At night in humid regions, the HIGH test can detect more sub-visual cirrus than can be found in the manual analysis. The aerosols attenuate the channel 5 radiance translating to a lower derived brightness temperature. Under extreme cases the resulting $T_4 - T_5$ difference can be large enough to exceed the cloud threshold. Since no upper air moisture information is available to TACNEPH, the potential for high humidity levels is assessed through the predicted clear-scene brightness temperature. If the predicted temperature is high then, following the assumption that increased capacity for moisture will result in increase aerosols, the cloud test thresholds are modified to reduce the incidence of false cloud detection. This method of parameterizing humidity levels could likely be improved with better humidity information such as can potentially be provided from the SSM/T and TOVS instruments.

Another problem for some cloud tests are multiple, vertically stacked cloud layers. While basic cloud detection is seldom a problem, AVHRR tests sensitive to thin cirrus can be confused when the ice cloud occurs over an optically thick water cloud. Since these AVHRR tests have potential for discriminating thin cirrus from other types of cloud, it is important to be aware of this condition for applications that require information on optically thin cirrus.

5.3.2 Validation Procedure

As discussed above, the TACNEPH cloud detection algorithms were routinely and extensively tested by visually comparing the intermediate cloud analysis (displayed as a color coded cloud mask) to the original satellite data. However, a separate objective algorithm validation procedure was developed to provide a more rigorous and quantitative measure of algorithm accuracy. The TACNEPH cloud algorithm validation plan was presented and approved at the 22-23 May 1990 contract program review. It called for statistical comparisons between manually analyzed sensor data and the automated algorithm results for globally varying scenes. This approach was used extensively on previous programs at the Phillips Laboratory to validate work done in support of the AFGWC RTNEPH program and for the SSM/I calibration/validation study (d'Entremont et al., 1989; Gustafson and Felde, 1988; 1989). In accordance with the accepted validation plan a formalized procedure for generating manual analyses from multispectral sensor data was developed. This procedure is similar to those used in the previous studies although it was extensively customized for the TACNEPH application. Case study data were collected to test the algorithms over a range of conditions using available ground station resources.

TACNEPH algorithm validation consists of objective comparisons between automated algorithm results and manually analyzed satellite imagery using case studies for four seasons over the East central United States and the Atlantic Ocean. The output of the manual analyses is used as ground truth for the purposes of these comparisons. This approach was selected because it was felt that a manual analysis of the available data by an experienced analyst provided the most accurate and consistent ground truth data possible for evaluating satellite nephalanalysis algorithms.

Case study data were selected to be representative of the range of conditions the algorithms were expected to encounter operationally. It was assumed that performance of the cloud algorithms is dependent on (at least) cloud type, scene illumination, and background conditions. However, case study selection was somewhat restricted in that the only sources of data readily available to the TACNEPH program were DMSP/RTD and NOAA/HRPT direct broadcast ground stations. Thus the geographic extent was limited to

the coverage area for these systems (i.e., the eastern US. and Canada to the western North Atlantic). To exercise the algorithms over as broad a range of conditions as possible given the input data constraints and available personnel resources, two ROIs within the coverage area were selected to represent terrestrial and oceanic backgrounds (Figure 10). Data were collected for each ROI over 8-10 day periods from four seasons: June, September, December, and March; for daytime, nighttime and near terminator orbits.

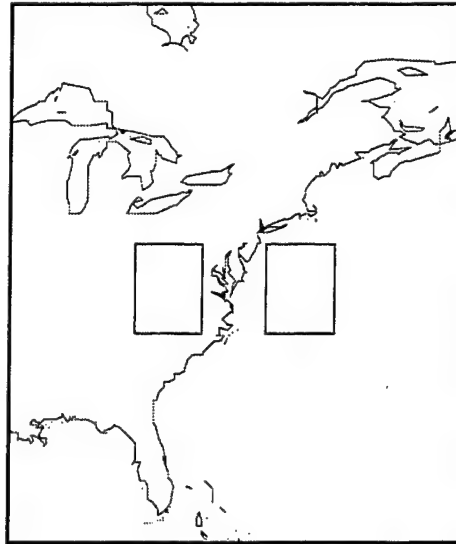


Figure 10. Selected regions of interest for validation study; the land ROI covers the area 35-40 N latitude, 78-83 W longitude; the water ROI covers the area 35-40 N latitude, 73.5 - 58.5 W longitude.

Considerable emphasis during the validation process was placed on the creation of accurate and consistent manual cloud analyses for the selected case study periods. This was necessary both because of the importance these analyses have as ground truth but also because this was by far the most time intensive part of the procedure. Processing of the selected case study data required analysis of approximately 120 AVHRR and 60 OLS scenes (differences in scene numbers result from the PL/GPA DMSP ground station limitation to receive transmissions from only one satellite at a time due to restrictions on the KG-44a decryption device as opposed to the NOAA ground station which can receive data from two satellites concurrently). To assist in manually classifying and cataloging such a large amount of data, a comprehensive interactive computer program called TBLANK was developed and implemented on the dedicated image processing computers available at the Phillips Laboratory (see Section 3.2 for a description). TBLANK provided both an automatic interface to the TACNEPH database and a formalized methodology for performing the analysis on whatever mix of visible, infrared and multispectral satellite imagery was available.

In addition to satellite data, the analyst also has access to conventional surface observations over the land background region of interest (Figure 10). Surface based reports of cloud cover are used only for guidance during the manual procedure and not to replace the satellite based analysis. For example, if an analyst suspected a fog or low stratus deck from examination of, say, an AVHRR composite 3.7 and 11 μm image, this could be confirmed by surface reports from that area. However, a surface report of fog, without supporting evidence in the satellite imagery, would not be extrapolated to the larger satellite scene.

The manual cloud analysis is considered as a single blind procedure (as opposed to a double blind) since the analyst has no knowledge of the automated algorithm results but is aware of the algorithm characteristics. Final output products of both the manual and automated algorithm analyses are binary images depicting the cloud-filled (1) and cloud-free (0) regions of the scene on a pixel-by-pixel basis. Fractional cloud amount can be readily calculated for any selected grid size. For this study, comparison statistics were computed over a 16 x 16 pixel grid selected to approximate the grid spacing expected to be used in the operational implementation of TACNEPH.

The TACNEPH algorithm validation study was a combination of objective and subjective analyses. First, a quantitative or objective analysis was performed on each case study via a statistical comparison of the fractional cloud amounts determined by the automated algorithm and the manual analysis. Second, a subjective analysis was done wherein the cloud detection results of each case were visually compared. This subjective analysis proved useful both as a means of verifying the statistics and explaining anomalous results.

Identification of statistics which accurately described the results proved difficult. A variety of statistical procedures were reviewed including analysis of variance, intraclass correlation coefficient and ordered rank statistics. These procedures were discarded because either the cloud fraction data did not meet the test requirements or the tests provided little useful information. It was decided that simple statistical measures (e.g., mean difference in cloud fraction, absolute mean difference in cloud fraction) in combination with the subjective analysis provided the clearest understanding of the validation study results.

5.3.3 Validation Results

Comparison statistics for the study periods of March, June, September and December are summarized in Table 13. The statistics are stratified by surface type (land and water) and by orbital time (day, night and near terminator) to highlight any differences in algorithm performance under varying scene illumination and background. A total of 120 AVHRR and 60 OLS satellite images were analyzed.

The AVHRR algorithm exhibits excellent agreement with the manual analysis, especially for the June, September and December time frames. The March cases include some anomalous results which will be addressed below. The mean absolute difference (MAD) in cloud fraction ($\sum |A_{TACNEPH} - A_{manual}|$) was determined to be the best descriptor of algorithm accuracy because it specifies the magnitude of the difference in fractional cloud amount irrespective of which analysis identified more cloud. The MAD for the entire AVHRR study averages 11% with a range of 3% to 25%. Excluding the March land cases, the average MAD is 9.5%. While the signed mean difference ($\sum (A_{TACNEPH} - A_{manual})$) has shortcomings in that it falsely reduces the discrepancies, it does show that there is no systematic bias in the automated algorithm toward under- or over-analysis of cloud. In just half of the categories in Table 5-7a (11 out of 24), more cloud was identified by the automated algorithm than by the manual analysis.

Results from scenes over land backgrounds from the March study are significantly poorer than the others. Generally, the automated algorithm detected more cloud than the manual analyst. Inspection of the March satellite imagery and analysis showed that a large

Table 13. Statistical Comparison of Fractional Cloud Amount Differences (%) for the AVHRR Algorithm (a) and the OLS Algorithm (b)

	DAY				NIGHT				TERMINATOR			
	March	June	Sept	Dec	March	June	Sept	Dec	March	June	Sept	Dec
LAND												
Mean	13.3	10.6	0.8	-2.3	18.9	-2.2	0.9	-10.2	23.6	-8.3	5.1	-7.9
Difference												
Mean	14.1	16.5	3.48	3.95	19.0	12.6	14.5	13.5	25.4	10.0	9.3	9.1
Abs Difference												
WATER												
Mean	3.6	-8.7	-8.7	-6.2	3.2	-6.4	2.3	-3.2	7.4	-2.2	-1.8	-11.5
Difference												
Mean	5.6	11.9	9.9	9.7	5.9	9.7	11.1	13.3	8.6	15.9	8.6	13.4
Abs Difference												

(a)

	DAY				NIGHT				TERMINATOR			
	March	June	Sept	Dec	March	June	Sept	Dec	March	June	Sept	Dec
LAND												
Mean	12.9	16.5	5.5	5.4	-22.7	-9.7	-13.4	-14.6	-21.3	4.8	-8.1	-7.6
Difference												
Mean	20.9	20.8	9.3	5.7	22.7	21.7	15.4	18.9	26.8	17.4	8.4	7.9
Abs Difference												
WATER												
Mean	-6.1	-10.7	-13.4	-4.1	-17.8	-8.9	-13.5	-19.3	-16.4	-8.8	-3.8	4.9
Difference												
Mean	9.1	12.7	17.1	8.3	19.0	9.9	14.9	19.9	17.7	10.8	7.9	12.3
Abs Difference												

(b)

snow field was incorrectly classified as cloud. During the case study period, there was a blizzard which produced a lot of snow and lowered the temperature of the land surface by up to 30 K. The cloud algorithm uses a threshold test which relies on a dynamically corrected reference surface temperature that is based on clear-scene information gathered from preceding days. The algorithm was unable to correct immediately for the drastic background temperature change and misclassified the anomalously cold surface as cloud. The analyses were poor for two days which resulted in a degradation in algorithm performance for March. However, once the algorithm adjusted to the new temperature conditions the statistics for the remainder of the March study were comparable to the other months.

The OLS algorithm performance exceeded expectations for the validation case study given the severe data limitations of the two-channel OLS compared to the five-channel AVHRR sensor. As described in Section 5.1, the OLS analysis is most often produced using only the single channel IR data. Use of visible data is problematic: at night the

quality of visible data obtained from the photomultiplier tube (PMT) is not particularly suitable for cloud detection, and during the day, the visible data is often not used because of the difficulty in characterizing the backgrounds correctly. So, the accuracy of the OLS algorithm is critically dependent on the single channel IR threshold and the ability to produce a valid estimate of the surface temperature.

In spite of this limitation, the algorithm performed well. In 16 of the 24 categories shown in Table 5.7b, the mean absolute difference in cloud fraction (MAD) between the automated and manual analyses was less than 30%; the average MAD for the entire case study was 25.2% with a range of 8.0% to 49.8%. Careful analysis of the individual cases in each category show that the large MADs (> 30) are usually the result of one or two very poor analyses which skewed the data within the category. For example, as in the AVHRR study, the March data was difficult to analyze correctly because of snow contamination. Scenes over water backgrounds proved unexpectedly difficult to classify especially during the winter months. During March and December, sunlight conditions are low; thus the algorithm relies more heavily on just infrared data. Thermally indistinct clouds (e.g. low cloud and cloud edges) were often missed by the algorithm resulting in cloud amount differences of between 10 and 20%. This problem was compounded by the manual analyst's misclassification of Gulf Stream eddies as low cloud decks. Misclassification problems, either automated or manual, occurred less often for land backgrounds. Why this difference exists is not well understood. It is conjectured that more very low cloud existed over water than land or that the reference climatology was not representative of the water temperature. However, of more concern than missed cloud edges is the apparent systematic bias of the OLS algorithm. In 20 out of 24 categories, the manual analyst detected more cloud than the automated algorithm (signed mean difference < 0). Visual examination and comparison of the manual and automated analyses show that the automated analysis is generally underanalyzing low cloud. Note that for the purposes of collecting comparison statistics on cloud fraction, data that were classed as partly cloudy by the algorithm were treated as cloud-filled.

In this validation study visual comparison of the algorithm and manual analysis results have provided important insight into the causes of disagreements between the manual and automated analyses. Interpretation of the results based on comparison statistics alone is difficult largely because it is not safe to assume that the manual analyses are always a perfect representation of truth. Situations have been identified where the automated analysis is superior to the manual analysis, yet, because of the way the validation study was set up, these differences contribute to the algorithm error statistics. For example, assume two theoretical scenes A and B. Scene A contains many small altocumulus clouds. The manual analyst interpreted the cloud edges differently than the algorithm resulting in a mean fractional cloud amount difference of 15%. Scene B is characterized by fog and low cloud in river and mountain valleys. The manual analyst misses all the fog and much of the low cloud while the algorithm identified it correctly resulting in a difference of 10%. The error in scene A is acceptable; the error in scene B is not because entire cloud fields were actually undetected. Careful visual comparison of results for each scene in the validation study have shown that most of the discrepancies occur at cloud edges. This is chiefly due to differences in the way that a person and the algorithm define edges. The analyst relies predominantly on textural information whereas the automated algorithm uses only spectral information. Cloud edges are often texturally or visually distinct from background surfaces while for thinner clouds enough background radiation can pass through the cloud as to make it difficult to detect using spectral measures.

6. QUALITY CONTROL AND TUNING

Interactive quality control (QC) techniques are required to ensure continued accuracy of the TACNEPH cloud analyses and to adjust algorithm sensitivity in response to mission specific requirements. Contract requirements were to investigate techniques to improve QC procedures for TACNEPH and recommend methods to reduce QC manpower. Work on this task was divided between development of quality control flags and tuning options. Quality flags were developed to provide an assessment of the relative accuracy or reliability of a given analysis. Since the TACNEPH algorithm is required to provide a cloud analysis for all possible data combinations that may be encountered in a tactical terminal, it was recognized that the quality of the analysis would vary with the available data mix. The requirement for data quality flags was established to provide the end user with an indication of the relative reliability of a given analysis. The main objective of the task is to determine what objective criteria should be used to measure algorithm accuracy. Several quantifiable measures were considered including the strength of the cloud signal (i.e., how close to the cloud threshold is the measured quantity), the number of tests that separately detect cloud, and the suitability of the analysis for a particular type of cloud (e.g., visible data for cirrus or thermal IR for low stratus).

Tuning options are needed to provide a tactical user with a measure of control over the sensitivity of the cloud algorithms while simultaneously providing guidance on how the options are to be applied. Much of the work on this task centered on how to provide a user who may have little or no knowledge of the cloud analysis algorithm, or even meteorological satellite data analysis, with a tuning mechanism that would be useful and easily understood. The approach is to limit what the user can do to fixed adjustments to modify the algorithm sensitivity to cloud. The available options are analogous to a dial with three settings. The center dial position corresponds to the optimal sensitivity setting for that layer, that is the setting determined to most accurately detect cloud without over analyzing. One position on either side will allow a relative increase in sensitivity (with the possibility with an increase in false alarms) and on the other a relative decrease. This should provide the user with sufficient control to adjust the algorithm sensitivity to match a particular application.

6.1 Analysis Confidence Flags

Data quality flags are added to a cloud analysis to provide the end user with an indication of the relative accuracy of the model at a given location under a given set of conditions. This was perceived as necessary since it is known that algorithm accuracy is affected by (at least) the mix of satellite data, background type, and time of day. However, it was concluded that providing end users with too much information would, in most cases, be counter productive and what would likely be most effective would be a single straightforward metric. The recommendation was for a three value expression indicating low, moderate, or high confidence in the cloud analysis since this is information that would likely be useful to tactical users and can be easily extracted from the algorithms. By using this type of categorization the quality measures for each cloud analysis can be coded as a 2-bit value. This in turn simplifies the presentation of the flag since they can be easily accommodated and displayed as synthetic, color-coded images on a tactical terminal.

An audit trail had also been previously suggested as information that would be potentially useful to an end user for evaluating cloud analysis robustness. However, in discussions at PL it was decided that an audit trail contains more specialized information than most users would want (or be able to interpret) so it was decided not to include one

with the data quality flag. Audit trails could, of course, be added as a separate model output parameter during operational implementation.

There was also considerable discussion about what criteria would feed into a data quality flag. Identification and quantification of conditions that affect algorithm accuracy became the major study topic during the task, several possibilities were examined:

- strength of the cloud signal (i.e., distance from the cloud detection threshold);
- in the multispectral algorithms, the number of separate tests that detect cloud;
- in the single channel IR tests, the likelihood that the climatology correction factor is cloud contaminated (i.e., distance from the statistical 2σ limits);
- the relative skill of individual tests in detecting specific cloud types (e.g., relatively low skill of single channel IR test for low cloud);
- potential impact of water vapor effects on measured radiation (e.g., suspected high humidity areas at low satellite zenith angles); and
- potential sun glint regions.

Data quality flags are provided separately by the OLS and AVHRR algorithms.

6.1.1 OLS Confidence Flag Determination

OLS algorithm accuracy estimates are based on pixel attributes that can be derived from information available to the analysis algorithm such. These include constraints imposed by external factors and the strength of the cloud signature as measured by the analysis algorithm. Accuracy estimates are intended to provided the end user with an indication of how much confidence to place in the analysis for any given pixel and, as such, are referred to as confidence flags. Three levels of confidence are defined: LOW, MIDDLE, and HIGH. The eleven pixel attributes listed in Table14 are used to establish the OLS analysis confidence level.

Table 14. Confidence Flag Criteria

Attribute	Source	Numeric Value
Sun Glint Contamination	Geometry Tests	-1
Coast Background	Geographic Type Database	-1
Desert Background	Geographic Type Database	-1
Default Temperature Correction	Clear-Scene Brightness Temperature	-1
Water Background	Geographic Type Database	+1
Land Background	Geographic Type Database	+1
Visible and IR Channels Available	Sensor Data	+1
Cloud and Within 15° K of T_{cld}	Cloud Algorithm	+1
Cloud and Within 10° K of T_{cld}	Cloud Algorithm	+1
Cloud and Within 5° K of T_{cld}	Cloud Algorithm	+1
Cloud and Within 3° K of T_{cld}	Cloud Algorithm	+1

A numeric value is assigned to each identifiable pixel attribute that affects confidence in the analysis (see Table 14). Note that pixels located over reflective or variable background surfaces (i.e., sun glint, coast, desert) are assumed to be more difficult to analyze and, as such, are assigned a negative value. Similarly, pixels located in an analysis box that require a default temperature correction in the calculation of the predicted clear-scene brightness temperature (Eq. 4-14) are considered to be more suspect than those that did not use a default correction and also carry a negative value.

The numeric value is positive for attributes felt to improve analysis accuracy. This includes cases when the cloud analysis is performed over a straight land or water background rather than one of the problem backgrounds listed above and when both visible and IR channels are available to the algorithm for analysis. The strength of the cloud signature, measured as the departure of the IR brightness temperature or visible count from the respective cloud cutoff value, is also used as a measure of confidence in the analysis.

Confidence flag values for each pixel are established by initially assigning a numeric value associated with middle level confidence and then adjusting up or down based on the attributes that apply. A final confidence value is calculated by summing the numeric value associated with all applicable attributes. For example, if the the following attributes applied to a given pixel: $T_{IR} = 256$, $T_{cld} = 268$, both visible- and IR-channel data are available, and the background surface is land; then the OLS algorithm would classify it as cloud and compute a confidence level as follows:

Initial confidence level of MIDDLE	5
Land background	+1
Visible and IR channels available	+1
Within 15° of IR cloud threshold	+1
Within 10° of IR cloud threshold	+1
Within 5° of IR cloud threshold	+1
Total Value	10

Conversion to a confidence flag value of LOW, MIDDLE, or HIGH is performed by subjecting the numeric value to the thresholds defined in Table 15. Thus, for the above example, the confidence flag assigned to the pixel has a value of HIGH since the total of 10 is greater than or equal to the HIGH confidence threshold of 9.

Table 15. DMSP Confidence Flag Assignment

Confidence Level Value	Confidence Flag
$0 \leq \text{Value} \leq 5$	LOW
$6 \leq \text{Value} \leq 8$	MIDDLE
$9 \leq \text{Value}$	HIGH

6.1.2 AVHRR Confidence Flag Determination

The AVHRR algorithm also produces information on the expected relative accuracy of the cloud analysis for each pixel. The level of confidence assigned to each pixel is based on the strength of the cloud signature relative to the cloud threshold level for each cloud test. Signature strength is defined in terms of quanta where a quanta is based on the magnitude of the cloud threshold associated with each test. A numeric value representing the relative strength of the cloud signature in quanta is calculated for each test based on the

magnitude of the cloud signal. Table 16 provides the quanta assignments for each cloud test. The convention used is that positive numbers indicate cloud-filled pixels and negative numbers indicate cloud-free pixels.

Quanta size are uniquely defined as fixed values for each cloud test with the exception of the Cirrus Cloud Test. The quanta size for the Cirrus Cloud Test is maintained as a function of the cirrus cloud threshold interpolated from tabulated values in Saunders and Kriebel (1988). The quanta size (n) for the Cirrus Cloud Test is calculated as:

$$n = \text{Cirrus Cloud Threshold} / 2 .$$

Thus, if the Cirrus Cloud Test threshold is determined to be 7.00 then the quanta size would be set to 3.5.

For example, if the COLD cloud test (Section 3.2.1) measured a $T_{\text{sfc}} - T_4$ difference of 16.3 K and the cloud threshold were 10 K, then the strength of cloud signature for that test would be 2 quanta:

$$\text{diff} = 6.3 \quad (\text{i.e., } 16.3 - 10)$$

and $5.0 < \text{diff} \leq 10.0$

therefore from Table 6-3: Quanta Magnitude = 2 and Confidence Level = MIDDLE

The procedure to assign a confidence flag to each pixel is to use the confidence level associated with the test that exhibits the strongest spectral signature. When performing the confidence flag determination, cloudy signatures always take precedence over clear signatures. Thus, if one cloud test detected cloud with a quanta magnitude of 1 and another test produced a cloud-free classification with a quanta magnitude of -2, the positive cloud result would take precedence and the pixel would be classified as cloud-filled with LOW confidence.

6.2 Tuning

Tuning options are required to allow tactical user adjustments to cloud algorithm accuracy to support specific mission requirements. For example, if a given tactical mission were particularly sensitive to low cloud cover, the analyst may choose to increase algorithm sensitivity to low cloud at the risk of falsely classifying some clear areas as cloud. Similar to the data quality flags, the decision was made to limit user choices to a few simple and easily understood options. This was in recognition of the limited understanding a tactical user is likely to have about how the algorithm operates. Tuning options adjust multiple cloud tests simultaneously using predefined sets of coefficients. Thus, when a user adjusts algorithm sensitivity upward or downward from the optimal point (as defined during the algorithm test and evaluation studies) through a mechanism analogous to a dial, the tuning algorithm makes the appropriate changes to all cloud thresholds simultaneously.

In the OLS algorithm, tuning can logically occur in two places. First is in the calculation of the predicted clear-scene brightness temperature (Section 4.2). The second is in the definition of the clear and cloud thresholds (Section 5.1).

Table 16. AVHRR Quanta Value Classification Assignments

Cloud Test Name	Quanta Size	Spectral Signature Departure From Threshold (diff)	Quanta Magnitude	Confidence Level
COLD	5.0	$0 < \text{diff} \leq 5.0$	+1	LOW/Cloud-Filled
		$5.0 < \text{diff} \leq 10.0$	+2	MIDDLE/Cloud-Filled
		$\text{diff} > 10.0$	> +2	HIGH/Cloud-Filled
		$0 \geq \text{diff} \geq -5.0$	-1	LOW/Cloud-Free
		$-5.0 > \text{diff} \geq -10.0$	-2	MIDDLE/Cloud-Free
		$\text{diff} < -10.0$	< -2	HIGH/Cloud-Free
CIRRUS	n	$0 < \text{diff} \leq n$	+1	LOW/Cloud-Filled
		$n < \text{diff} \leq 2n$	+2	MIDDLE/Cloud-Filled
		$\text{diff} > 2n$	> +2	HIGH/Cloud-Filled
		$0 \geq \text{diff} \geq -n$	-1	LOW/Cloud-Free
		$-n > \text{diff} \geq -2n$	-2	MIDDLE/Cloud-Free
		$\text{diff} < -2n$	< -2	HIGH/Cloud-Free
n = Cirrus Cloud Threshold / 2				
CLF	6.0	$0 < \text{diff} \leq 6.0$	+1	LOW/Cloud-Filled
		$6.0 < \text{diff} \leq 12.0$	+2	MIDDLE/Cloud-Filled
		$\text{diff} > 12.0$	> +2	HIGH/Cloud-Filled
		$0 \geq \text{diff} \geq -6.0$	-1	LOW/Cloud-Free
		$-6.0 > \text{diff} \geq -12.0$	-2	MIDDLE/Cloud-Free
		$\text{diff} < -12.0$	< -2	HIGH/Cloud-Free
RATIO	0.075	$0 < \text{diff} \leq 0.075$	+1	LOW/Cloud-Filled
		$0.075 < \text{diff} \leq 0.15$	+2	MIDDLE/Cloud-Filled
		$\text{diff} > 0.15$	> +2	HIGH/Cloud-Filled
		$0 \geq \text{diff} \geq -0.075$	-1	LOW/Cloud-Free
		$-0.075 > \text{diff} \geq -0.15$	-2	MIDDLE/Cloud-Free
		$\text{diff} < -0.15$	< -2	HIGH/Cloud-Free
BRIGHT	0.03	$0 < \text{diff} \leq 0.03$	+1	LOW/Cloud-Filled
		$0.03 < \text{diff} \leq 0.06$	+2	MIDDLE/Cloud-Filled
		$\text{diff} > 0.06$	> +2	HIGH/Cloud-Filled
		$0 \geq \text{diff} \geq -0.03$	-1	LOW/Cloud-Free
		$-0.03 > \text{diff} \geq -0.06$	-2	MIDDLE/Cloud-Free
		$\text{diff} < -0.06$	< -2	HIGH/Cloud-Free
FLS	0.75	$0 < \text{diff} \leq 0.75$	+1	LOW/Cloud-Filled
		$0.75 < \text{diff} \leq 1.50$	+2	MIDDLE/Cloud-Filled
		$\text{diff} > 1.50$	> +2	HIGH/Cloud-Filled
		$0 \geq \text{diff} \geq -0.75$	-1	LOW/Cloud-Free
		$-0.75 > \text{diff} \geq -1.50$	-2	MIDDLE/Cloud-Free
		$\text{diff} < -1.50$	< -2	HIGH/Cloud-Free
HIGH	1.0	$0 < \text{diff} \leq 1.0$	+1	LOW/Cloud-Filled
		$1.0 < \text{diff} \leq 2.0$	+2	MIDDLE/Cloud-Filled
		$\text{diff} > 2.0$	> +2	HIGH/Cloud-Filled
		$0 \geq \text{diff} \geq -1.0$	-1	LOW/Cloud-Free
		$-1.0 > \text{diff} \geq -2.0$	-2	MIDDLE/Cloud-Free
		$\text{diff} < -2.0$	< -2	HIGH/Cloud-Free

Accurate prediction of clear-scene brightness temperatures is predicated on accurate classification of reference pixels used in Eq. 4-9 as either cloud-free or cloud contaminated. This decision is in turn dependent on the ΔT limits calculated in Eqs. 4-10 and 4-11 correctly describing the natural variability between the surface temperature climatology and the satellite observed IR brightness temperature. Limiting the range between the ΔT limits would have the effect of reducing algorithm sensitivity to low cloud (i.e., cloud temperatures close to surface temperature). This is accomplished by adjusting the 2σ factor in Eq.

4-7 to a smaller value. Thus, the tuning option would be to replace the 2σ in Eq. 4-7 to a variable:

$$\Delta T_{\min_i} = \overline{\Delta T_i} - p_0 \sigma_i \quad (6-1)$$

where p_0 is a decimal number that can be adjusted up, to increase sensitivity to low cloud, or down, to decrease sensitivity. Use of this approach has the beneficial aspect of maintaining the influence of local variations in surface temperature on the cloud detection process. However, it may have the undesirable side effect of contaminating the clear-scene statistics with cloudy pixels that will generally degrade the algorithm performance. A more direct approach is to adjust the thresholds α_{cld} and α_{clr} in the IR algorithm (Eqs. 5-1 and 5-2) and ρ_{cld} and ρ_{clr} in the visible algorithm (Eqs. 5-5 and 5-6). Changing the magnitude of α_{cld} and ρ_{cld} will have an inverse effect on the algorithm sensitivity to low cloud (i.e., raise the threshold to decrease sensitivity). Similarly, adjusting α_{clr} and ρ_{clr} will affect the contribution from partially filled pixels relative to clear pixels. Increasing the thresholds will decrease the number of pixels classified as partially cloud-filled.

The AVHRR algorithm can also support tuning of cloud detection tests. Tuning capabilities allow the user to either increase or decrease algorithm sensitivity to low, optimal and high. The interface can best be thought of as a dial, each with three settings: -1, 0, +1. In the case of the AVHRR algorithm, algorithm sensitivity can be adjusted separately for low, middle, or high cloud. Thus, in the dial analogy, three independent dials would exist for each cloud level; sensitivity to low cloud can be modified without affecting algorithm sensitivity to mid or high level cloud. Changing the dial settings changes the cloud thresholds in the appropriate tests. Figure 11 provides a schematic showing which tests are affected when sensitivity to one or more cloud types is changed.

One relationship is used to tune all thresholds simultaneously by modifying the optimal threshold by a predefined increment as follows:

$$\text{new_threshold} = ((p_A * \text{increment}) + 1) * \text{old_threshold}$$

where $p_A = -1, 0, 1$ indicates whether sensitivity to a type of cloud is increased or decreased and increment gives the percent change in the threshold. Table 17 provides default increment values for each cloud test. The sign of p_A is used to change the threshold value in the correct direction (i.e., decreased sensitivity generally requires a higher threshold). In the current TACNEPH implementation, the dial settings are manually-input command line qualifiers, /LOW = c, /MID = c, /HIGH = c, where $c = +1$ or -1 for increased or decreased sensitivity respectively. Rather than using default (optimum) values, the increment and decrement values applied to the cloud test thresholds may also be set on the command line. However, this option should only be used by persons with good understanding of the algorithm. It was included for testing purposes and to aid setting of the default threshold values.

Table 17. Default Threshold Increments

TEST	% CHANGE
BRIGHT	.25
RATIO	.2
CLF	.2
FLS	.7
HIGH	.25
COLD	.2
CIRRUS	.2

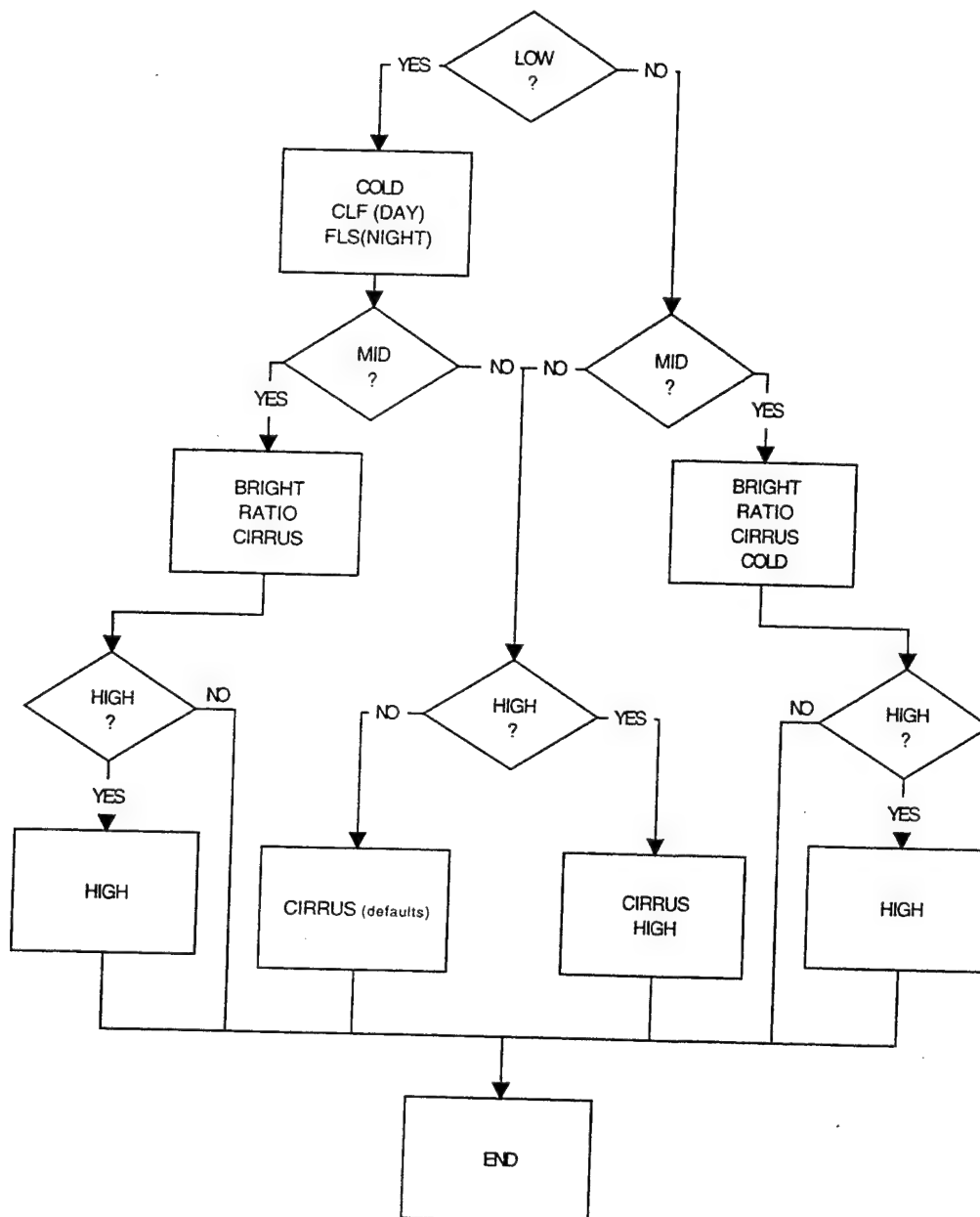


Figure 11. Schematic of recommended AVHRR cloud algorithm tuning option.

6.3 Quality Control Recommendations

Quality Control guidelines formulated at TACNEPH program reviews specified that manual interaction or bogusing of analyzed cloud fields would not be supported. However, that did not exclude the possibility of performing some type of operation outside of TACNEPH since, for example, the Mark IV-B has the capability to bogus cloud analysis files maintained on-line in the database. Recommendations were required for display options that support manual examination and evaluation of input data and analysis products for the purpose of quality control. Interactive QC of algorithm results has been a feature of the TACNEPH development program since its inception (see for example the discussion on algorithm testing in Section 5.3.1). Many of these types of operations can be supported in a tactical terminal and, as such, are potentially useful for real-time QC and in-depth analysis of cloud products.

The most useful diagnostic product used during TACNEPH algorithm development were interactive displays of intermediate algorithm products overlaid on satellite imagery. Intermediate products represented pixel-by-pixel results of individual cloud tests from both the OLS and AVHRR algorithms. Each individual test result was carried as a 1-bit value (cloud or clear) that was used to generate a synthetic image describing the test results over the spatial range of the input image. The BIT_TOGGLE program described in Section 3.2 was used to interactively manipulate synthetic algorithm result images and the input satellite imagery. BIT_TOGGLE allow an analyst to select for display any individual satellite channel image, or combination of channels, from the satellite sensor (i.e., OLS or AVHRR). Single channel images are displayed as gray shades, multispectral images as color composites. On top of the satellite imagery, the algorithm result images were displayed as color coded values in a non-destructive overlay. Algorithm results were combined into groups of eight so that they could be carried in a single 8-bit values in accordance with the limitations of the display hardware. BIT_TOGGLE options allowed the user to view results from any single test or combined results using any mix of the eight possible tests.

This approach would transfer well to a tactical terminal since the image display capability is well within the scope of modern imaging computers. All functions can be implemented using color look up tables. Generation of multispectral color composites requires some preprocessing to be done using look up tables, but even that restriction is eliminated with 24-bit, full color systems. The benefits of implementing this type of capability are consistent with the stated objective of improving QC procedures and reducing manpower requirements since it allows the QC analyst to quickly and accurately evaluate the algorithm results through direct comparison with the satellite imagery. In the tactical environment this approach has the following desirable attributes:

- allows knowledgeable users to evaluate and interrogate intermediate products as guidance on second order cloud characteristics (e.g., type, phase);
- provides visual clues on where the algorithm detected cloud using spectral signatures that the human analyst might otherwise miss;
- gives an easy to understand and interpret representation of algorithm results; and
- supports fast QC of analysis accuracy.

7. ASSIGNMENT OF CLOUD TOP ALTITUDES

Required TACNEPH cloud parameters are cloud amount and altitude. As discussed in Section 1, these parameters are to be generated using only the resources available on a transportable tactical terminal. For this reason, the use of real time satellite sensor data is indicated. The previous sections have provided information on the TACNEPH analysis approaches for cloud amount from both DMSP OLS and TIROS AVHRR cloud imagers. Cloud location and amount are analyzed on a pixel-by-pixel basis, leaving it up to the user to decide how to use this information. It is assumed that the cloud amount results will be calculated over some type of analysis grid (e.g., GWC 16th mesh polar stereographic grid).

The requirements for cloud top altitude are driven both by the need to define cloud layer heights to predict their movement and other field requirements. The most recent Operational Requirements Document (ORD) states that cloud layers are required at high vertical resolution (300 m) with a horizontal resolution at tactical sites equal to that of the fine data cloud imagery (i.e. on a pixel by pixel basis). TACNEPH was not tasked with this requirement. Given the tactical constraints on the problem, a reasonable way to establish cloud altitude consistent with that for cloud cover described in Section 5 would be to take an average cloud top temperature over the analysis grid cell using an appropriate infrared window channel (i.e., using only those pixels determined to be cloudy by the cloud detection algorithm) and assign this temperature to an altitude based on the use of a reliable temperature profile. This altitude would be reported as the cloud altitude for the analysis grid box. The window channel average equivalent black body brightness temperature (EBBT) for cloudy pixels would represent the temperature of the average cloud top with the analysis grid box when corrected for atmospheric effects as discussed below. (This algorithm would also be applicable to determine the altitude of each cloudy pixel in which case no averaging is required.) Appropriate window channels include the OLS thermal channel and channels 4 and 5 of the AVHRR (channel 3 may be used at night). The simple algorithm defined above is summarized in Figure 12.

In the context of the cloud top altitude algorithm defined here, this section provides a simple evaluation of the utility of SSM/T derived temperature profiles for the assignment of cloud top altitude. This evaluation treats the original TACNEPH task. Additionally, we provide guidance on tailoring the TACNEPH cloud top altitude determination based on forecaster inputs. We contend that understanding of regional synoptic situations is essential to the interpretation of TACNEPH guidance. Finally recognizing the planned availability of additional satellite data resources at tactical terminals not addressed in the original TACNEPH tasking, we recommend improvements to the determination of cloud top altitude. These include use of SSM/T-2 moisture data and application of TOVS sounder data for AVHRR applications.

7.1 Quantitative Relationships of Cloud Top Altitude and Temperature Profile

As discussed in Section 1, the TACNEPH algorithms are designed to operate in the absence of any dynamic data source other than direct satellite sensor transmission, to automatically select the optimal processing algorithm in response to data availability or quality, and provide techniques for customization and quality control of derived products. The assignment of the cloud height is based upon the derived EBBT of the cloud field and its association to the satellite derived vertical temperature profiles. A description of the characteristics of the microwave temperature sounder from DMSP, the SSM/T-1 and the NOAA TOVS can be found in Falcone and Isaacs (1987) and will not be elaborated here.

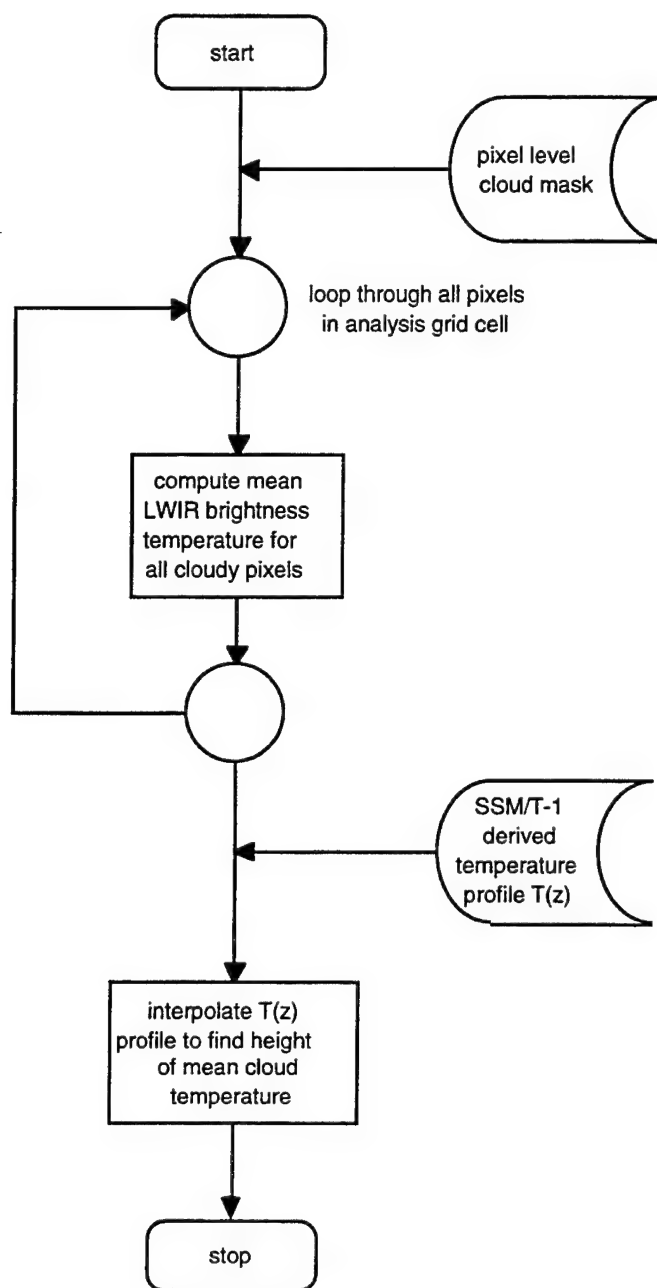


Figure 12. Cloud altitude algorithm flow chart.

As discussed above the ORD states that layers are required to be distinguishable with a minimum vertical resolution of 300 m. In order to evaluate the applicability of the SSM/T-1 in cloud top altitude assignment, we have identified sources of error in the determination of cloud top altitude using the simple algorithm defined above. This provides a means to allocate the uncertainties attributable directly to the temperature profile determination and hence the SSM/T-1 retrieval. Sources of error include: (a) instrumental errors (due to sensor calibration, noise and quantization of the LWIR channel from which the EBBT in Figure 12 above is obtained), (b) errors due to uncertain knowledge of atmospheric attenuation in the IR channel, and (c) errors in the temperature profile itself. The

last source of uncertainty addresses the use of SSM/T-1 for temperature profile retrieval. In this context, we treat the errors in the temperature profiles retrieved from SSM/T-1 "system". This includes instrument and retrieval algorithm sources of error together.

For evaluation purposes we translate temperature errors from each source defined above into equivalent cloud altitude errors using a typical atmospheric lapse rate. This is based on the assumption that cloud top altitude assignment is performed as shown in Figure 12 associating an IR channel EBBT corrected for atmospheric attenuation with a height on a profile. Thus, using a typical value of 6.8 K/km, an error of 1 K in determining the appropriate EBBT corresponds to a cloud top altitude error of 150 m. It should also be noted that the approach assumes unit emissivity or so called "black" clouds. For transmissive clouds such as cirrus cloud, measured IR radiation transferred through the cloud has the effect of biasing the cloud top altitude to lower values, i.e. high cloud is analyzed as lower cloud. For the AVHRR/TOVS applications an approach to address these situations is suggested later.

Instrumental errors arise due to sensor calibration, noise, and to quantization of the data. Sensor calibration is an issue in that absolute IR radiance values provide the most accurate measure of cloud top emission. The DMSP OLS is designed to provide an EBBT output scaled to the sensor response output, however it is not absolutely calibrated. The AVHRR is calibrated. Overall, each 1 K of drift in EBBT results in potential 150 m shifts in cloud top altitude. This may or may not be an issue depending on the importance of relative or absolute measurements in the final user application. In the context of the analysis here, we judge sensor noise sources of error to be small enough not to affect cloud top determination. However, quantization of the OLS in 8 bits over its dynamic range introduces a granularity of about a 0.5 K. This corresponds to an uncertainty in cloud top of about 75 meters. Thus no OLS cloud top determination can be more accurate than this number even assuming no sensor noise. (The AVHRR uses a 10 bit quantization.) Both calibration and quantization are issues for the OLS rather than the AVHRR. For the OLS an estimate of total error due to these sources might be 1.5 K on average or 225 m.

The source of error due to uncertainty in water vapor profile in the estimation of cloud top altitude based on the single IR channel plus temperature profile approach described above can be understood in the context of the radiative transfer equation (RTE) below:

$$R_o = B(T_c) \tau(Z_c) + \int_{Z_c}^{\infty} B[T(Z)] d\tau(Z) \quad (7-1)$$

This RTE describes the radiance signal, R_o , measured by the IR channel for a completely overcast pixel. The IR channel EBBT is the inverse Planck function, i.e. $B^{-1}(T)$, of R_o evaluated at the appropriate average wavelength of the IR Channel used. The two contributing terms: (a) are the Planck blackbody radiation emitted by the cloud at the temperature of the cloud top T_c (i.e., at cloud top altitude assuming a non transmissive cloud) which is attenuated by absorption by the atmosphere between the cloud top and the top of the atmosphere along the sensor's line of sight and (b) the emission by the atmosphere over the same path. If the atmosphere were transparent, the transmission factor multiplying the Planck function would be unity, the integral would be zero, and the measured radiance would be identically the Planck function of the cloud top temperature. Although both the OLS thermal channel and channels 4 and 5 of the AVHRR are so called "window" channels, there are sources of atmospheric attenuation. The predominant mechanism for attenuation is absorption by the water vapor continuum. Additional effects

are due to carbon dioxide 0.1-0.2 K, aerosol 0.1-0.4 K, and transmissive cirrus. Presumably, much cirrus will be identified by the cloud detection algorithm.

The net effect of this attenuation is that the black body temperature equivalent to R_0 is generally a few degrees cooler than that of the actual cloud top. This effect can be treated. Quantitatively, the "correction" for water vapor attenuation, is a function of satellite look angle and integrated water vapor amount between the sensor and cloud top. The latter means that corrections are larger for lower clouds and in regions of high precipitable water. We have evaluated the difference between actual cloud top temperature and cloud top temperature obtained by assuming an uncorrected equivalent black body temperature using an RTE computer code. As a worse case, the cloud top was assumed to be at the ground (i.e., maximum water vapor path). Results for a mid latitude atmosphere as a function of integrated water vapor and sensor look angle are shown in Figure 13. Note that corrections of 2-5 K are required at nadir and corrections of 8 K may be required at large viewing angle/water vapor paths. If uncorrected, these temperature deficits correspond to incorrect altitude assignments of 500-750 m, all systematically biased to put cloud higher in altitude.

This source of uncertainty can be mitigated by using a climatological water vapor correction or a collocated water vapor sounding sensor. The required climatological correction would be location and seasonally dependent. The error associated with using a climatological profile would depend on the local variance of water vapor. For the case discussed above the error in EBBT using a climatological profile is about 1.5 K corresponding to about 225 m using our assumed lapse rate. This estimate is based on knowledge of the climatological variance about the mean profile. Note that for any specific situation, the error in using the mean profile may be much larger. Note that if the water vapor retrievals from the SSM/T-2 are used there is potential to reduce the corresponding error in EBBT by a factor of about three, i.e. to less than 0.5 K.

The final source of error is that due to the temperature profile retrieval accuracy available from the sounder collocated with each imager (SSM/T-1 for the OLS and TOVS package for the AVHRR). Statistical information on the error characteristics of the vertical temperature profile (VTP) assignment provided by the satellite sensors is compiled on an ongoing basis at NESDIS. Figure 14 provides an analysis of mean error and bias between VTP's obtained from the DMSP SSM/T-1 and NOAA TOVS and RAOBS for various height levels in the atmosphere (Reale et al., 1992). These data are for a six day period and have been stratified into three latitudinal (only the N. hemisphere extra tropics are shown).

As noted in Figure 14, the characterization of temperature retrieval error by Grody et al. (1985) seems to hold true with an RMS error of 2.5-3.0 K through the troposphere (corresponding to altitude assignment errors of up to 450 m) and linear surface errors of 4.0 K or 600 m. These errors appear consistent for the SSM/T regardless of latitude or season. The TOVS accuracy for clear soundings are about 2 K. For cloudy soundings, results are similar to the SSM/T-1. There are some subtle differences in way the errors are reported between the SSM/T-1 and TOVS. TOVS statistics are stratified into clear and cloudy (this distinction is not made for SSM/T-1). In the SSM/T-1 statistics, differences are noted between the retrievals over the oceans versus those from over land. This is attributed to the difference in the surface emissivity between the differing backgrounds and the impact on the retrievals. It should be noted that the combined effects of temperature profile and water vapor uncertainty increase for the determination of cloud top altitude for clouds lower in the atmosphere.

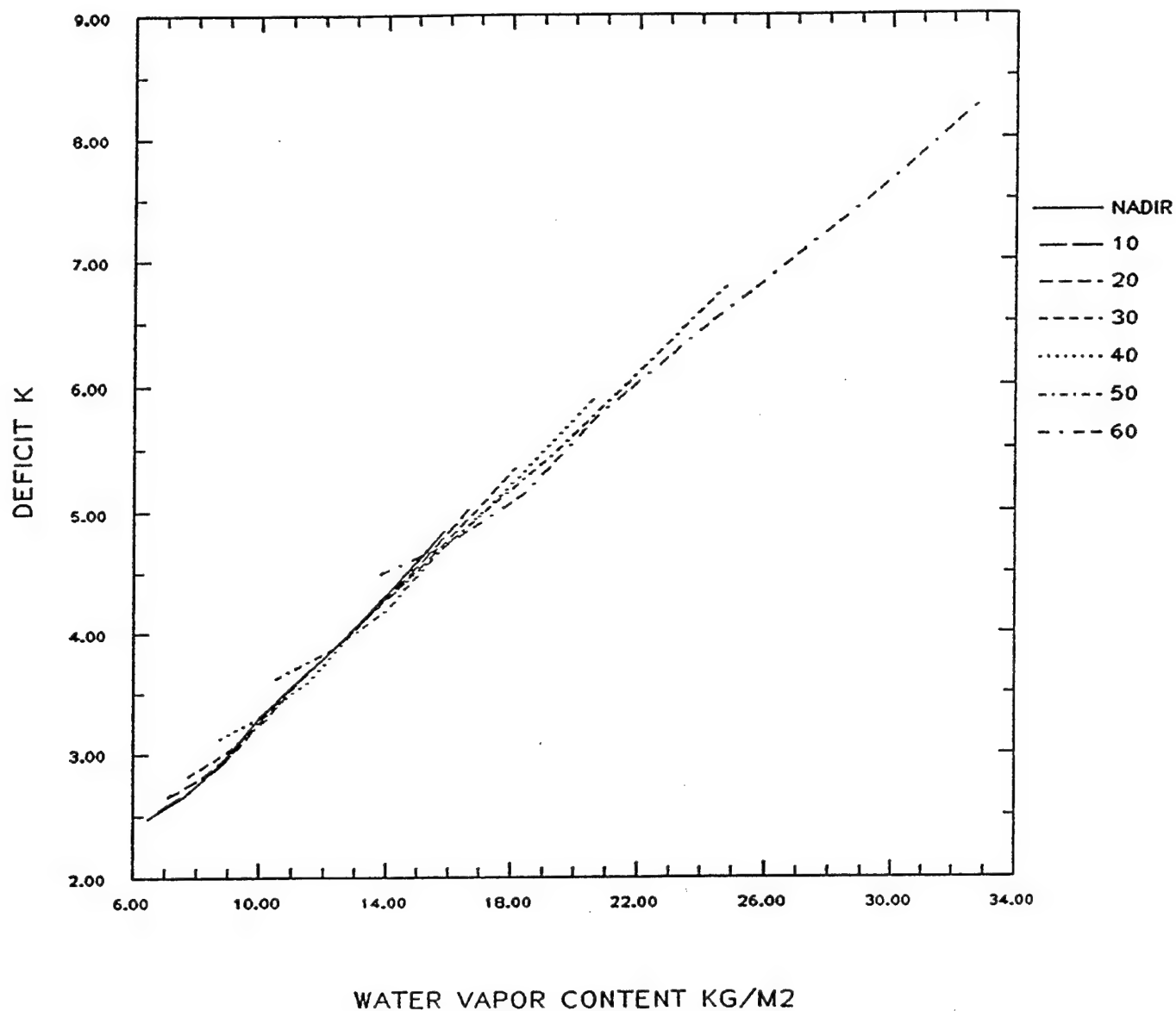


Figure 13. Deficit between cloud top and EBBT as a function of look angle and integrated water vapor for a mid latitude atmosphere.

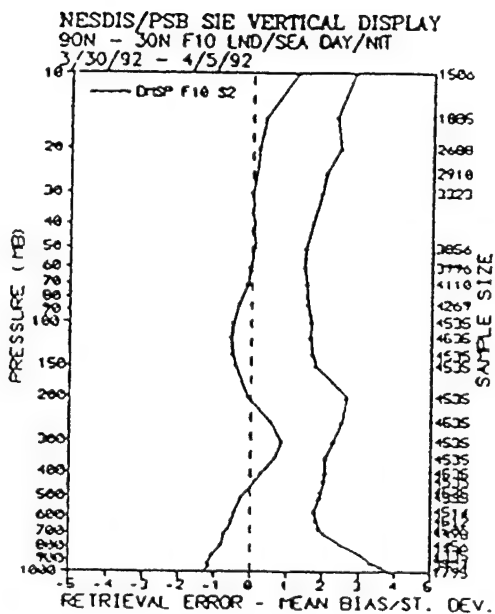
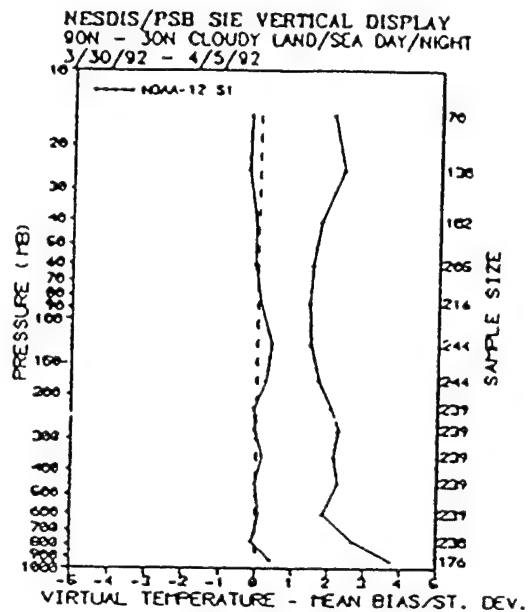
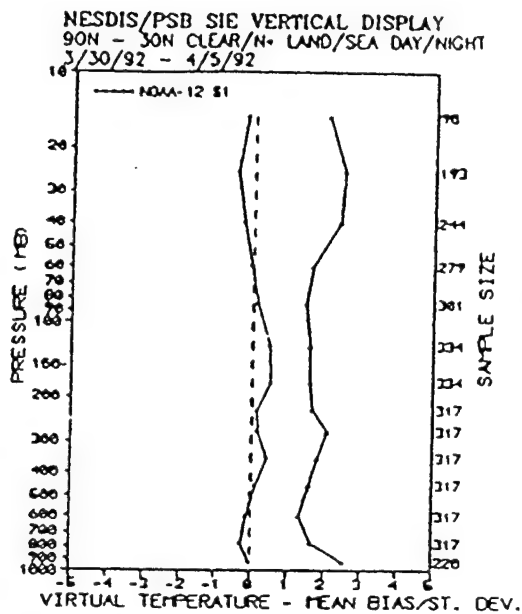


Figure 14. Vertical distribution of SSM/T-1 temperature profile retrieval errors.

The data discussed above are routinely extracted by NOAA and analyzed for use in tailoring the VTP for use in large scale global NWP models. Stratification by latitude, season, etc. would potentially assist in providing statistics for TACNEPH guidance. However, direct application of the error characterization to TACNEPH guidance customization is a monumental task. The difficulty results from the sheer amount of data available (NESDIS runs error statistics on the VTP's on a continuing basis year round) and the expected application of the VTP to NWP and not to a tactical mission, *per se*. Developing generalities from this small sample is not recommended. Further analysis of larger stratified data sets is required before reliable quantitative evaluations are possible.

Summarizing the discussion of error sources noted above, Table 18 gives typical temperature errors. Assuming that water vapor is corrected for using climatology, the error in the temperature profile retrieval becomes the dominant source of uncertainty in the assignment of a cloud top temperature and hence cloud top altitude. Based on using a climatological water vapor correction, a typical lapse rate and assuming these errors are uncorrelated gives a total uncertainty of almost 1 km for the OLS and 0.6 km for the AVHRR.

*Table 18. Temperature Error Budget (K) for Cloud Top Temperature Assignment
(multiply by 0.15 for cloud top altitude error in km)*

Error Source	DMSP (OLS/SSM/T)	NOAA (AVHRR/TOVS)
Instrument	1.5	negligible
EBBT Correction		
None	2-8	2-8
Climatology	1.5	1.5
Sounder	.5	.5
Temperature Retrieval		
Troposphere	2.5-3.0	2.0-2.5
Near Surface	4.0	2.0-3.0

7.2 Qualitative Tailoring of TACNEPH Guidance

The combined uncertainty discussed above is large enough to suggest that the quality of the TACNEPH cloud top altitude guidance be evaluated carefully by the forecaster. The duty forecaster's awareness of the synoptic situation, is the basis upon which any tailoring of the cloud height assignment from TACNEPH should be based. The temporal continuity of the cloud fields as determined through the local and synoptic observation network is a powerful tool in maintaining a credible association between the mission planning and execution forecasts. Information garnered from other sources can also assist in the specific tailoring of the TACNEPH provided guidance. Sources of additional information include local radiosondes, observations by deployed units, pilot reports, mission debriefings, and satellite interpretation discussions available through communication channels. The integration of all or some of these data sources with the TACNEPH guidance can result in spatially and temporally consistent analysis and subsequent development of the theater or battlefield level cloud height fields. Another important aspect is the understanding by the forecaster of the specific needs of the mission planning system in terms of the impacts of the cloud height assignment. Weapon system

selection, loading, and deployment is usually contingent on operating within specified rules of engagement and locally developed tactics. For example, if the local situation requires a weapons delivery after visual sighting of the target within a specified height range, the height of the cloud fields becomes critical in determining the probability of mission success and the assignment of mission alternates should the primary be unobtainable.

Another source of potential information regarding the tailoring of the TACNEPH guidance is climatology. We have already mentioned the potential role of water vapor profile climatology in correcting EBBTs for water vapor attenuation. There are two aspects of the climatological cloud height, itself, pertinent to the use within a tactical environment. First, the regional climatology of the specific deployment area should provide general spatial and temporal characteristics of the cloud fields and heights. This information may be based on cloud type information using empirically derived relationships between specific types of cloud and expected vertical height placement and development. For example, stratus cloud usually resides near the 900 mb level but local climatology may alter that assignment based on local affects (i.e., topography, wind flows, nearby water masses, etc.). Another pertinent aspect of climatology for the forecaster to consider in TACNEPH tailoring is the use of climatological vertical temperature profiles to assist in the final height assignment. Areas of expected cloud development may be reflected in the climatological profiles which characterize seasonal and latitudinal influences of moisture flows. It is important to note, that the TACNEPH guidance will probably provide a spatially more consistent and temporally more timely assessment of the cloud heights than climatology alone. However, the integration of the TACNEPH guidance within the context of expected climatological behavior of the region provides for increased opportunities for reliable mission forecasts.

The verification of the cloud height assignment through the vehicle of the mission debriefing and/or pilot report is helpful in developing local rules-of-thumb regarding TACNEPH guidance tailoring. It is important to keep track of the original TACNEPH guidance prior to any modification by using climatology or synoptic awareness so that the TACNEPH could possibly be tuned. In the same sense, keeping track of whatever modifications which are applied to TACNEPH guidance, can assist in further refining rules-of-thumb and determining the most effective combination of TACNEPH guidance and specific tailoring.

7.3 Expected Improvements in VTP/Cloud Height Assignment Characterization

The above discussion has suggested a number of areas for improvement of cloud top altitude assignment accuracy. In this section we summarize these as recommendation for future study. First and most obvious is the use of collocated moisture sounder retrievals to support the determination of water vapor corrections for the measured EBBTs. In the case of DMSP, the SSM/T-2 data are available for this application. In the calculations in Section 7.1 above we have assumed SSM/T-2 water vapor retrieval accuracies like those reported by the SSM/T-2 calibration/ validation effort (Falcone et al., 1992). Integration of the T-2 moisture retrievals for this purpose was not tasked as part of TACNEPH, however. Likewise, cloud top altitude assignment for AVHRR using the TOVS temperature and moisture retrievals was not investigated.

There are ongoing efforts, particularly within the NOAA/NESDIS community to improve the accuracy, precision, and usefulness of the VTPs for operational NWP uses. In addition, efforts are also focusing on better methods of cloud retrieval using VTP radiance measurements (McMillin and Zhou, 1994). The TACNEPH guidance for the

cloud height assignment is one of the ways DoD is addressing this problem. Other efforts are involved in SERCAA (Neu et al., 1994) and also in improving weather communication within theater and battlefield environments. In particular, the cloud layering algorithm from SERCAA should have direct tactical applications.

It's obvious that further analysis of available error statistics of the VTPs could assist greatly in providing better understanding and application potential for the TACNEPH guidance. In addition, better techniques for assigning IR EBBT to the vertical temperature level could also assist in meeting this goal.

NESDIS, in their effort to improve the NWP assimilation of the VTP, is developing (and partially implementing) an imagery based display method of the error characteristics (T. Reale, personal communication). These imagery provide information on a global basis of the errors between the VTP and co-located RAOBS. The advantage of the imagery based system is the ease of viewing a global pattern and the inherent data compaction involved in the imagery display itself. There is potential for further investigating the usefulness of these error fields in characterizing TACNEPH guidance effectiveness. The fields could be provided as at the time of deployment to assist in the qualitative tailoring of the TACNEPH guidance and then updated within a certain timeliness after field deployment. Possibilities may also exist for extracting imagery specific to a deployment area after initial set up is accomplished. Modes of data transfer would also have to be assessed and optimized.

A temperature retrieval process which used a physical approach and explicitly estimated surface emissivity rather than using a statistical value, would likely improve the retrieval accuracy. NESDIS is in the process of assessing the differences between statistical methods (D-matrix) and physical retrievals but error statistics are not readily available as yet. In using the TOVS error data, these retrievals appear to have RMS errors about half of what the SSM/T-1 values are. However, the comparison of TOVS to SSM/T-1 must be done with consideration of the combined IR/microwave character of the TOVS versus the microwave only of the SSM/T-1. Consequently, the TOVS error statistics are based on comparisons between cloudy and clear retrievals. This probably makes direct comparisons of SSM/T-1 and TOVS a problem from a scientific approach but probably irrelevant to an operational user who's trying to use whatever data is available.

A more direct comparison is available based on the unified retrieval approach (Isaacs, 1989; Moncet and Isaacs, 1994) which combines DMSP 5D-2 sensor data (OLS, SSM/T-1, SSM/T-2, and SSM/I) in a physical retrieval combined with nephanalysis. From the discussion above, the advantage of this approach is that it tackles the problem in its entirety to obtain temperature and moisture profiles, surface emissivity, and cloud information directly and simultaneously. For example, temperature profile retrieval accuracy using 5D-2 data is up to 1-1.5 K superior to statistical approaches in the lower atmosphere and moisture profile is obtained simultaneously. Additionally, cloud liquid water information is also retrieved. In the context of cloud top altitude determination, this retrieval approach integrates the 5D-2 sensor data to provide the optimal temperature and water vapor retrieval to support correcting EBBTs and assigning an altitude. It is worth noting that the same approach is applicable to the TOVs package.

Cloud top temperature determination is difficult for cirrus cloud. The RTE defined in 7-1 is not applicable to cirrus cloud since it can be transmissive (i.e., its emissivity can be less than unity). In the case of the NOAA AVHRR/TOVS system, two approaches may be used to treat this problem. First, we can exploit the ability of the TACNEPH AVHRR cloud detection algorithm to identify cirrus cloud situations. Once this is accomplished, a correction factor can be developed and applied to account for cirrus cloud emission. This

correction factor would be in the form of a blackbody temperature in degrees (K) which would be subtracted from the measured IR EBBT to account for transmission of radiation from below cloud top level. Essentially this would be based on a cirrus cloud microphysical properties used to compute a cirrus cloud model emissivity for the bandpass of the IR channel which would then be used to evaluate the required "correction" in an average environment. An additional level of sophistication would be to use the magnitude of the cirrus cloud signature in the AVHRR test to adjust the magnitude of the correction (larger cirrus cloud signatures in the 4-5 test would correspond to smaller corrections). A second and more sophisticated approach would be to employ the CO₂ slicing technique (d'Entremont et al., 1992) to the analysis of the TOVs data. This would provide the cloud top pressure directly.

Finally, we note that there is considerable potential in applying modified forms of the SERCAA geostationary (d'Entremont et al., 1994) algorithms to the determination of cloud cover and top altitude (see, for example, Wylie and Menzel, 1989). Tasking of TACNEPH did not include treatment of geostationary sensor data. This is certainly an oversight.

We have summarized these recommendations in Table 19. As a consequence of these techniques and suggestions for the qualitative tailoring of the TACNEPH guidance, the possible eventual development of rules-of-thumb as viable analysis and forecast aids is indicated.

Table 19. Summarized Recommendations for Improved Retrieval of Cloud Top Altitude in a Tactical Environment

	DMSP	TIROS	GEO
Cloud Cover and altitude			Implement GEO algorithms
EBBT "Correction"	Water vapor climatology Use SSM/T-2 Retrievals	Water vapor climatology Use TOVS	Water vapor climatology Use GEO sounder channel data (if available)
Temperature Retrievals	Physical (unified) retrieval	Physical (unified) retrieval	Physical (unified) retrieval
Cirrus Cloud		AVHRR test based correction CO ₂ Slicing	Imager based correction CO ₂ Slicing

8. CLOUD THICKNESS AND BASE FROM MULTISPECTRAL CLOUD IMAGER DATA

An algorithm was developed which utilizes multispectral radiance data from cloud imagers such as the AVHRR to provide cloud optical thickness information. Cloud optical thickness is related to cloud physical thickness by ascertaining cloud type and using off line radiative transfer look up tables which are dependent on cloud type microphysical properties such as the cloud droplet size distribution. Cloud base is determined from the estimated cloud thickness and cloud top heights derived from thermal infrared channel data.

Knowledge of cloud base is important for a variety of defense tactical operations as well as for the determination of downward infrared flux required in climate modeling applications. The current RTNEPH approach for cloud base specification uses cloud type dependent thickness based on climatological models and cloud height determined from sensor data (Hamill et al., 1992). Sensor data itself, however, can be exploited to provide cloud thickness information. This is accomplished by using cloud microphysical models based on cloud type to define the relationship between sensor radiance values and cloud

thickness. Studies have investigated retrieval of cloud properties, including cloud optical thickness, from passive multispectral sensor data (King, 1987; Minnis et al., 1990, 1992; Nakajima and King, 1989; Twomey and Seton, 1980; Isaacs et al., 1990; Berendes et al., 1992). Results indicate that single channel sensor data depends on many cloud parameters, such as phase, particle size distribution and cloud thickness. For a given cloud type, we assume a specific particle size distribution which is used to relate sensor incident radiances and cloud thickness.

In this section, we describe a research grade algorithm developed to address the task requirement to develop an algorithm which would be an improvement over the existing RTNeph "climatology based" approach. In accomplishing this goal, we focused on utilizing the cloud optical thickness information potentially available from back scattered solar radiation. The algorithm was designed to exploit calibrated cloud imager data such as that from AVHRR to "measure" cloud thickness. The interplay of several algorithms is fundamental in the determination of cloud thickness. These algorithms include cloud cover, cloud type, and cloud height. The TACNEPH cloud base approach uses the TACNEPH AVHRR cloud cover algorithm (Section 5.2) and TACNEPH derived cloud heights (Section 7). Since there was no explicit requirement for a TACNEPH cloud type algorithm, we employed a straightforward cloud typing scheme described below. The main purpose of cloud type is to select the appropriate cloud microphysical model to relate cloud optical and cloud physical thicknesses. This is done through off-line radiative transfer calculations. These look up tables (LUTs) are cloud type dependent.

Although cloud height is derived after cloud type, the results of the cloud height algorithm may be used to improve on the cloud types, should discrepancies occur between the computed cloud type and the height assigned to it by standard cloud models.

8.1 Algorithm Description

The algorithm for cloud thickness and base determination requires: (a) identification of cloudy regions using the TACNEPH cloud cover analysis; (b) typing of the clouds to assign the appropriate radiative transfer based LUT, and (c) calculation of cloud top height. Cloud top height information is obtained by comparing corrected equivalent black body brightness temperature (EBBT) from an infrared channel to a temperature profile for the same region. Figure 15 provides an illustration of the procedure used to determine cloud thickness and base using this approach.

The input data for the algorithm consists of calibrated cloud imager data (such as AVHRR). The requirement for calibration is based on the need to qualitatively associate back scattered radiance in the visible channels with cloud optical thickness through the off-line radiative transfer calculations. The multispectral imager data is used in three ways: (1) determination of cloud type; (2) determination of cloud optical thickness, and (3) determination of cloud height. The TACNEPH innovation is the merging of cloud type related information (cloud microphysics), and cloud optical thickness (derived from visible channel data using off line radiative transfer calculations based on cloud type) to infer cloud physical thickness and the subsequent use of cloud height to obtain cloud base.

The functional flow of the algorithm proceeds in the following steps:

- The TACNEPH AVHRR cloud cover algorithm is used to delineate cloud covered regions. Cloud thickness and base are only inferred for cloudy regions. An description of this algorithm is provided in Section 5.2.

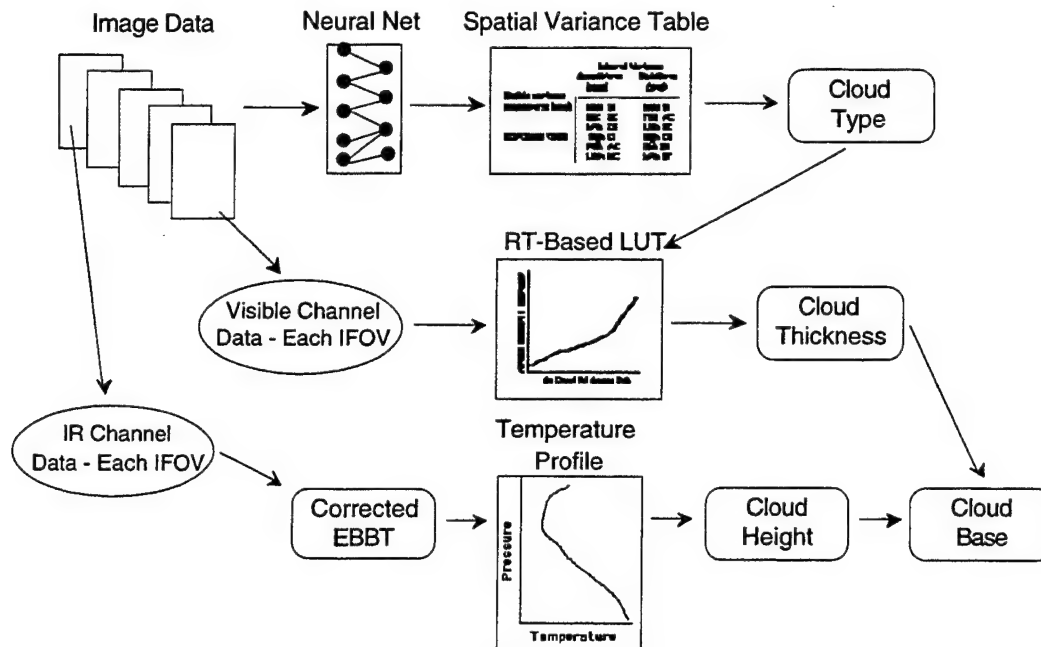


Figure 15. Cloud thickness and base procedure.

- Multispectral data are used to infer cloud type. There are many possible ways to accomplish this using spatial, spectral, and morphological cloud features. We have not developed a standalone TACNEPH cloud type algorithm, but have implemented a straightforward hybrid approach which uses a neural net to accomplish this step. This is described in Section 8.2. Any cloud typing scheme (including that available on the Mark IV-B tactical terminal or the current RTNEPH spatial variance approach) can be used (we used salient aspects of this into our approach). The cloud type output is used to identify one of the off line radiative transfer LUTs for use in the optical thickness determination.
- A visible channel (we have used AVHRR channel 2) is used to infer cloud optical thickness. The key to this procedure is the use of a look up table based on radiative transfer calculations which relates measured radiance in the channel to the cloud optical thickness. Sample look up tables and the procedure we used to generate them are provided in Section 8.3. Look up tables are dependent on cloud type (from the step above), satellite viewing angle, and solar zenith angle. By using the cloud type dependent look up table, the measured visible radiance is related to cloud optical thickness and cloud physical thickness. The latter relationship derives directly from the type dependent microphysical assumptions used in the off line generation of the LUTs. Output of this step is the cloud thickness in kilometers (or meters) and is based on synthesis of the information from the first step and the visible channel radiance data.
- The final step is the determination of cloud base. This is done by using the cloud top height information provided by assigning a height to the equivalent blackbody brightness temperature (EBBT) from an infrared window channel using a collocated temperature sounder profile or other vertical temperature

profile (tactically this may be done with a ground based sounder or local sonde release). We have sketched a procedure for cloud top height determination in Section 8.4 using AVHRR channel 5 which allows for correction of the EBBT using water vapor profile information (again either a satellite sounder data source or in situ data may be available). Once the cloud top height is determined the cloud base is obtained by subtracting the cloud thickness obtained above from the cloud top.

8.2 Cloud Type

Cloud type is used to fix the correct cloud microphysics upon which the relationship between measured visible radiance and cloud thickness is determined. Cloud type per se was not a TACNEPH requirement and a specific cloud type algorithm was not developed. To prototype the cloud base algorithm we implemented the following approach to cloud type retrieval. Any viable cloud typing scheme which is consistent with the input data may be used to obtain cloud type for the purpose of the TACNEPH cloud thickness and base algorithm.

The cloud typing portion of the algorithm uses both spectral and spatial information applied to pixels identified as cloud-filled to determine the cloud type category. Spectral information alone is not sufficient to identify the correct cloud type because clouds with similar radiative signatures may have different morphologies. The algorithm employed here uses spectral information to separate the cloud-filled pixels into four classes from which, using spatial information, the final cloud type is determined. The cloud typing approach is illustrated in Figure 16. The spectral information content of the cloud-filled pixels enables the grouping of clouds into four categories, which are:

- Cumulus, Stratus, Stratocumulus, Nimbostratus (Low Level Cloud)
- Altostratus, Altocumulus (Middle Level Cloud)
- Cirrostratus, Cirrocumulus, Cirrus (High Level Cloud)
- Cumulonimbus

This sub-typing process is performed by a neural network that uses the spectral content of visible and infrared channels, together with background information (land or water) to discriminate among the four classes. For example, cumulonimbus clouds can be easily separated from the other three classes due to their high albedo values and cold temperatures. Although different in a morphological sense, the cloud types in each of the four classes have similar spectral properties.

The neural network was trained on a preliminary set of test cases (~30) taken from four different images. Each cloud type had a few corresponding test cases. The training method employed was back propagation. In the training session, the network is presented an output corresponding to the given inputs. During training the weights of the connections between nodes in the network are adjusted in such a way as to minimize the output error. Negative weights indicate inhibitory connections; positive weights, disinhibitory ones. The inputs are normalized before being used by the neural network so that albedo values and brightness temperatures fall in the same range of values.

The network is composed of an input layer (the five channels and background information), a hidden layer with six nodes, and an output layer with four nodes each for a possible cloud type. There is not a general rule to determine the optimal number of hidden-layer nodes, however, a practical rule (based on direct experimentation and hidden

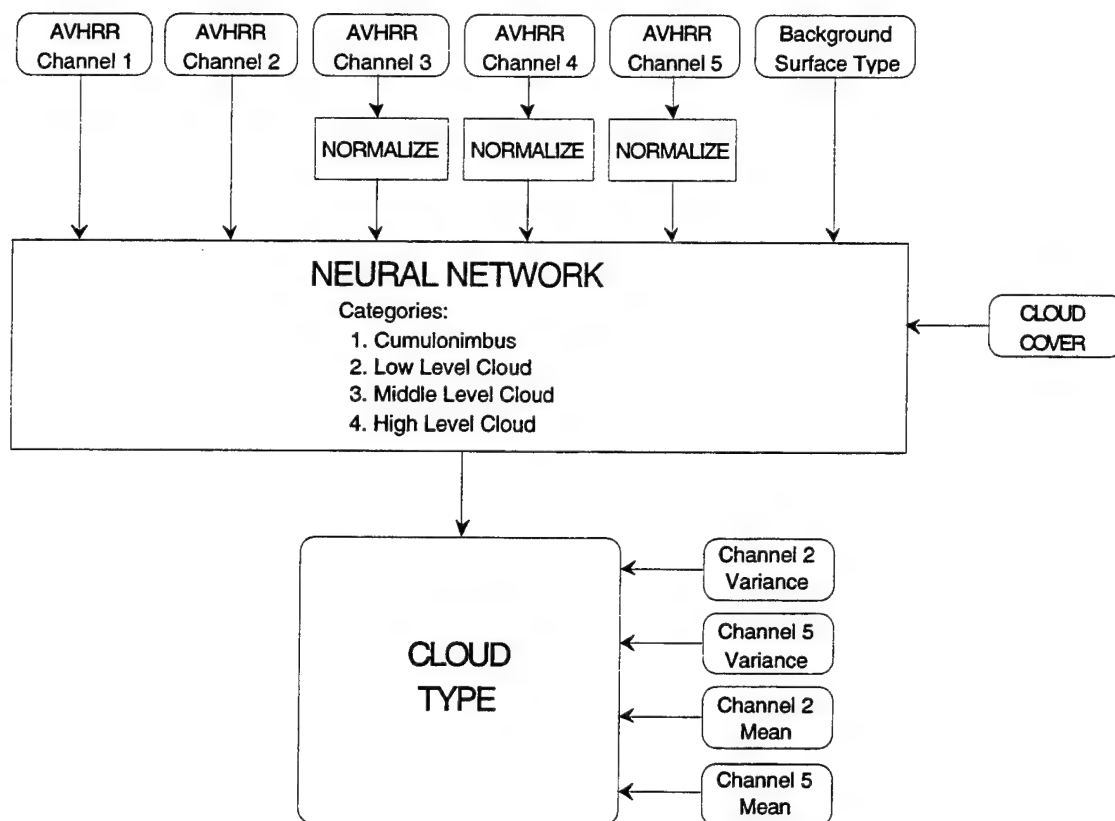


Figure 16. Cloud type calculation.

nodes used by the other implementations) was used: hidden nodes = (the number of input nodes / 2) + 3. Increasing the number of hidden nodes does not significantly improve the network; it requires a longer training period.

The second part of the cloud typing procedure uses spatial information to differentiate the cloud types within each of the four cloud categories. More specifically, mean and variance for $n \times n$ pixel boxes in both a visible and infrared channel are used. The assumption behind the variance test is that the higher the variance, the more cumuliiform the cloud. Table 20 demonstrates how variance in a visible and infrared channel is used to determine individual cloud types for low level clouds.

The output of the algorithm is compared with the output of the cloud height algorithm to improve on the performance of both.

Table 20. Variance Table for Low Level Clouds

Visible Variance	Infrared Variance	Cloud Type
Low	Low	Stratus
Low	High	Stratocumulus
High	Low	Stratocumulus
High	High	Cumulus

8.3 Cloud Thickness

Knowledge of cloud type is used in the determination of cloud thickness. The algorithm uses visible channel radiance information to determine cloud optical thickness and cloud thickness through the use of cloud type dependent look up tables (LUTs). These LUTs, which provide relationships between sensor channel radiance and cloud thickness, are built off line using radiative transfer calculations. Here we describe the procedure we used in building a few prototype LUTs for testing purposes. The particular implementation used to derive these tables is not significant. Any state-of-the-art multiple scattering, radiative transfer simulation model may be used.

Inputs to LUT generation are a model atmosphere, an indication of cloud type, thickness and height, surface properties, sun/sensor geometry, and sensor characteristics. The model atmosphere defines such attributes as temperature, moisture, and aerosol background for latitudinal zones such as tropical, mid latitude, and Arctic. Cloud type information describes droplet size distribution and phase. Surface property information defines the geography type, such as land or water background, as well as its respective albedo value. Geometry information provides sun elevation, sensor viewing angle, and azimuth. Sensor characteristics provide channel response functions and dynamic range. Figure 17 illustrates the procedure used to generate LUTs. In subsequent application of the LUTs generated by this procedure, it is assumed that of the above input characteristics, cloud type and geometry are most important in determining the relationship between measured radiance and cloud thickness.

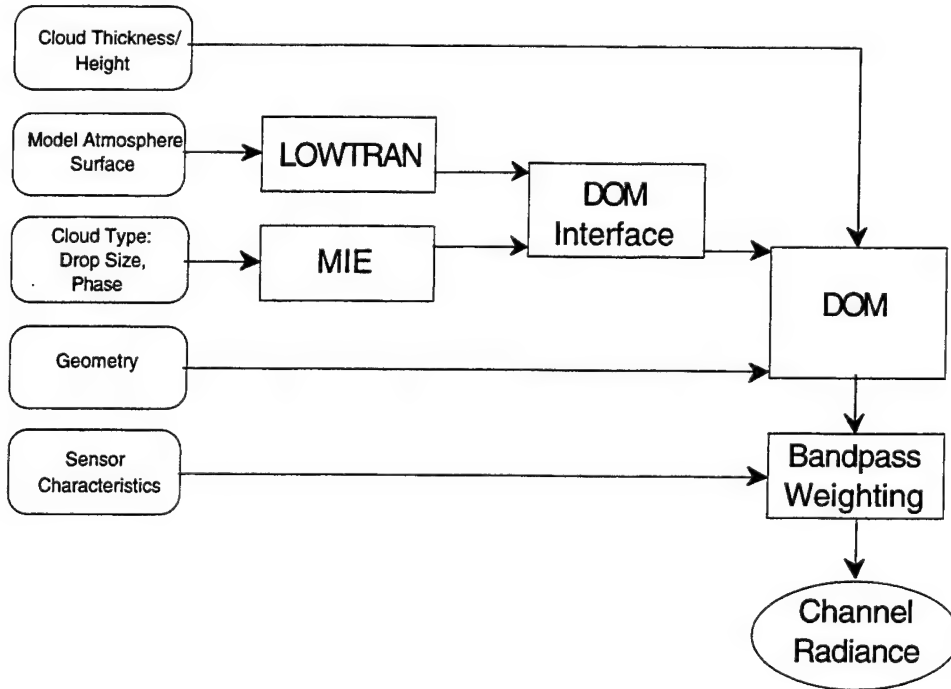


Figure 17. Radiative transfer-based LUT generation.

Low spectral resolution transmittance for clear atmospheres, aerosols, and the surface is calculated using the LOWTRAN radiative transfer code module. The MIE module provides cloud optical properties from characteristics based on cloud microphysics. Multiple scattering radiative transfer code is provided by the DOM module which employs a discrete ordinate method (DOM) approach. As indicated in Figure 17, all of these radiative transfer code modules are employed in LUT generation (Lindner and Isaacs, 1993).

Cloud optical properties are determined by their microphysical properties such as droplet size distribution and phase (water/ice). The key optical properties used in radiative transfer are the extinction coefficient, single scattering albedo, and angular scattering function. These are computed using Mie theory routines which require complex index of refraction and droplet size distribution as input, as indicated in Figure 17. Index of refraction is determined by phase while droplet size distribution is dependent upon cloud type. Droplet size distribution is defined as:

$$n(r) = Ar^{\alpha} \exp(-Br^{\gamma}) \quad (8-1)$$

Inputs to the relationship shown above are provided in Table 21.

Table 21. Cloud Type Dependence

Cloud Type	Density (gm ⁻³)	Mode Radius (μm)	A	α	B	γ
Cirrus	0.10	40	3.6 (-8)	6	1.90	0.5
Altostratus	0.15	10	6.0 (-4)	6	0.60	1.0
Low Lying Stratus	0.25	10	1.0 (-3)	6	0.60	1.0
Alto cumulus	0.15	10	5.6 (-2)	6	3.79	0.5
Strato cumulus	0.25	10	9.4 (-2)	6	3.79	0.5
Fair Weather Cumulus	0.70	10	2.6 (-1)	6	3.79	0.5

Figure 18 illustrates a set of typical AVHRR Channel 2 LUTs for five cloud types at a look angle of 0 degrees. Based on this table and determination of the cloud type, a cloud thickness is determined. The effect of cloud liquid water content is obvious. For a given sensor incident radiance, the higher liquid water content clouds are thinner. Given this cloud thickness and a determination of cloud top height, base is evaluated as illustrated in Figure 15.

8.4 Cloud Top Height

Cloud top height is obtained by comparing corrected equivalent black body brightness temperature (EBBT) from an infrared channel to a temperature profile for the same region. The brightness temperature of an IR channel (AVHRR channel 5) is adjusted to account for the integrated water vapor in the atmosphere (computed from the vertical moisture profile). Subsequently, the nearest temperature profile is used to obtain the height and pressure of the cloud. Finally, by using information from the cloud type algorithm, the height of cumulonimbus and cirrus clouds is corrected. In fact, cumulonimbus clouds, being cold, are at times placed higher than they are, and cirrus clouds, for their low emissivity, might be placed lower than they are. The cloud height algorithm is shown in Figure 19.

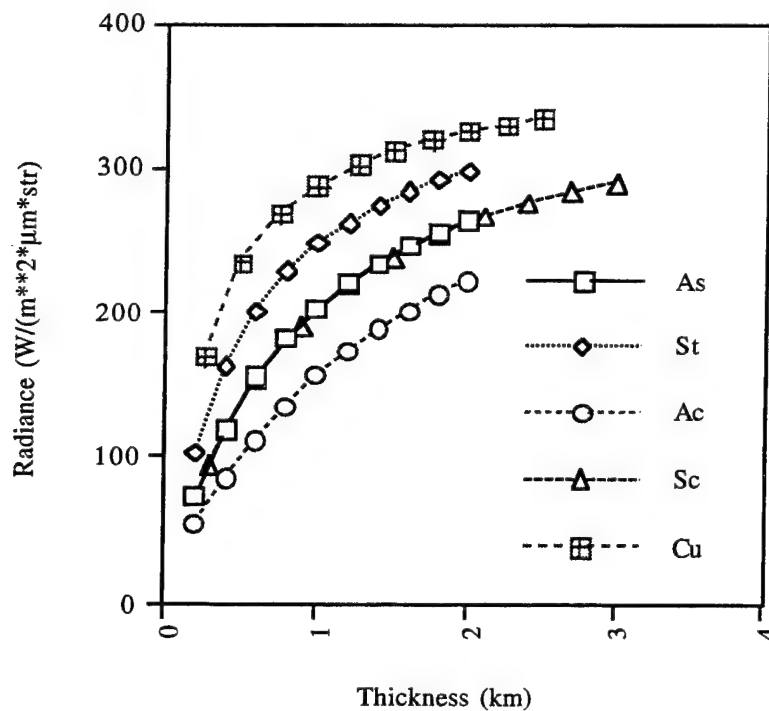


Figure 18. Cloud thickness look up tables (LUTs) for five cloud types.

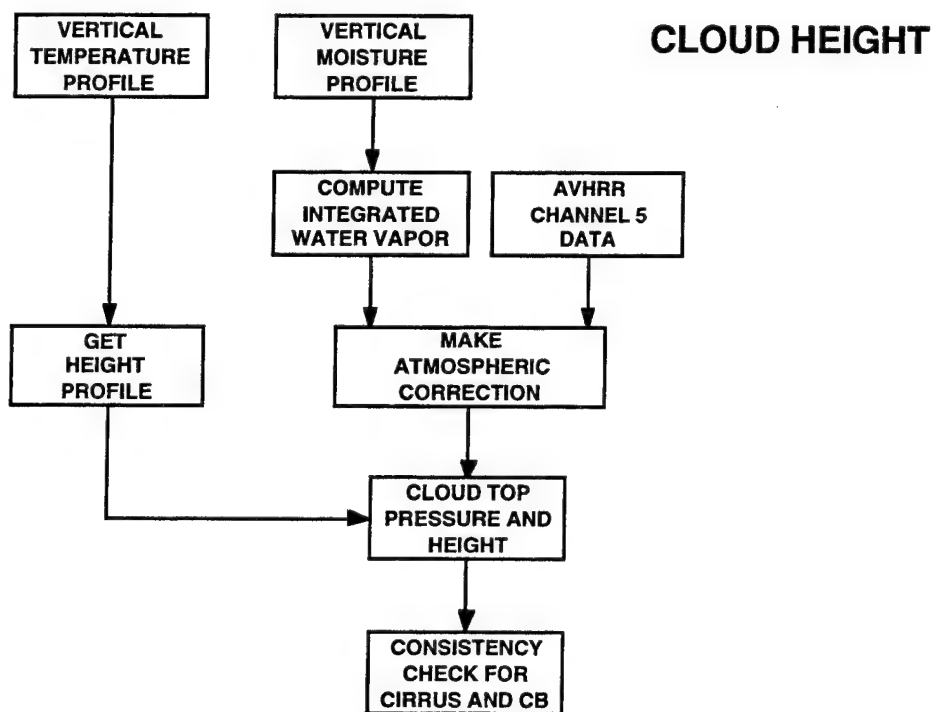


Figure 19. Integrated cloud height calculation.

8.5 Results

The cloud thickness and base algorithm described in Section 8.1 has been implemented in research grade code consisting of both Khoros and C routines for testing and evaluation. The algorithm was applied to a test case over the North East with both land and water background. A partly cloudy (43%) area was selected as the test image. Figure 20 corresponds to AVHRR channel 2 of that image. The date of the image is Julian Day 183 in the year 1992. The image is 512x512 pixels, with a resolution of approximately 1 km per pixel.

The progressive steps in the algorithm procedure as described in Section 8.1 are illustrated by the output images in Figures 21 through 25 for the test case study. The first step is the determination of cloud cover. Figure 21 is the derived cloud mask of the image. Cloudy pixels are represented in white; clear pixels, in black. Figures 21 and 22 can be compared for a qualitative validation of the cloud mask.

Figure 22 contains the results of the cloud typing algorithm described in Section 8.3. These results are derived using the full daytime complement of five AVHRR channels. The cloud types that are present in the image are the following:

1. Cumulonimbus (black)
2. Cumulus
3. Stratus
4. Stratocumulus
5. Altostratus
6. Altocumulus
7. Cirrostratus
8. Cirrus
9. Clear (white)

A gray shade look up table was used to render the different cloud types. Gray shade values go up in intensity (transition from black to white) from type 1 (Cb) to type 10 (clear). We have performed a manual cloud type analysis on this image to determine the validity of the typing procedure. Based on comparison of the manual and objective analysis, there is considerable quantitative skill demonstrated particularly for so called compatible cloud types (for example, cirrus and cirrostratus). In particular it can be seen by comparing to Figure 8-6 that the very bright areas in the original image correspond to convective regions where cumulonimbus clouds are identified by the typing algorithm. Notably, the algorithm does well in identifying clouds with similar liquid water contents which is important to the assignment of the appropriate microphysics models used in the radiative transfer based LUTs.

Figure 23 contains the results of the cloud height algorithm described in Section 8.5. Cloud height is derived using AVHRR channel 5 EBBTs. The range in height is approximately 300-9000 meters. Lower values are rendered in white; higher values, in black. A sanity check for the cloud height determination is possible by comparing it to the original image (Figure 20) and the cloud type results (Figure 22). Note that the highest cloud types (Cbs) are assigned the highest heights, the middle clouds (grays in both figures) the middle level heights, and the lowest clouds (see the isolated Cu and St in the central portion of Figure 15) the lowest heights.

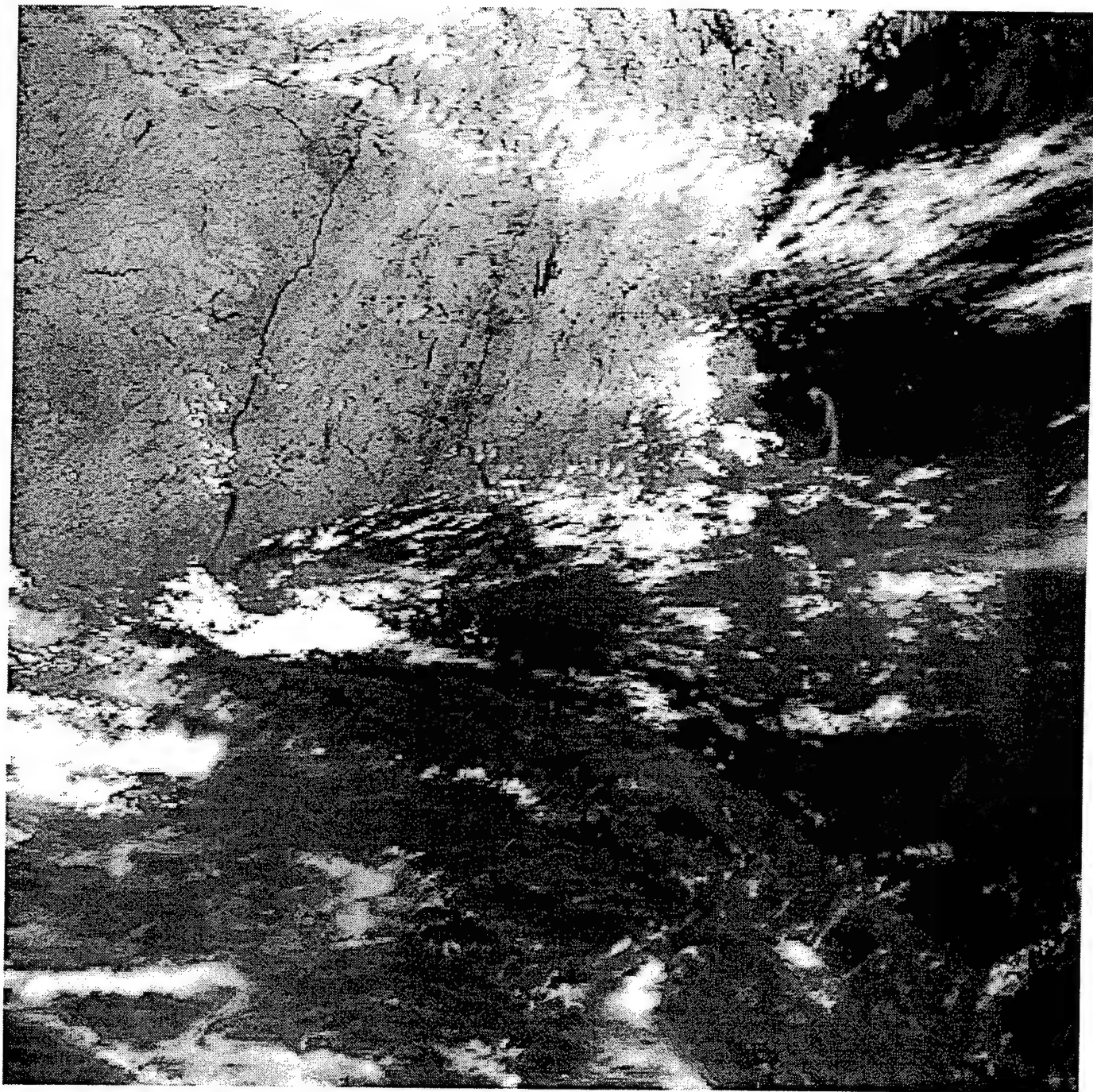


Figure 20. AVHRR channel 2. Julian day: 183; Year: 1992.

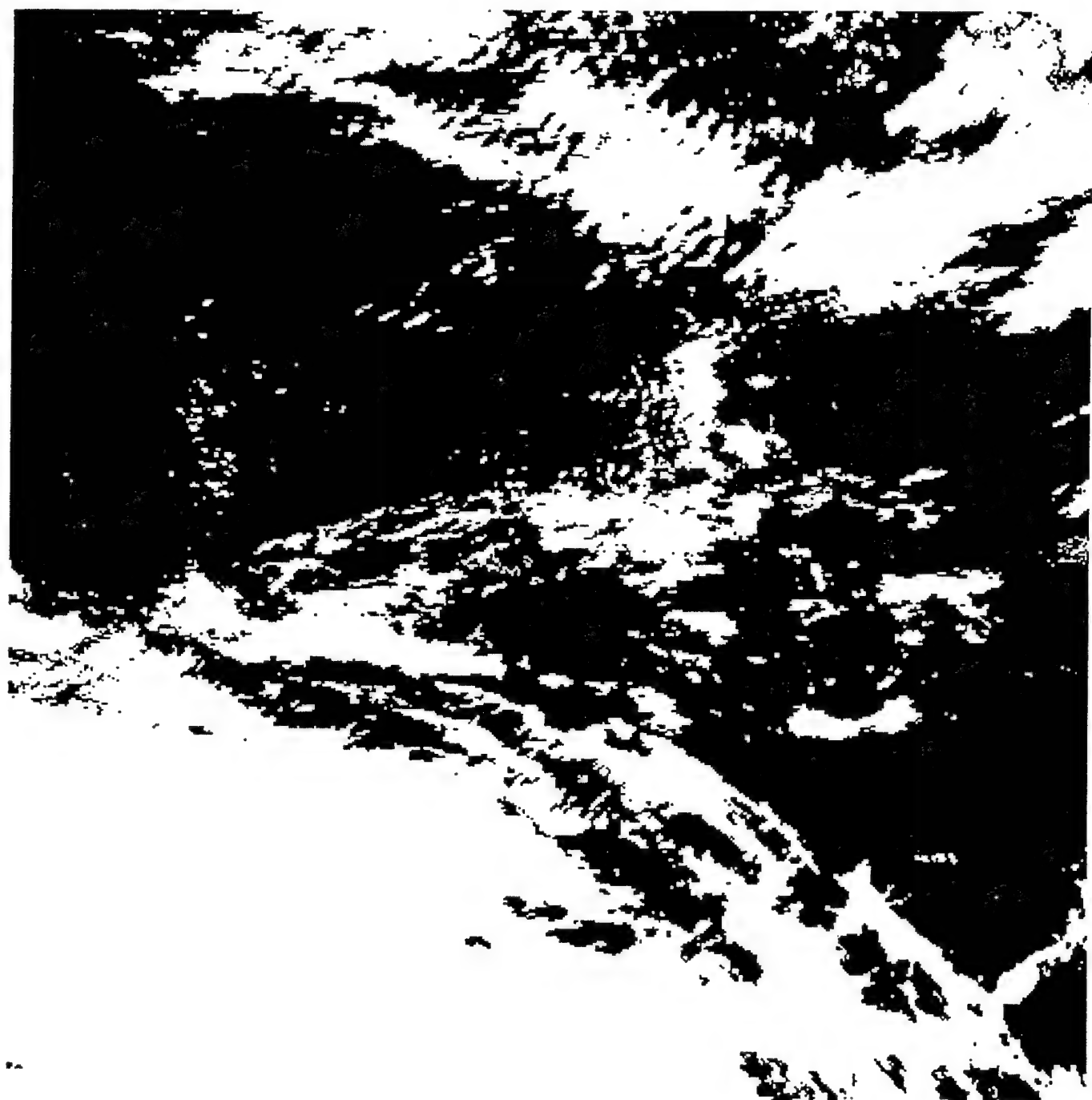


Figure 21. Cloud mask (cloudy pixels are white).

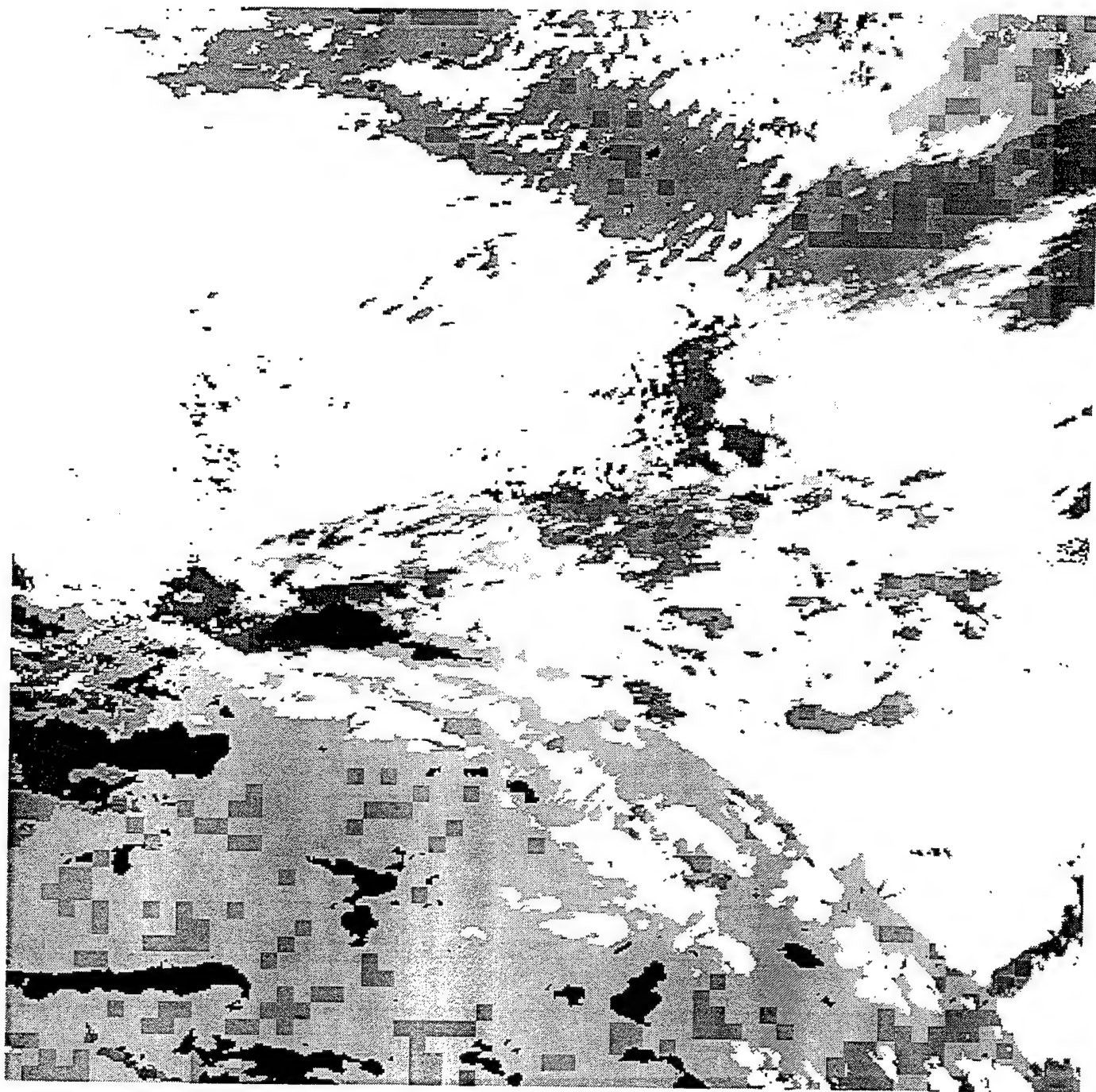


Figure 22. Cloud typing: 1: cumulonimbus (black); 2: cumulus; 3: stratus; 4: stratocumulus; 5: altostratus; 6: altocumulus; 7: cirrostratus; 8: cirrus; 9: clear.

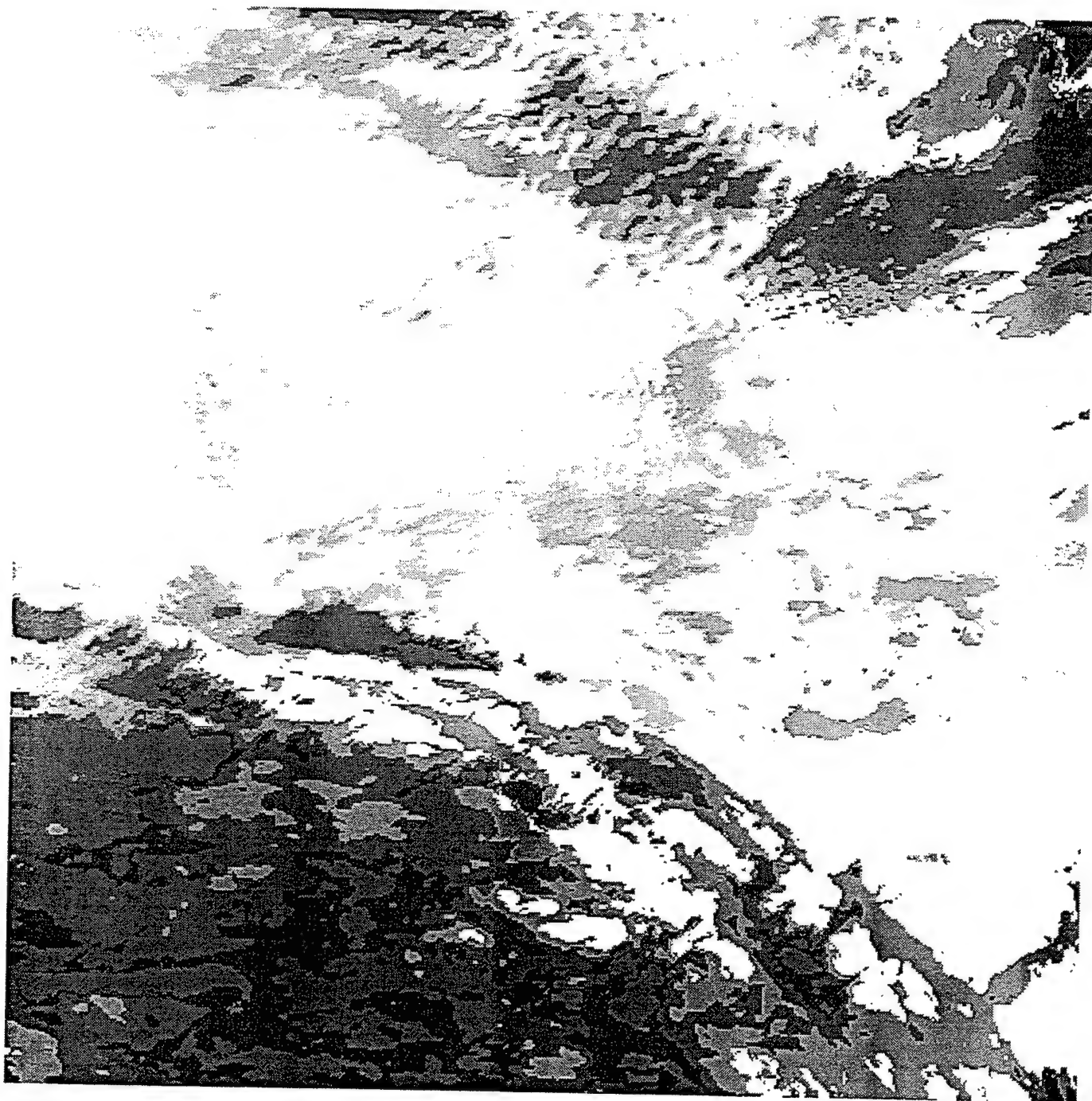


Figure 23. Cloud height. Low - 300 m (white); high - 9000 m (black).

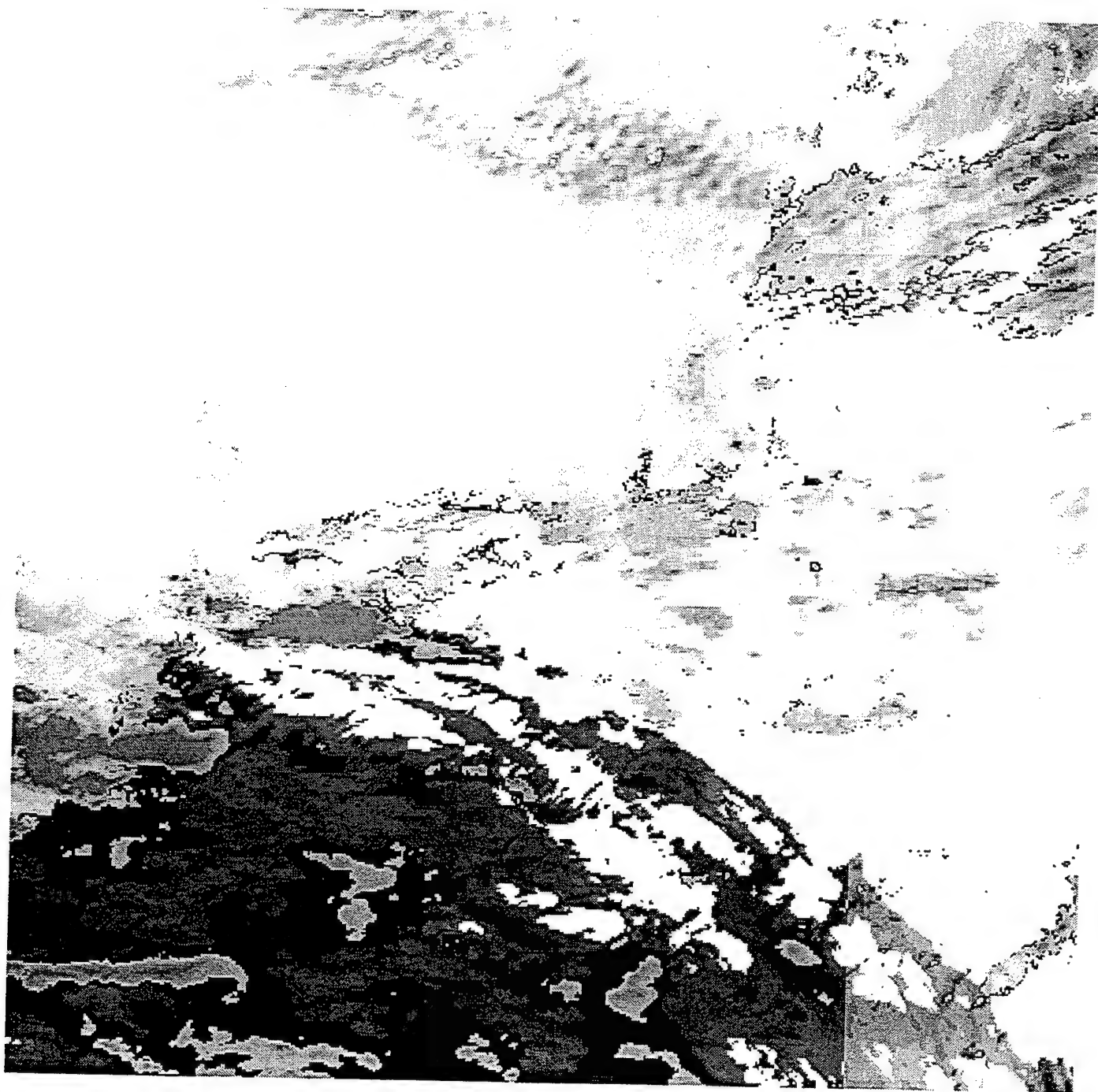


Figure 24. Cloud thickness. Low - 200 m (white); high - 6000 m (black).

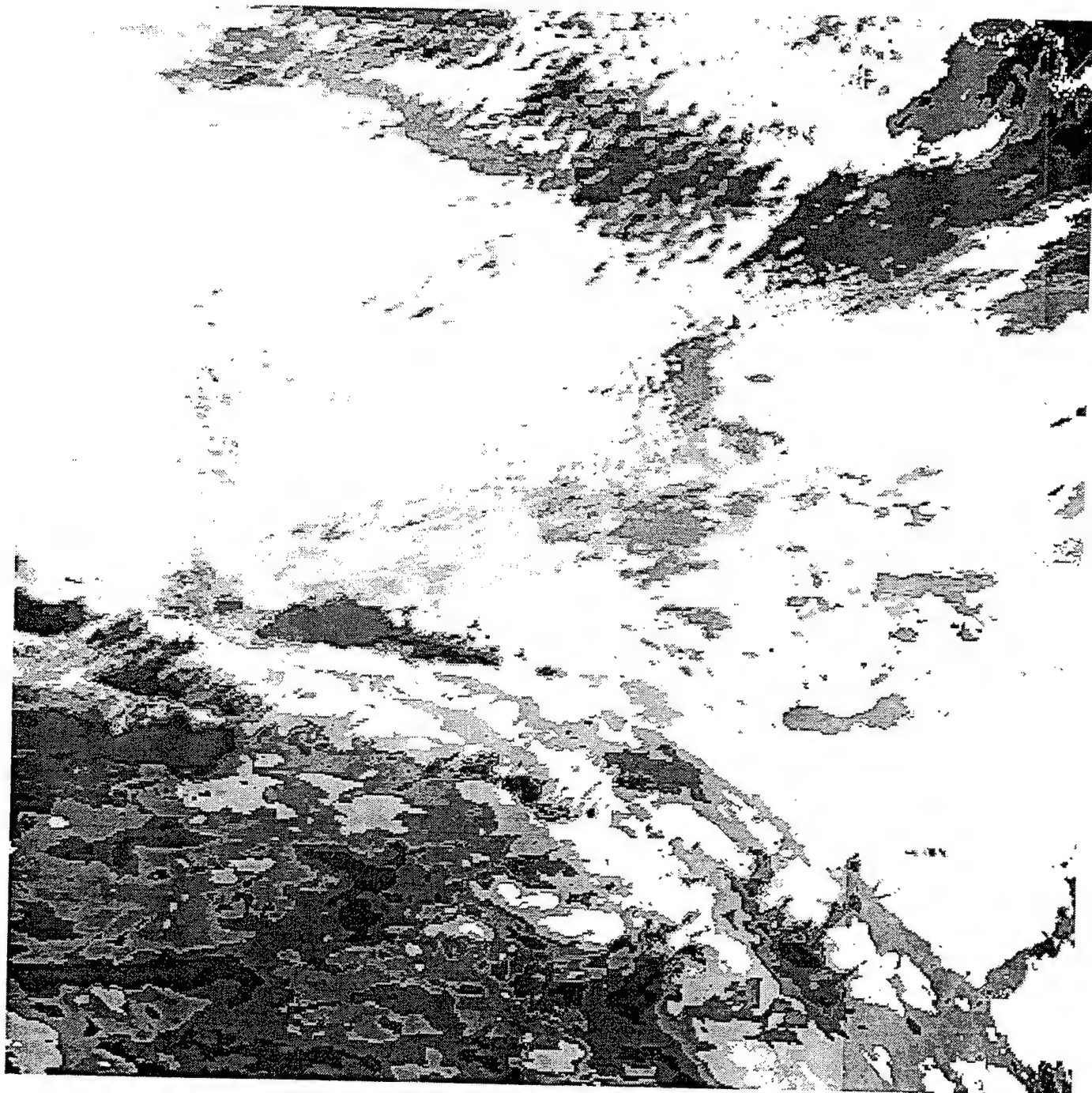


Figure 25. Cloud base. Low - 100 m (white); high - 8000 m (black).

Figure 24 contains the cloud thickness values. These are obtained by using the cloud types in Figure 22 to select appropriate LUTs to determine cloud thickness based on the approach described in Section 24. The range in thickness is approximately 200-4000 meters. Lower values are rendered in white; higher values, in black. In general the larger cloud thicknesses in Figure 24 correspond to the Cbs and Cs/Ci areas. The low and middle clouds are determined not to be as thick.

The final step in the algorithm consists of subtracting the cloud thicknesses in Figure 24 from the cloud heights in Figure 23. Figure 25 contains the cloud base values. The range in the cloud base values is approximately 100-8000 meters. Lower values are rendered in white; higher values, in black. In general, the results make sense when compared to cloud types in Figure 22. Low clouds (dark in Figure 23; exception Cb) have the lowest bases (light in Figure 25). High clouds (light in Figure 23) have the highest bases (dark in Figure 25). The middle clouds have mid level bases (intermediate in both figures). An exception to the above are the Cbs which have middle level bases.

While the above test case results are certainly not a definitive validation of the algorithm, they demonstrate skill in determining both cloud thickness and base. It should be pointed out that the current RTNEPH approach for cloud base is to assign a climatological base to each cloud type. Based on that approach, the cloud base results would have spatial properties identical to the cloud type result shown in Figure 22. The improved TACNEPH approach illustrated in Figure 25 provides a much more realistic spatial variation and dynamic range of cloud base by exploiting the information content of the visible channel radiance data.

8.6 Conclusions

We have outlined an algorithm to determine cloud base using multispectral imager radiance data. In this prototype, the cloud type is used to assign a particle size distribution which related physical cloud thickness and optical cloud thickness for a given imager channel bandpass. Off-line radiative transfer calculations then support the creation of look up tables (LUTs) to provide cloud thicknesses per cloud type based on sensor radiance data. As described in the previous section, we have applied a research version of this algorithm implemented on a workstation to a test case and obtained reasonable results. This work was reported at the 1993 CIDOS meeting (Isaacs et al., 1993). However, no extensive testing and validation of the algorithm has been performed. We have made a preliminary investigation of potential data sources for validation and testing including the use of field ceilometer data. This should be pursued in the future to obtain direct validation of the procedure developed in this task.

9. RECOMMENDATIONS FOR USE OF SURFACE OBSERVATIONS OF CLOUD

The use of conventional data in TACNEPH was suggested and requested primarily because cloud bases and cloud amounts in the lower atmosphere are often better observed from the ground than from satellite, especially when higher clouds obscure them. Although a sensible approach, it must be recognized foremost that tactical terminals in general, and the Mark IV-B in particular, have no capability to handle conventional data. Therefore it is not possible to integrate such data into the TACNEPH cloud analysis during and even after completion of the satellite-only portion of the analysis. Thus the capabilities of the Mark IV-B must be taken into account when determining how best to utilize conventional data as a supplement to the TACNEPH satellite cloud analysis product.

Since surface observations of cloud are not available on tactical terminals, their use either during or after satellite data processing is precluded. During TACNEPH conventional data assimilation techniques were explored that depart from the current RTNEPH merge processor philosophy in which surface observations are essentially force-fit into the satellite part of the analysis. Such techniques included making run-time adjustments to the cloud/no-cloud thresholds so that the satellite-observed cloud fractions agree with the surface-observed fractions. Adjustments would have to be made to account for differences in viewing geometries; surface observers view clouds from below that are hundreds of meters away, while satellite sensors observe clouds from above that are hundreds of kilometers away. Although technically appealing, such approaches were never seriously considered for TACNEPH because the prime constraint is a lack of surface data in the tactical environment.

Because of this limitation, it was decided that any conventional data processing has to be limited to post-processing of the satellite-only TACNEPH analysis in an external tactical weather facility that does have access to surface reports such as the proposed Combat Weather System (CWS). However, it is important to point out that conventional observations typically are not available until many minutes and even hours after the satellite image time. This even further constrains the use of conventional data in a timely sense within the TACNEPH analysis process. This essentially limits conventional data assimilation to at best an RTNEPH merge type of processing capability. Because the "force-fit" philosophy of the RTNEPH merge process typically manifests itself as sharp discontinuities in the final RTNEPH cloud product, it is recommended that surface observations of cloud cover be used only to interactively supplement the TACNEPH cloud analysis displays. If it is decided that a more invasive approach be taken, then TACNEPH cloud analysis quality flags can be used to provide information on when and how strongly to integrate surface observations of cloud. This represents a change from the current RTNEPH, which replaces satellite observations of cloud with surface observations *whenever* they are available. For example, spectral signatures that lie close to the cloud detection thresholds or clouds that are only detected by one cloud test have a low confidence in the TACNEPH analysis. Such points can be considered for conventional data assimilation in a more strongly weighted fashion than for points whose cloud detection signatures are very strong (i.e., whose confidence flags are high). Other information that is available from the TACNEPH analysis includes cloud phase and cloud top height, which can be used to help determine whether a conflicting surface observation should override a satellite-derived cloud analysis.

10. TACNEPH COMPUTER PROGRAM

The TACNEPH program had requirements in two areas:

- 1) development of algorithms capable of generating gridded fields of cloud amount and altitude from data sources available in a tactical terminal and
- 2) implementation of those algorithms as research grade FORTRAN code with sufficient documentation to support transition to operational programs on the Mark IV-B.

In previous sections, this report has primarily addressed the first requirement area. However, a considerable part of the TACNEPH program was devoted to development of working software to implement the new algorithms in a working environment (see for example the discussion on algorithm testing and validation in Section 5.3). In this section we provide a brief description of that process with the assumption that "lessons learned"

will be of value during operational implementation on a tactical terminal. Detail on the individual software modules is provided separately in the relevant software design reports.

TACNEPH processing requirements were designed to be consistent with typical low-end mini-computers, although, depending on the implementation, the algorithm can be memory intensive. The research grade code was developed to run in batch mode on a Micro-VAX 3900 with 20 MB of memory and interactively on a VAX-station 3600 with 16 MB of memory. Both systems run VMS version 5.5 and the software makes extensive use of the virtual memory capabilities of the operating system. Currently the program requires approximately 25 MB of virtual memory and can process a typical 1K by 1K image in about 8 minutes of CPU time running batch mode. Typically data are processed in 32 x 32 pixel arrays to approximate a 16th mesh grid size, this translates into memory requirements for storage of 32 lines of sensor and supporting data plus diagnostic information and the internal results buffer. This can and should be optimized to accommodate specific constraints of the target tactical terminal processing environment. These numbers are provided as guidelines only and should not be interpreted as hard requirements for the operational program since the research grade code is not optimized for efficiency in either memory or CPU usage.

10.1 Research Grade Code

During the TACNEPH development program, and at program reviews, there was considerable confusion about the definition of Research Grade Code (RGC). The stated requirement for tasks that required software development was that all software shall be implemented as Research Grade Code. In this application, RGC is defined as software written to run on the AIMS computer system for the sole purpose of demonstrating, testing, and validating satellite data processing algorithms developed under TACNEPH. No attempts were made to optimize the software to meet operational processing requirements. Several internal data buffers are maintained solely to provide a record of intermediate analysis products for use as a diagnostic of algorithm performance.

Necessarily, the TACNEPH computer program was closely tied to the TACNEPH Database (Section 3.1) to provide all data management functions. Database management was the most important implementation consideration since TACNEPH operates on large satellite databases that are frequently updated (Section 2). In fact, much of the required code is dedicated to the data management function. It is implicitly assumed that whatever tactical platform the TACNEPH algorithms are eventually implemented on will have an advanced capability to manage satellite data. Consequently the TACNEPH code will be tailored to accommodate that data management strategy.

TACNEPH RGC is useful as documentation in addition to the algorithm descriptions contained in this report. It provides examples of one way to implement the cloud algorithms. However, it is emphasized that RGC software should not be considered as a model for operational implementation. It was developed to meet the unique requirements of the TACNEPH research program and, as such, contains many features that would likely be superfluous in an operational implementation.

10.2 Implementation on the AIMS System

This section is intended to provide a general synopsis of the implementation of the TACNEPH computer algorithm on AIMS. A detailed description of the software is provided in the separate software design reports that accompany the OLS, AVHRR, and

clear-scene background characterization computer programs. The data analysis process consists of five separate components:

- 1) collection and calibration of satellite data via the two satellite ground stations,
- 2) ingest of the data into TDB,
- 3) application of the cloud detection algorithms,
- 4) updating of the infrared and visible dynamic supporting databases, and
- 5) manual analysis of the results.

All steps except the manual analysis are automated and require no user input. The algorithm is triggered by receipt of a satellite overpass by one of the PL ground station computers.

The first step in the TACNEPH cloud detection scheme on AIMS is collection of the satellite data. Recall that two ground stations are available to collect DMSP/RTD and NOAA/HRPT data in real-time. Every pass within the ground station line-of-site is collected for NOAA-11, NOAA-12 and F-11 on a continuing basis. Included with the ground station system is software to handle automatic scheduling of data capture and ingest, unpacking of the raw data stream, and calibration of the sensor data. When a pass is collected, a command script is automatically run which initiates the TACNEPH algorithm. The data stream is written both to hard disk and to permanent storage on tape. Next, the relevant sensor data (OLS or AVHRR) are unpacked from the data stream and calibrated. At this point, the data are in a ground station-specific format. The imagery can be displayed for the purposes of a manual check of the data quality. The data are then reformatted for ingest into TDB. OLS fine mode data are sampled to match the resolution of the smooth mode channel. Each sensor channel image is stored as a separate file (Section 3.1). Recall that the TACNEPH cloud analysis is performed on scan-formatted data so that no sampling of the original data is required. In addition to the sensor channel imagery, files of sampled latitude, longitude and solar/satellite angles are also created. Using additional software written expressly to manage the transfer of data from the ground stations to AIMS, the imagery, supporting ephemeris and satellite pass information are copied into a temporary file space on AIMS. When the transfer is complete, a TDB ingest script is initiated.

The ingest of data into TDB involves creating a data dictionary entry for each file and moving the files from temporary to permanent space on the AIMS hard disk. TDB is detailed in Section 3.

Once the data are registered in TDB, the automated script executes the satellite appropriate cloud algorithm. As discussed in Section 5, the cloud algorithms handle the graceful degradation issue internally. A series of paths through the code are traversed according to solar illumination constraints, data availability and quality. Note that automated quality checks are limited to detection of missing data and do not include checks for anomalous data. Cloud detection results are stored in permanent files and registered with TDB.

Using the newly created data files which contain cloud analyses for this satellite pass, clear-scene visible and infrared pixel values are identified and the visible and infrared dynamic databases described in Section 4.1 and 4.2 are updated. At this point, the automated process ends.

The final step is manual analysis of the cloud detection results using the interactive techniques described in Section 5.3.1.

11. REFERENCES

- Berendes, T, S.K. Sengupta, R.M. Welch, B.A. Wielicki, and M. Navar, 1992: Cumulus cloud base height estimation from high resolution Landsat data: A Hough transform approach. *IEEE Trans. Geo. and Remote Sens.*, **30**, 3, 430-443.
- Coakley, J.A. and F.P. Bretherton, 1982: Cloud Cover From High-Resolution Scanner Data: Detecting and Allowing for Partially Filled Fields-of-View, *J. Geophys. Res.*, **87**, 4917-4932.
- d'Entremont, R.P., L.W. Thomason, and J.T. Bunting, 1987: Color-composite image processing for multispectral meteorological satellite data. Proceedings, Conference on Digital Image Processing and Visual Communications Technologies in Meteorology, **846**, SPIE, 27-28 October 1987, Cambridge, MA, pp 96-106.
- d'Entremont, R.P., G.B. Gustafson, J.T. Bunting, M.K. Griffin, C. Barker Schaaf, P.M. Nowak, J.M. Ward, R.S. Hawkins, 1989: Comparisons between the RTNEPH and AFGL cloud layer analysis algorithms. GL-TR-89-0175, Geophysics Laboratory, Hanscom, AFB, MA. ADA216637
- d'Entremont, R.P., D.P. Wylie, J.W. Snow, M.K. Griffin, J.T. Bunting, 1992: Retrieval of cirrus radiative and spectral properties using independent satellite data analysis techniques. *Proceedings, Sixth Conference on Satellite Meteorology and Oceanography*. AMS. January 5-10, 1992, pp. 17-20.
- d'Entremont, R.P., G.B. Gustafson, and B.T. Pearson, 1994: Analysis of geostationary satellite imagery using a temporal differencing approach. Preprints, Seventh Conference on Satellite Meteorology and Oceanography. American Meteorological Society, Boston, MA.
- Falcone, V.J., and R. G. Isaacs, 1987: The DMSP microwave suite. In NOAA (Ed.), Proceedings, NOAA Conference on Passive Microwave Observing from Environmental Satellites. U.S. Department of Commerce. pp. 174-185.
- Falcone, V.J., M.K. Griffin, R.G. Isaacs, J.D. Pickle, J.F. Morrissey, A.J. Jackson, A. Bussey, R. Kakar, J. Wang, P. Racette, D.J. Boucher, B.H. Thomas, A.M. Kishi, 1992. SSM/T-2 Calibration and Validation Data Analysis, PL-TR-92-2293, Phillips Laboratory, Hanscom AFB, MA 01731-5000. ADA265817
- Grody, N.C., D.G. Gray, C.S. Novak, J.S. Prosad, M. Piepgrass and C.A. Dean, 1985: Temperature Soundings from the DMSP microwave Sounder, *Advances in Remote Sensing retrieval Methods*, A. Deepak Publishing, pp 249-267.
- Gustafson, G.B. and G.R. Felde, 1988: Interactive Image Processing Applied to Cloud Detection. Preprints: 4th International Conference on Interactive Information and Processing Systems for Meteorology, Hydrology, and Oceanography, AMS, Boston, MA.
- Gustafson, G.B. and G.R. Felde, 1989: Validation of automated cloud detection from microwave imagery. Preprints: 5th Conference on Interactive Information

Processing Systems for Meteorology, Hydrology, and Oceanography, AMS, Boston, MA.

- Gustafson, G.B., R.G. Isaacs, R.P. d'Entremont, J.M. Sparrow, T.M. Hamill, C. Grassotti, D.W. Johnson, C.P. Sarkisian, D.C. Peduzzi, B.T. Pearson, V.D. Jakabhazy, J.S. Belfiore, and A.S. Lisa, 1994: Support of Environmental Requirements for Cloud Analysis and Archive (SERCAA). PL-TR-94-2114, Phillips Laboratory, Hanscom AFB, MA, pp 105. ADA283240
- Hamill, T.M., R.P. d'Entremont and J.T. Bunting, 1992: A description of the Air Force real-time nephanalysis model. *Wea Forecasting*, **7**, 288-306.
- Heacock, L.E., 1985: ENVIROSAT-2000 Report; Comparison of the Defense Meteorological Satellite Program (DMSP) and the NOAA Polar-orbiting Operational Environmental Satellite (POES) Program, US Department of Commerce/NOAA/NESDIS, Washington, D.C.
- Hoke, J.E., J.L. Hayes, and L.G. Renniger, 1981: Map Projections and Grid Systems for Meteorological Applications, *AFGWC Technical Note 79/003*, USAF AFGWC, Offutt AFB NE 86 pp.
- Hollinger, J., R. Lo, G. Poe, R. Savage, J. Peirce: 1987: Special Sensor Microwave/Imager User's Guide. Naval Research Laboratory, Washington, D.C.
- Hughes, N.A. and A. Henderson-Sellers, 1983: Analysis of cloud characteristics derived from archived satellite data. *Int. J. Remote Sensing*, **4**, 1, 159-173.
- Isaacs, R.G., 1989: A Unified Retrieval Methodology for the DMSP Meteorological Sensors, RSRM '87: Advances in Remote Sensing Retrieval Methods, A. Deepak Publishing.
- Isaacs, R.G., B.L. Lindner, and R.N. Hoffman, 1990: Multispectral cloud property retrieval. Final Report. Contract No. F04701-87-C-0145, HQ Space Systems Division, Los Angeles, CA 90009.
- Isaacs, R. G., A. Bianco, G. Gustafson, and C. Sarkisian, 1993: Remote Sensing of Cloud Thickness and Base from Multispectral Cloud Imager Data. Paper presented at the Cloud Impacts on Defense Operations and Systems (CIDOS'93) 16-19 November 1993, Fort Belvoir, VA.
- Ivaldi, C.F., G.B. Gustafson, and J. Doherty, 1992: The Air Force Interactive Meteorological System: A research tool for satellite meteorology. PL-TR-92-2327, Phillips Laboratory, Hanscom AFB, MA., 85 pp. ADA265957
- Kidwell, K.B., 1988: NOAA Polar Orbiter Data Users Guide, NOAA/NESDIS/NCDC/SDSD, Washington, D.C.
- King, M.D., 1987: Determination of the scaled optical thickness of clouds from reflected solar radiation measurements. *J. Atmos. Sci.*, **44**, 1734-1751.
- Lindner, B.L. and R.G. Isaacs, 1993: Remote Sensing of Clouds by Multispectral Sensors. *Appl. Optics*, **32**, 15, 2744-2746.